

การศึกษาพลศาสตร์ของลำอิเล็กตรอน  
ของเครื่องกำเนิดแสงสยาม

นายฤทธิไกร ไชยงาม

วิทยานิพนธ์นี้เป็นส่วนหนึ่งของการศึกษาตามหลักสูตรปริญญาโทมหาบัณฑิต

สาขาวิชาฟิสิกส์

มหาวิทยาลัยเทคโนโลยีสุรนารี

ปีการศึกษา 2543

ISBN 974-7359-89-8

**ELECTRON BEAM DYNAMICS STUDIES  
OF  
THE SIAM PHOTON SOURCE**

**Mr. Ritthikrai Chai-ngam**

**A Thesis Submitted in Partial Fulfillment of the Requirements  
for the Degree of Master of Science in Physics**

**Suranaree University of Technology**

**Academic Year 2000**

**ISBN 974-7359-89-8**

## **Thesis Title**

### **Electron Beam Dynamics Studies of the Siam Photon Source**

Suranaree University of Technology Council has approved this thesis submitted in partial fulfillment of the requirements for a Master's Degree.

#### **Thesis Examining Committee**

.....  
( Assoc. Prof. Dr. Prasart Suebka )  
Chairman

.....  
( Prof. Dr. Takehiko Ishii )  
Thesis Advisor

.....  
( Assoc. Prof. Dr. Samnao Phatisena )  
Member

.....  
( Dr. Saroj Rujiwat )  
Member

.....  
( Dr. Prayoon Songsiririthigul )  
Member

.....  
( Assoc. Prof. Dr. Kasem Prabripataloong )  
Vice Rector for Academic Affairs

.....  
( Assoc. Prof. Dr. Tassanee Sukosol )  
Dean, Institute of Science

ฤทธิ์ไกร ไชยงาม: การศึกษาพลศาสตร์ของลำอิเล็กตรอนของเครื่องกำเนิดแสงสยาม  
(ELECTRON BEAM DYNAMICS STUDIES OF THE SIAM PHOTON SOURCE)  
อ. ที่ปรึกษา: ศ. ดร. ทาเกฮิโกะ อิชิอิ, 125 หน้า. ISBN 974-7359-89-8

อิเล็กตรอนพลังงาน 40 MeV จากเครื่องเร่งอนุภาคแนวตรง (Linear Accelerator (LINAC)) จะเคลื่อนที่ผ่านส่วนลำเลียงพลังงานต่ำ (Low-Energy Beam Transport Line (LBT)) ไปยังเครื่องเร่งอนุภาคซินโครตรอน (Booster Synchrotron (SYN)) ต่อมาอิเล็กตรอนจะถูกเร่งจนมีพลังงานสูงถึง 1 GeV จากนั้นจะถูกผลัก (kicked out) ออกจากเครื่องเร่งอนุภาคซินโครตรอนให้เคลื่อนที่ผ่านส่วนลำเลียงพลังงานสูง (High-Energy Beam Transport Line (HBT)) ไปกักเก็บไว้ในวงแหวนสะสม (Storage Ring (STR))

การศึกษาพลศาสตร์และลักษณะของลำอิเล็กตรอนของเครื่องกำเนิดแสงสยาม เริ่มด้วยการศึกษาอธิบายและวิเคราะห์ ลักษณะและการเคลื่อนที่ของอิเล็กตรอนในเครื่องเร่งอนุภาควงกลม (circular accelerator) แล้วคำนวณพารามิเตอร์ (parameters) ที่สำคัญต่างๆ ที่บ่งบอกถึงลักษณะของลำอิเล็กตรอน โดยใช้โปรแกรมคอมพิวเตอร์ LATTICE และ BETA และใช้การประมาณอันดับแรก (first-order approximation) ในการคำนวณเชิงตัวเลข ค่าความเข้มของสนามแม่เหล็ก (magnetic field strength) ของแม่เหล็กสี่ขั้ว (quadrupole magnet) จะถูกแปรผันไปจนกระทั่งได้ลักษณะของลำอิเล็กตรอนที่ต้องการ ผลการคำนวณจะถูกแสดงทั้งในรูปของตัวเลขและกราฟ สำหรับวงแหวนสะสมได้มีการจำลอง (simulation) dynamic aperture อีกด้วย

ในวิทยานิพนธ์นี้ ไม่เพียงแต่ศึกษาพลศาสตร์และลักษณะของลำอิเล็กตรอนในวงแหวนสะสมเท่านั้น แต่ยังสามารถศึกษาทางเดิน (path) ของลำอิเล็กตรอนผ่าน ส่วนลำเลียงพลังงานต่ำ, เครื่องเร่งอนุภาคซินโครตรอน และ ส่วนลำเลียงพลังงานสูงอีกด้วย

สาขาวิชาฟิสิกส์

ลายมือชื่อนักศึกษา \_\_\_\_\_

ปีการศึกษา 2543

ลายมือชื่ออาจารย์ที่ปรึกษา \_\_\_\_\_

RITTHIKRAI CHAI-NGAM: ELECTRON BEAM DYNAMICS  
STUDIES OF THE SIAM PHOTON SOURCE, THESIS  
ADVISOR: PROF. DR. TAKEHIKO ISHII, Ph.D. 125 PP. ISBN  
974-7359-89-8

The 40 MeV electrons from the Linear Accelerator (LINAC) pass through the Low-Energy Beam Transport Line (LBT) and reach the Booster Synchrotron (SYN). Then, the electrons are accelerated to 1 GeV, kicked out from the Booster Synchrotron into the High-Energy Beam Transport Line (HBT) and finally injected into the Storage Ring (STR).

The electron beam dynamics and characteristics of the accelerator complex of the Siam Photon Source have been studied. First, the characteristics and motion of electrons in circular accelerators are described analytically. Then, the parameters characterizing the accelerators are calculated numerically with programs LATTICE and BETA to the first-order approximation. In the numerical calculation, the gradient fields of the quadrupole magnets are varied until the desired beam characteristics are carried out. The results of calculations are displayed both numerically and graphically. For the Storage Ring, the dynamic aperture is simulated.

In this thesis, not only the beam dynamics and characteristics of the electron beam in the Storage Ring but also the paths from the Low-Energy Beam Transport Line, the Booster Synchrotron, and the High-Energy Beam Transport Line are considered.

School of Physics

Student's signature \_\_\_\_\_

Academic Year 2000

Advisor's signature \_\_\_\_\_

## Acknowledgements

I would like to express my sincere thanks to the following persons who guided and helped me during the course of this thesis study:

Professor Takehiko Ishii, my advisor, for his patient guidance, encouragement and assistance throughout my study.

Professor Masumi Sugawara, ex-advisor to NSRC, for his helpful discussion about the beam dynamics and program computers, LATTICE and BETA.

Dr. Prayoon Songsiriritthigul and Dr. Saroj Rujiwat, members of my advisor committee, for their kind support and valuable suggestions.

Dr. Su Su Win and Mr. Somchai Tancharakorn, staff members of NSRC, for their useful advises on the various computer programs needed in completing this study.

Members of the Chai-ngam and Sri-ampai families, for their sincerity, encouragement, understanding and support all along. Without them, I could not have come this far.

Ritthikrai Chai-ngam

# Contents

	Page
<b>Abstract (Thai)</b> .....	I
<b>Abstract (English)</b> .....	II
<b>Acknowledgments</b> .....	III
<b>Contents</b> .....	IV
<b>List of Tables</b> .....	VII
<b>List of Figures</b> .....	VIII

## Chapter

### I. Introduction

1.1 Siam Photon Project.....	1
1.2 Siam Photon Source.....	2
1.3 Beam Dynamics.....	5
1.4 Purposes of the Work.....	6

### II. Electron Motion in a Storage Ring

2.1 A General First-Order Theory of Beam Transport Matrix.....	7
2.1.1 The Coordinate System.....	7
2.1.2 First and Second-Order Expansion of a Magnetic Field.....	9
2.1.3 Equation of Motion to Second-Order.....	10
2.1.4 The Solutions of the Equations of Motion.....	12
2.1.5 The Transfer Matrix R.....	13
2.2 The Betatron Oscillation.....	21
2.2.1 Betatron Functions.....	21
2.2.2 Phase Ellipse.....	22
2.2.3 Betatron Tune or Betatron Wave Number; $\nu_x, \nu_y$ .....	25
2.3 Beam Parameters.....	26
2.3.1 Momentum Compaction Factor $\alpha_c$ .....	26
2.3.2 Closed Orbit.....	28
2.3.3 Transition Energy $\gamma_T$ .....	28
2.3.4 Energy Loss per Turn $U_0$ .....	29
2.3.5 Damping Partition Numbers $J_x, J_y, J_E$ .....	30

## Contents (Continued)

	Page
2.3.6 Damping Times $\tau_x, \tau_y, \tau_E$ .....	31
2.3.7 Energy Spread $\sigma_E$ .....	31
2.3.8 Bunch Length $\sigma_L$ .....	32
2.3.9 Beam Size $\sigma_x, \sigma_y$ .....	32
2.3.10 Natural Emittance $\epsilon_x^0$ .....	33
2.3.11 Chromaticity, $\xi_x, \xi_y$ .....	33
2.3.12 Harmonic Number $k$ .....	34
2.3.13 Dynamic Aperture .....	35
<b>III. Beam Dynamics Calculation</b>	
3.1 Data Collection .....	37
3.1.1 Low-Energy Beam Transport Line (LBT) .....	40
3.1.2 Booster Synchrotron (SYN) .....	41
3.1.3 High-Energy Beam Transport Line (HBT) .....	42
3.1.4 Storage Ring (STR) .....	43
3.2 Software .....	45
3.3 Twiss Parameters .....	46
3.3.1 Twiss parameters of LBT .....	46
3.3.2 Twiss parameters of SYN .....	48
3.3.3 Twiss parameters of HBT .....	49
3.3.4 Twiss parameters of STR .....	51
3.4 Result of Calculation and Discussion .....	53
3.4.1 LBT .....	53
3.4.2 SYN .....	54
3.4.3 HBT .....	56
3.4.4 STR .....	58
<b>IV. Conclusion</b>	
4.1 Beam Dynamics .....	62
4.2 Beam Characteristics .....	62
4.3 Future Perspective .....	63
<b>References</b> .....	<b>64</b>
<b>Appendices</b> .....	<b>67</b>
Appendix A: Equation of Motion .....	68
Appendix B: Magnetic Field Expansion to Second-Order Only .....	72
Appendix C: The First-Order Solutions of the Equation of Motion .....	75



## Contents (Continued)

	Page
Appendix D: Betatron Functions.....	79
Appendix E: Radiation Damping and Excitations.....	80
Appendix F: The Results of Calculations.....	103
F1. The Results of Calculations for the Low-Energy Beam Transport Line (LBT) by the Program LATTICE.....	103
F2. The Results of Calculations for the Booster Synchrotron (SYN) by the Program LATTICE.....	108
F3. The Results of Calculations for the High-Energy Transport Line (HBT) by the Program LATTICE.....	111
F4. The Results of Calculations for the Storage Ring (STR) without Chromaticities Compensation by the Program LATTICE.....	116
F5. The Results of Calculations for the Storage Ring (STR) with Compensation Chromaticities by the Program LATTICE.....	117
F6. The Results of Calculations for the Storage Ring (STR) by the Program BETA.....	122
<b>Curriculum Vitae</b> .....	125

## List of Tables

Table		Page
3.1	Magnet parameters of LBT.....	40
3.2	Parameters of SYN.....	41
3.3	Magnet parameters of HBT.....	42
3.4	Parameters of STR.....	43
3.5	Twiss parameters of LBT.....	47
3.6	Twiss parameters of SYN.....	48
3.7	Twiss parameters of HBT.....	50
3.8	Twiss parameters of STR.....	52
3.9	Main parameters of SYN.....	54
3.10	Main parameters of STR.....	58
3.11	The field gradient of the quadrupoles in STR.....	60

# List of Figures

Figure	Page
1.1	Layout of component accelerators in the Siam Photon Source..... 2
1.2	Injector Linac..... 3
1.3	A Low-Energy Transport Line (LBT) and Booster Synchrotron (BS)..... 4
2.1	Coordinate system ..... 8
2.2	Illustration of interior of the quadrupole magnet..... 11
2.3	Rectangular coordinate system ..... 15
2.4	Field boundary for bending magnets..... 20
2.5	The Phase space ellipse due to the Courant-Snyder invariant, where $\epsilon$ is the beam emittance, $\beta, \alpha, \gamma$ are the betatron amplitude functions..... 22
2.6	Transformation of a phase ellipse along drift space at different locations.... 24
2.7	Chromatic focusing errors..... 34
2.8	Dynamic aperture for a perfect machine and a realistic Machine with error... 35
3.1	Bending magnet of BS..... 37
3.2	Quadrupole magnets and steering magnets..... 38
3.3	Sextupole magnet ..... 39
3.4	RF cavity in STR ..... 39
3.5	Transfer magnet elements of LBT ..... 40
3.6	Magnet structure of BS..... 41
3.7	Magnet structure of HBT..... 42
3.8	Unit cell of magnet lattice..... 43
3.9	Magnet structure of STR ..... 44
3.10	The schematic layout of LBT..... 46
3.11	The schematic layout of BS..... 48
3.12	The schematic layout of the HBT ..... 49
3.13	The schematic layout of the STR..... 51
3.14	Betatron functions and dispersion function in LBT..... 53
3.15	Beam sizes in LBT, electron energy 40 MeV..... 54
3.16	Betatron functions and dispersion function in BS..... 55
3.17	Beam sizes for BS in a unit cell of Lattice..... 56
3.18	Betatron functions and dispersion function in HBT..... 57
3.19	Beam sizes in HBT..... 57
3.20	Betatron functions and dispersion function in a unit cell of STR ..... 59
3.21	Beam sizes in a unit cell of lattice of STR..... 60
3.22	The dynamic aperture for perfect machine at the center of the long straight section. The dashed line is the physical aperture of the vacuum chamber.... 61
A.1	Deflecting of a particle trajectory, ideal trajectory $s$ and individual trajectory $\mathbf{s}$ ..... 70

## List of Figures (Continued)

E.1	Longitudinal motion of an electron within a bunch.....	84
E.2	Effect of energy gain from rf accelerating system on the vertical betatron oscillations.....	88
E.3	Effect of energy changes at $s_0$ on the horizontal betatron displacement .....	90

# Chapter I

## Introduction

### 1.1 Siam Photon Project

The Ministry of Science, Technology and Environment of Thailand started the Siam Photon Project in early 1996. For implementing the project, the National Synchrotron Research Center (NSRC) of Thailand was established in May 1996. The Center received an accelerator complex for a synchrotron light source from SORTEC CORPORATION. The components of the dismantled SORTEC ring and its injector system arrived at NSRC in January 1997. It is now installed in the Siam Photon Laboratory of NSRC which is located in the campus of Suranaree University of Technology. This light source, named as the *Siam Photon Source*, is the first light source accelerator in Thailand.

In the Siam Photon Project, the SORTEC ring is modified so that the beam emittance is reduced and the insertion devices can be installed. Therefore, lattice structure is changed from quadrupole doublet lattice to double bend achromat lattice (DBA) and the ring with four long straight sections is built. The Project aims at promoting the scientific research based on spectroscopic methods in the vacuum ultraviolet and soft x-ray (VUV-SX) region in the first stage, and later the applications of x-ray from the superconducting wiggler will be considered. Also, applications of synchrotron radiation to the development of the new technology will be considered. The Project is promoted as a part of the human resources development plan. Young scientists and engineers will be trained in various fields of technology, beam line optics, measurement technology and practical technology, and various fields of accelerator physics (Pairsuwan, W. and Ishii, T., 1998). More specifically, the Siam Photon Project is summarized as follows:

- 1 A 1.0 GeV electron storage ring with four long straight sections for insertion devices will be constructed. Future up grade of the electron energy to 1.2 GeV is considered.
- 2 Beam lines and experimental stations for advanced spectroscopic studies on gases, solid, materials, surfaces and interfaces will be built. Experiments are planned as follow:
  - 2.1 Spin- and angle-resolved photoemission.
  - 2.2 Soft x-ray fluorescence.
  - 2.3 Magnetic circular dichroism.
  - 2.4 Photoelectron-photoion coincidence measurements.
  - 2.5 Two-color experiments by simultaneous irradiation with laser and synchrotron light.
  - 2.6 High-resolution spectroscopy of gaseous atoms and molecules.

- 3 Conventional beam lines for routine photoabsorption experiments and radiation biology will be built.
- 4 A beam line for basic researches on metrology using synchrotron radiation as intensity standard of light and on microlithography and micromachining will be built.
- 5 The installation of superconducting wiggler magnets is considered. Beam lines will be built for x-ray experiments associated with:
  - 5.1 Protein crystallography
  - 5.2 X-ray microscopy
  - 5.3 Applications to metallurgy and mineralogy
  - 5.4 X-ray microanalysis

## 1.2 Siam Photon Source

The Siam Photon Source consists of the following component accelerators, an injector linac, a booster synchrotron and beam transport lines, a low-energy beam transport line, high-energy beam transport line, as shown in Fig.1.1:

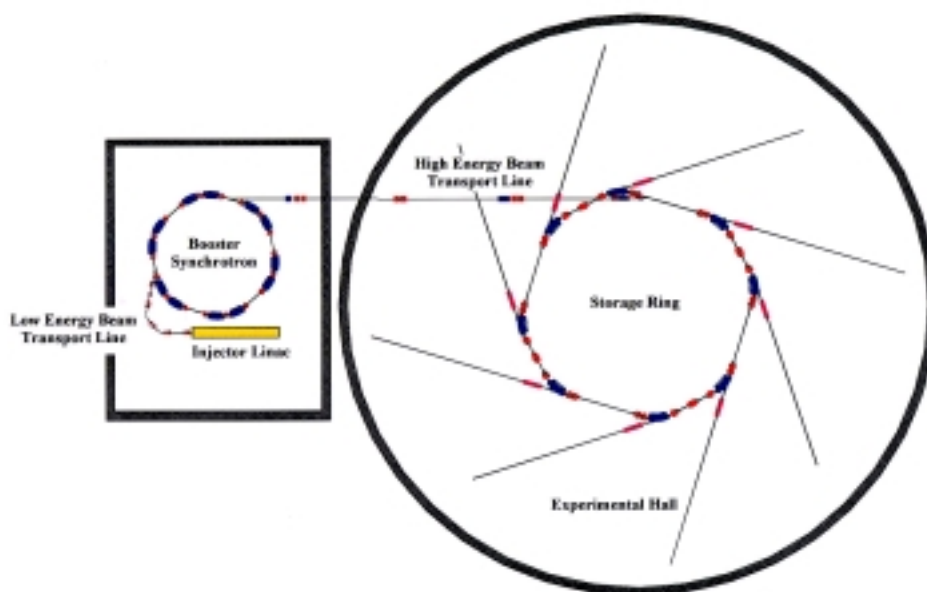


**Figure. 1.1** Layout of component accelerators in the Siam Photon Source

### 1.2.1 Injector Linac (LINAC)

The injector of the SORTEC facility is used in the Siam Photon Source without modification. The injector linac is shown in Fig.1.2. The *linear accelerator*, abbreviated as LINAC, is about 9.5 m long. A pair of acceleration tubes is used in the linac, the length of one acceleration tube is 2.3 m. The RF power to the tubes is supplied by a Klystron, PV-3035, maximum output power is 35 MW. In this thesis we will not simulate the electron beam in the

LINAC, so some designed parameters of the SORTEC system are used in simulation of other paths. The electron beam is accelerated to 40 MeV with a large current of 60-80 mA. The electron beam has properties as the low energy dispersion, energy width  $\Delta\varepsilon/\varepsilon$  of 0.7 %, and a low emittance of 700 nm rad. LINAC is installed in an underground room.



**Fig. 1.2** Injector Linac

### **1.2.2 A Low-Energy Beam Transport Line (LBT)**

The low-energy electron beams, 40 MeV, from LINAC are led to the booster synchrotron. This path is, therefore, called the *Low-Energy Beam Transport Line*, abbreviated as LBT. The LBT is located between the injector linac and the booster synchrotron. The LBT of SORTEC system is used without reformation, but the new beam position monitors comprising of fluorescent screen monitors are used. LBT is shown by Fig 1.3.

### **1.2.3 A Booster Synchrotron (SYN)**

The synchrotron of SORTEC system is also used without modification in the Siam Photon Source, which receives electrons of 40 MeV from LBT and accelerates them to 1 GeV. Therefore, it is called the *Booster Synchrotron*, abbreviated as SYN. It is shown in Fig 1.3. The circumference is 43.19 m. The lattice structure is FODO type. The yokes of the bending and quadrupole magnets are made of laminated silicon steel plates of 0.5 mm thickness. The inflector magnet and four bump magnets are used for beam injection. The 118 MHz RF acceleration cavity is of reentrant type and made of copper. The details of the synchrotron are discussed in Chapter III.



**Fig.1.3** A Low-Energy Beam Transport Line (LBT) and Booster Synchrotron (SYN)

### 1.2.4 A High-Energy Beam Transport Line (HBT)

This path is located between SYN and the storage ring. The 1 GeV electrons from SYN are transported through the high-energy beam transport line (HBT) to the storage ring. Because LINAC and SYN are installed underground and the configuration of the storage ring is modified, HBT is newly built. The inflector magnets and bending magnets deflect the electron beams. The electron beams are deflected of  $17.5^\circ$  in the vertical plane and deflected twice in the horizontal plane: first by  $4^\circ$  at a 5.1 m point away from the injector magnet of the storage ring and second by  $2^\circ$  at an about 1.7 m point from the inflector. The details are also discussed in Chapter III.

### 1.2.5 Storage Ring (STR)

A storage ring accumulates and stores electrons that have been accelerated and transport them from the injection system to produce the synchrotron light. The SORTEC ring has a beam emittance about  $500 \text{ nm } \pi \text{ rad}$ . It is not necessary to have a small beam size, because it was optimized for microlithography. To reduce the emittance and install insertion devices, the storage ring is reformed as:

- The lattice structure is changed from the quadrupole doublet lattice to the double bend achromat (DBA) lattice. To fulfill this modification, the quadrupole magnets and the sextupole magnets are increased.
- Four long straight sections are built to install the insertion devices, three undulators and a superconducting wiggler will be installed.
- New vacuum chambers will be built.



The STR circumferences 81.3 m, the structure of the lattices are discussed in details in Chapter III, and important parameters of the modified ring are calculated in this thesis.

Not only these, all of the machine control system was newly built. This is because the control system of the SORTEC machine is too old and inadequate for controlling the new machine system. The maintenance of the old system is not easy.

In order to force the high-energy beam to move in the desired direction and to confine the beam in the space near the ideal orbit, the locations and sizes of magnets and associated magnetic fields should be known. In addition, necessary collection such as chromatic collection should also be known. The electron beam motion in a given magnet structure is called the beam dynamics. In this thesis, numerical calculation will be carried out by the computer codes, LATTICE and BETA. We obtain the characteristics of the electron beam with various parameters calculated with these programs.

### 1.3 Beam Dynamics

Beam dynamics is the word for calling the revolution of particle trajectories under the influence of Lorentz force. In this thesis we will discuss the theory of linear beam dynamics, the mathematical description of particular trajectories in the presence of only the linear field.

After electrons are accelerated and transported from the injection system, the electrons are stored in packets called bunches which are held together in the direction of motion by the bunching effect of the radio frequency system in RF cavity. Since the injected electrons are displaced with respect to the ideal orbit, the betatron oscillations around this orbit occur in transverse directions. The electrons lose energy due to synchrotron radiation and their energy losses are compensated in the RF cavity. This loss and gain of energy causes the synchrotron oscillations. The electrons circulate inside a vacuum chamber in which a high vacuum is maintained. The chamber is delimited by metallic wall. The bending magnets curve the electron trajectories and the focusing magnets, quadrupole, keep them close together in the plane perpendicular to the direction of motion.

Obviously, it is essential to carry out the electron beam dynamics analysis in designing an accelerator. Thus, we need to perform the beam dynamics calculation for the new magnet lattice in the Siam Photon Source. In this thesis, the calculation is implemented. In what follows, simple analytic parts of the beam dynamics are described. The change and characteristics of the beam are expressed by the basic equation of motions which are described in reference system, ideal orbit, with an azimuthal axis tangent to the orbit, and the transverse horizontal and vertical coordinates, lying in the plane perpendicular to the ideal orbit. The betatron oscillation is used to describe an oscillation of the electrons around the ideal orbit. The Courant-Snyder invariant, the Twiss parameters and the phase ellipses are used to characterize the electron beams. For each element of the transport, the transformation matrix conveniently describes the system.

## 1.4 Purposes of the Work

In this thesis, the calculation is limited only to the case of the ideal arrangement of the magnetic field. Thus, the field error arising from magnet misalignment, mechanical imperfection and energy spread at the time of the beam injection are not taken into account. The effect of correction fields, such as those of sextupole and steering magnets are not introduced in the calculation explicitly. These correction fields are considered only to make bending and focusing fields to be ideal and perfect and assumed to be involved in the perfect fields. In this sense, the data to be obtained here is not realistic. However, the data will provide us with the basic characteristics that are necessary in designing the magnet lattice structure as the starting point.

The purposes of this work, therefore, are to study the beam dynamics summarized as follows:

- 1.4.1 Describe the analytical part of the electron motion in a storage ring.
- 1.4.2 Calculate the important beam parameters.
- 1.4.3 Illustrate the beam size and dispersion function graphically. They are the  $\beta$  function (betatron function) and the  $\eta$  function (dispersion).
- 1.4.4 Illustrate the dynamic aperture.
- 1.4.5 Calculations will be carried out for LBT, SYN, HBT and STR.

## Chapter II

### Electron Motion in a Storage Ring

#### 2.1 A General First-Order Theory of Beam Transport Matrix

##### 2.1.1 The Coordinate System

In order to describe charged particle beam dynamics we must choose the appropriate coordinate system to maximize physical clarity and minimize mathematical complexity. So the reference plane should be imposed on the field configuration that will be designated as the magnetic midplane. The magnetic midplane is defined as the reference plane with which the magnetic scalar potential  $\varphi$  shall be an odd function in the transverse coordinate  $y$ , i.e.,  $\varphi(x, y, s) = -\varphi(x, -y, s)$ . We suppose a particle in the *ideal trajectory* toward the directions, see Fig.2.1. The ideal trajectory lines on the magnetic midplane. The radius of curvature of the ideal trajectory,  $\rho_0$ , in its bending part is given as:

$$\rho_0 = \frac{P_0}{eB_0} \quad (2.1)$$

Here,  $B_0$  is the strength of the magnetic field that is perpendicular to the magnetic midplane, and  $P_0$  is the momentum of the particle on the ideal trajectory. Obviously,  $\rho_0$  is equal to the radius of the circular orbit of the charged particle moving in a uniform magnetic field directed toward the  $y$  direction.

In Fig.2.1  $\mathbf{R}$  is the position vector of the electron and  $\mathbf{O}$  is the origin. We use the coordinates  $(x, y, s)$ , variable  $s$  is the coordinate vector that is the arc length measured along the ideal trajectory and  $y$  is positive on the upward side of the magnetic midplane while  $y$  is designate of negative for downward. Coordinate vector  $x$  may have any direction as long as the  $x$  direction is orthogonal to  $s$  and  $y$ ,  $x$  is the distance from the ideal trajectory in the median plane. In other words,  $x, y$  and  $s$  form the right-handed curvilinear coordinate system. Since the ideal trajectory is known and fixed, we are only interested in the deviation of the individual particle trajectories from the ideal trajectory. This path is called *individual trajectory*.

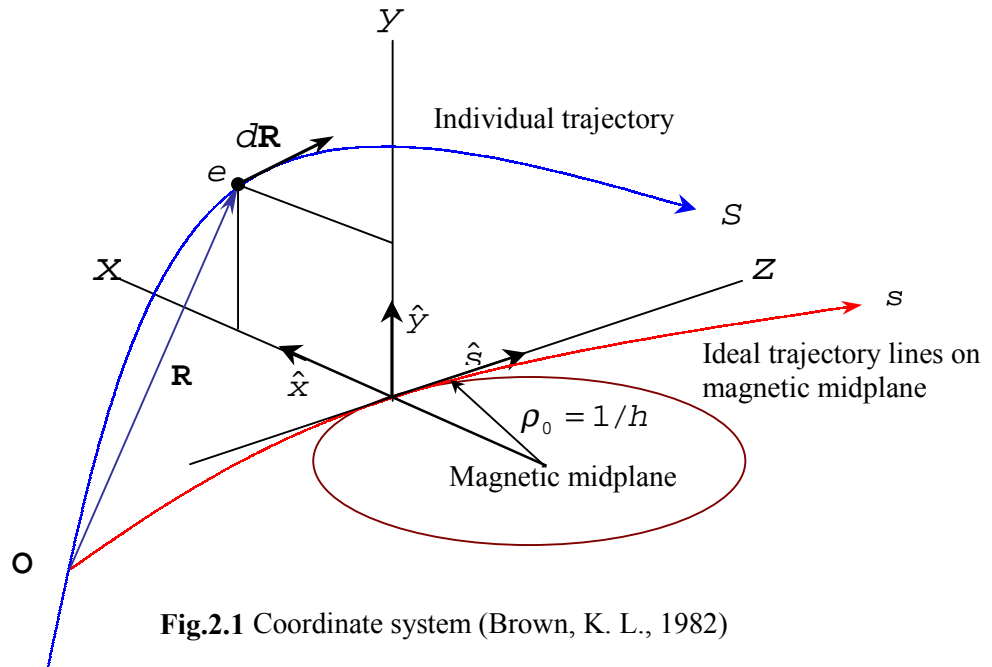


Fig.2.1 Coordinate system (Brown, K. L., 1982)

To bend and direct the charged particle beam close to the ideal trajectory, a dipole magnet is used. We indicate the static magnetic field of the bending magnet by  $\mathbf{B}$ , the velocity vector of the particle by  $\mathbf{v}$  and the charge of the particle by  $e$ . We may write the relation of the time rate of the change of the momentum  $\mathbf{P}$  according to the *Lorentz force* as:

$$\frac{d\mathbf{P}}{dt} = e(\mathbf{v} \times \mathbf{B}) \quad (2.2)$$

Comparing the partial differential of equation (2.2) with the partial differential of coordinate vector  $\mathbf{R}$ . By expressing the equation in terms of  $d\mathbf{R}/dR$  (the unit tangent vector of the trajectory) and  $d^2\mathbf{R}/dR^2$  (the deviation of the unit tangent vector) and  $S$  is the distance transversed (see Appendix A for details), we expect the momentum to be constant. Note that  $S = \int dR$ . We obtain the equation of motion in the form of:

$$\mathbf{R}'' - \frac{1}{2} \frac{\mathbf{R}'}{(R')^2} \frac{d}{ds} (R')^2 = \frac{e}{P} R' (\mathbf{R}' \times \mathbf{B}) \quad (2.3)$$

We use the prime to indicate the operation  $d/ds$ . Then, we substitute the coordinate vector  $d\mathbf{R} = \hat{x}dx + \hat{y}dy + (1 + hx)\hat{s}ds$  (see Appendix A, (A.6)). Here  $\hat{x}, \hat{y}$  and  $\hat{s}$  are unit vectors in the  $x, y$  and  $s$  directions, respectively. (see Appendix A for details), we obtain the general equation of motion in the form of:

$$\begin{aligned}
& \left( x'' - h(1+hx) - \frac{x'}{(R')^2} (x'x'' + y'y'' + (1+hx)(hx' + h'x)) \right) \hat{x} + \\
& \left( y'' - \frac{y'}{(R')^2} (x'x'' + y'y'' + (1+hx)(hx' + h'x)) \right) \hat{y} + \\
& \left( (2hx' + h'x) - \frac{(1+hx)}{(R')^2} (x'x'' + y'y'' + (1+hx)(hx' + h'x)) \right) \hat{s} \quad (2.4) \\
& = \left( \frac{e}{P} R' (y'B_s - (1+hx)B_y) \right) \hat{x} + \left( \frac{e}{P} R' (1+hx)B_x - x'B_s \right) \hat{y} \\
& \quad + \left( \frac{e}{P} R' (x'B_y - y'B_x) \right) \hat{s}
\end{aligned}$$

Note that in this equation form, the equation of motion is still valid to all orders in the variables  $x, y$  and their derivatives. If we approximate

$$\frac{1}{(R')^2} = 1 - 2hx + \dots \text{ and keeping up terms only to the second-order we obtain:}$$

$$x'' - h(1+hx) - x'(hx' + h'x) = \frac{e}{P} R' (y'B_s - (1+hx)B_y) \quad (2.5)$$

$$y'' - y'(hx' + h'x) = \frac{e}{P} R' (1+hx)B_x - x'B_s$$

So far we have used the ideal trajectory as the reference trajectory. For the ideal trajectory  $x, y, x', y', x''$  and  $y''$  equal to zero under this condition, we obtain:

$$h = \frac{e}{P_0} B_y(0,0,s) \quad \text{Or} \quad B_y \rho_0 = \frac{P_0}{e} \quad (2.6)$$

If we put  $B_y = B_0$ , we obtain equation (2.1). Equation (2.6) is well known as the *beam rigidity*.

### 2.1.2 First and Second-Order Expansion of a Magnetic Field

In the coordinate system, we have already chosen the reference trajectory on the magnetic midplane. The magnetic scalar potential is an odd function in direction  $y$ ,  $\phi(x, y, s) = -\phi(x, -y, s)$ . This is equivalent to saying that on the midplane  $y=0$ , the components of the magnetic fields are such that  $B_x = B_s = 0$  and only  $B_y$  remains nonzero (see Appendix B). In other words, on the midplane  $\mathbf{B}$  is always normal to the plane. For the particle in the vacuum the magnetic field,  $\mathbf{B}$ , may be expressed by the relation  $\mathbf{B} = \nabla\phi$ , and  $\phi$  derived from Laplace equation (we omit the minus sign for convenience since we are restricting the problem to static magnetic fields):

$$\nabla^2 \phi = 0 \quad (2.7)$$

Finally, the expression for the magnetic field components may be expressed in the forms of (see also Appendix B):

$$\begin{aligned} B_x(x, y, s) &= \left( \frac{P_0}{e} \right) [-nh^2 y + 2\beta h^3 xy + \dots] \\ B_y(x, y, s) &= \left( \frac{P_0}{e} \right) [h + -nh^2 x + \beta h^3 x^2 - \frac{1}{2} (h'' - nh^3 + 2\beta h^3) y^2 + \dots] \quad (2.8) \\ B_s(x, y, s) &= \left( \frac{P_0}{e} \right) [(h'y - (n'h^2 + 2nhh' + hh')xy + \dots)]. \end{aligned}$$

where  $P_0$  is the momentum of the ideal trajectory.

### 2.1.3 Equation of Motion to Second-Order

Combining equation (2.5) and equation (2.8) we obtain:

$$\begin{aligned} x'' - h(1 + hx) - x'(hx' + h'x) &= \frac{P_0}{P} R' \{ (1 + hx) [h + nh^2 x - \beta h^3 x^2] \\ &\quad + \frac{1}{2} (h'' - nh^3 + 2\beta h^3) y^2 + h'yy' + \dots \} \quad (2.9) \\ y'' - y'(hx' + h'x) &= \frac{P_0}{P} R' \{ -x'h'y - (1 + hx) [nh^2 y - 2\beta h^3 xy] + \dots \} \end{aligned}$$

Let

$$\frac{P_0}{P} = \frac{P_0}{P_0(1 + \delta)} = 1 - \delta + \delta^2 + \dots \quad (2.10)$$

And we have

$$R' = [x'^2 + y'^2 + (1 + hx)^2]^{\frac{1}{2}}$$

Substituting them into equation (2.9) we obtain the expression of the equation of motion to the second-order as:

$$\begin{aligned} x'' + (1 - n)h^2 x &= h\delta + (2n - 1 - \beta)h^3 xx' + h'xx' + \frac{1}{2} hx'^2 \\ &\quad + (2 - n)h^2 x\delta + \frac{1}{2} (h'' - nh^3 + 2\beta h^3) y^2 + h'yy' - \frac{1}{2} hy'^2 \\ &\quad - h\delta^2 + \text{higher order terms} \quad (2.11) \\ y'' + nh^2 y &= 2(\beta - n)h^3 xy + h'xy' - h'xy + hx'y' + nh^2 y\delta \\ &\quad + \text{higher order terms} \end{aligned}$$

From this equation, the equation of motion for the first-order terms may be extracted as:

$$\begin{aligned}x'' + (1-n)h^2 x &= h\delta \\ y'' + nh^2 y &= 0\end{aligned}\tag{2.12}$$

where  $\delta$  may be approximated as being equal to  $\Delta P/P_0$  where  $\Delta P = P - P_0$  (see equation (2.10)).

Consider the case of quadrupole field. Because the interior of the quadrupole (Fig.2.2) field is current-free, one can define the scalar magnetic potential which can be calculated with Laplace equation in two dimensions. Assuming that the length effect is negligible, we derive the ideal quadrupole as:

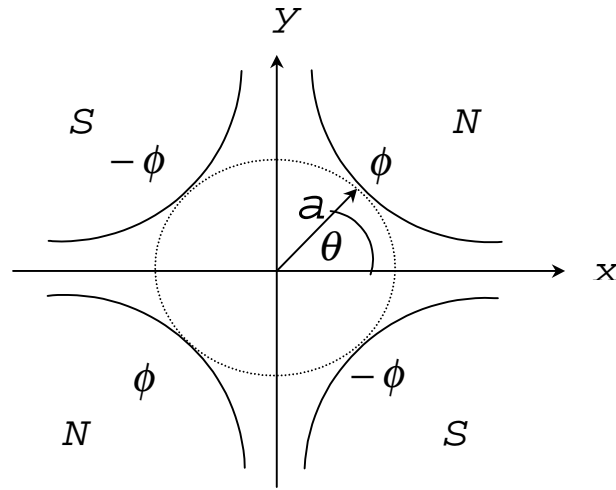


**Fig2.2** Illustration of interior of the quadrupole magnet

Solving the Laplace equation in the cylindrical coordinate, we obtain the scalar potential of the pure quadrupole field as:

$$\phi = \left(\frac{B_0 r^2}{2a}\right) \sin 2\theta = \frac{B_0}{a} xy$$

where  $B_0$  is the field at the pole,  $a$  is the radius of the quadrupole aperture and  $r$  and  $\theta$  are the cylindrical coordinates (see Fig.2.2), respectively. From  $\mathbf{B} = \nabla\phi$ , we obtain the constant gradient field as:

$$\left.\frac{\partial B_y}{\partial x}\right|_{x=0, y=0} = \frac{B_0}{a} = -nh^2 \left(\frac{P_0}{e}\right)\tag{2.13}$$

If we define the quantity  $k_q^2$  as follows:

$$k_q^2 = -nh^2 = \frac{B_0}{a} \frac{e}{P_0} = \frac{B_0}{a} \frac{1}{B\rho_0} \quad (2.14)$$

Then, substitute equation (2.14) into (2.11), in case of quadrupole  $h \rightarrow 0$ ,  $h' \rightarrow 0$  we find that the equations of motion up to second-order for a pure quadrupole are:

$$\begin{aligned} x'' + k_q^2 x &= k_q^2 x \delta \\ y'' - k_q^2 y &= -k_q^2 y \delta \end{aligned} \quad (2.15)$$

This equation is useful in the matrix elements for the pure quadrupole.

#### 2.1.4 The Solutions of the Equations of Motion

Equation (2.12) is the first-order equation of motion of charged particle in the magnetic static field. The solutions are presented in Appendix C. The Taylor expansion and the boundary conditions are used to express the first-order solutions in the forms:

$$\begin{aligned} x &= \sum (x|x_0, y_0, x'_0, y'_0, \delta) x_0, y_0, x'_0, y'_0, \delta \\ y &= \sum (y|x_0, y_0, x'_0, y'_0, \delta) x_0, y_0, x'_0, y'_0, \delta \\ x &= c_x x_0 + s_x x'_0 + \eta_x \delta \\ y &= c_y y_0 + s_y y'_0 \end{aligned} \quad (2.16)$$

where

$$\begin{aligned} (x|x_0) &= c_x & (x|x'_0) &= s_x & (x|\delta) &= \eta_x \\ (y|y_0) &= c_y & (y|y'_0) &= s_y \end{aligned} \quad (2.17)$$

The symbols shown by parameters are the Taylor expansion coefficients of the first-order. We assume that the solutions  $x$  and  $y$  are given by the Taylor expansion as to parameters  $x_0, x'_0, y_0, y'_0$  and  $\delta$ .  $\delta$  is defined in the expansion shown in equation (2.10). For general expressions, see Appendix C. When we insert these solutions into the equation of motions and then compare the coefficients of  $x_0, x'_0, y_0, y'_0$  and  $\delta$ , we find the differential equations, both homogeneous and inhomogeneous forms. For homogeneous equations, after deriving with boundary conditions, we find that the coefficients of Taylor's expansions are in forms of *cosine like solutions* and *sine like solutions*, namely (see Appendix C for detail):



$$\begin{aligned}
c_x(s) &= \cos k_x s & s_x(s) &= \left(\frac{1}{k_x}\right) \sin k_x s \\
c_y(s) &= \cos k_y s & s_y(s) &= \left(\frac{1}{k_y}\right) \sin k_y s
\end{aligned} \tag{2.18}$$

And for  $k_x, k_y$  with negative values:

$$\begin{aligned}
c_x(s) &= \cos |k_x| s & s_x(s) &= \left(\frac{1}{|k_x|}\right) \sin |k_x| s \\
c_y(s) &= \cos |k_y| s & s_y(s) &= \left(\frac{1}{|k_y|}\right) \sin |k_y| s
\end{aligned} \tag{2.19}$$

where  $k_x^2 = (1-n)h^2$  and  $k_y^2 = nh^2$ . At this stage, we are only interested in the positive  $k_x, k_y$ , because both forms are similar. For the inhomogeneous equation Green's function method is used. The particular solution of the inhomogeneous equation is expressed by (see Appendix C, (C.14), (C.15)):

$$\eta_x = s_x(s) \int_0^s h(\tau) c_x(\tau) d\tau - c_x(s) \int_0^s h(\tau) s_x(\tau) d\tau \tag{2.20}$$

Using equation (2.18), we assumed that  $h(\tau)$  is constant. Finally, the solutions are expressed by:

$$\eta_x = \frac{h}{k_x^2} [1 - \cos k_x s] = \frac{h}{k_x^2} [1 - c_x] \tag{2.21}$$

where  $k_x$  is positive value. The function of  $\eta_x$  is called *dispersion function*. The physical interpretation is simply that the particular solution of the equation of motion, (see equation (2.16)),  $\eta_x \delta$ , determines the offset of the trajectories of the particles with a relative energy  $\delta$  from the ideal trajectory. We note that the right side of the equation has the term of  $h=1/\rho_0$ , i.e., the first-order dispersion is generated only in regions where the ideal orbit is deflected, in dipole magnet or bending magnet.

### 2.1.5 The Transfer Matrix R

So far the first-order solutions of the equation of motion have been expressed in terms of the coordinate system  $(x, y, s)$ . To facilitate matching boundary conditions between the various components comprising a beam transport system, we transform this coordinate system to the rectangular coordinate system  $(x, y, z)$ , as shown in Fig.2.3. And introduce the angular

coordinates  $\theta$  and  $\phi$ , defined as follows (use approximation  $\tan\theta = \theta$  and  $\tan\phi = \phi$ ):

$$\begin{aligned}\theta &= \frac{dx}{dz} = \frac{x'}{z'} = \frac{x'}{(1+hx)} \\ \phi &= \frac{dy}{dz} = \frac{y'}{z'} = \frac{y'}{(1+hx)}\end{aligned}\quad (2.22)$$

Using these definitions, equation (2.16) and their derivatives (may be see in Appendix C, C.2), we may express the solutions of the equation of motions for  $x, \theta, y, \phi$  and  $\delta$  in terms of rectangular coordinate system. The expressions  $x, \theta, y, \phi$  and  $\delta$  at the end boundary of a system as a function of initial variables are given below:

$$\begin{aligned}x &= (x|x_0)x_0 + (x|\theta_0)\theta_0 + (x|\delta)\delta \\ \theta &= (\theta|x_0)x_0 + (\theta|\theta_0)\theta_0 + (\theta|\delta)\delta \\ y &= (y|y_0)y_0 + (y|\phi_0)\phi_0 \\ \phi &= (\phi|y_0)y_0 + (\phi|\phi_0)\phi_0\end{aligned}\quad (2.23)$$

$$\begin{aligned}x &= c_x x_0 + s_x \theta_0 + \eta_x \delta \\ \theta &= c'_x x_0 + s'_x \theta_0 + \eta'_x \delta \\ y &= c_y y_0 + s_y \phi_0 \\ \phi &= c'_y y_0 + s'_y \phi_0\end{aligned}\quad (2.24)$$

where

$$(\theta|x_0) = c'_x, \quad (\theta|\theta_0) = s'_x, \quad (\phi|y_0) = c'_y, \quad \text{and} \quad (\phi|\phi_0) = s'_y$$

It is useful to regard the equations as these which treat charged particle motion through a system of magnetic fields by the matrix multiplication. To describe the characteristics of such particles, any specified position of an arbitrary charged particle is represented by a single column matrix  $\mathbf{x}$ , whose components are the positions, angles, and momenta of the particle with respect to the ideal trajectory.

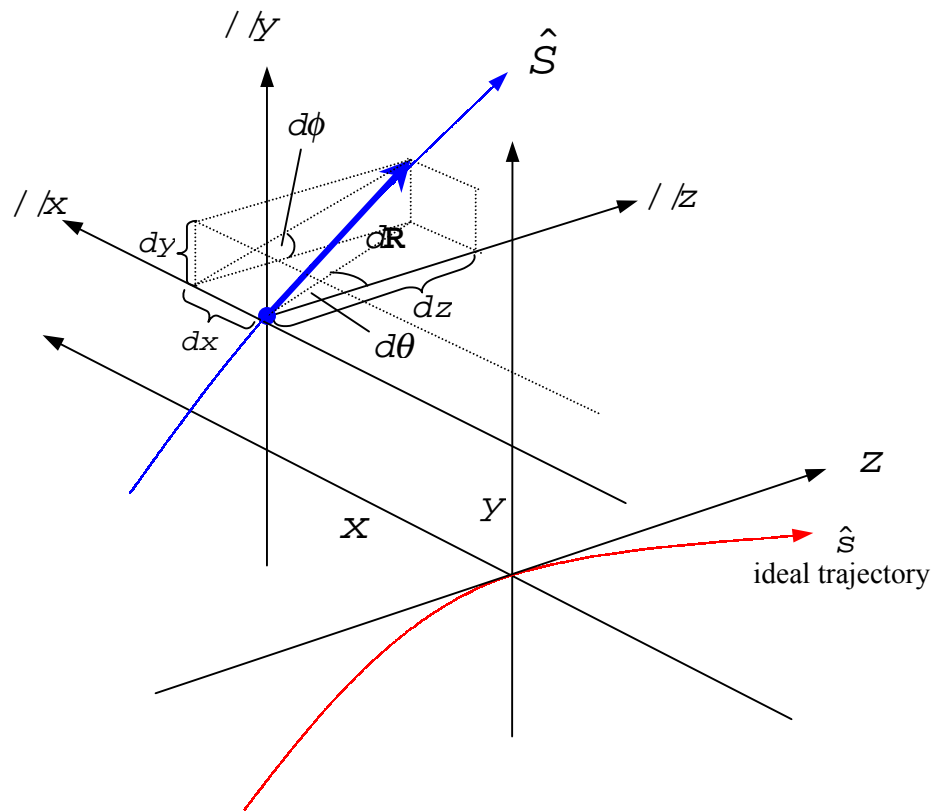


Fig.2.3 Rectangular coordinate system

$$\mathbf{x} = \begin{bmatrix} x \\ \theta \\ y \\ \phi \\ l \\ \delta \end{bmatrix} \quad (2.25)$$

Here the definitions are:

$x$ : The horizontal displacement of a beam with respect to the ideal trajectory.

$\theta$  : The angle that the beam makes in the horizontal plane with respect to the ideal trajectory.

$y$ : The vertical displacement of a beam with respect to the ideal trajectory.

$\phi$ : The angle that the beam makes in the vertical plane with respect to the ideal trajectory.

$l$ : The path length difference between the beam trajectory and the ideal trajectory.

$\delta = \frac{\Delta P}{P}$ : The fractional momentum deviation of the beam from the ideal trajectory.

The trace of the three-dimensional vectors  $(x, y, z)$  forming a part of vector, for a given particle, generates a beam. Suppose  $\mathbf{x}$  the initial coordinate vector is represented by  $\mathbf{x}(0)$ . It can be transformed to the final coordinate vector,  $\mathbf{x}$ , by the transfer matrix,  $R$ , namely:

$$\mathbf{x} = R\mathbf{x}(0) \quad (2.26)$$

The traversing of several magnets and interspersing drift spaces are described by the same basic equation (2.26), but with  $R$  now being replaced by the product matrix  $R = R(n) \dots R(3)R(2)R(1)$  of the individual matrices of  $n$  system elements. Using first-order Taylor's expansion, the beam transport matrix is expressed as:

$$\begin{bmatrix} x \\ \theta \\ y \\ \phi \\ l \\ \delta \end{bmatrix} = \begin{bmatrix} \langle x|x_0 \rangle & \langle x|\theta_0 \rangle & \langle x|y_0 \rangle & \langle x|\phi_0 \rangle & \langle x|l_0 \rangle & \langle x|\delta \rangle \\ \langle \theta|x_0 \rangle & \langle \theta|\theta_0 \rangle & \langle \theta|y_0 \rangle & \langle \theta|\phi_0 \rangle & \langle \theta|l_0 \rangle & \langle \theta|\delta \rangle \\ \langle y|x_0 \rangle & \langle y|\theta_0 \rangle & \langle y|y_0 \rangle & \langle y|\phi_0 \rangle & \langle y|l_0 \rangle & \langle y|\delta \rangle \\ \langle \phi|x_0 \rangle & \langle \phi|\theta_0 \rangle & \langle \phi|y_0 \rangle & \langle \phi|\phi_0 \rangle & \langle \phi|l_0 \rangle & \langle \phi|\delta \rangle \\ \langle l|x_0 \rangle & \langle l|\theta_0 \rangle & \langle l|y_0 \rangle & \langle l|\phi_0 \rangle & \langle l|l_0 \rangle & \langle l|\delta \rangle \\ \langle \delta|x_0 \rangle & \langle \delta|\theta_0 \rangle & \langle \delta|y_0 \rangle & \langle \delta|\phi_0 \rangle & \langle \delta|l_0 \rangle & \langle \delta|\delta \rangle \end{bmatrix} \begin{bmatrix} x_0 \\ \theta_0 \\ y_0 \\ \phi_0 \\ l_0 \\ \delta \end{bmatrix} \quad (2.27)$$

We may write equation (2.26) in the full form as:

$$\begin{bmatrix} x \\ \theta \\ y \\ \phi \\ l \\ \delta \end{bmatrix} = \begin{bmatrix} R_{11} & R_{12} & R_{13} & R_{14} & R_{15} & R_{16} \\ R_{21} & R_{22} & R_{23} & R_{24} & R_{25} & R_{26} \\ R_{31} & R_{32} & R_{33} & R_{34} & R_{35} & R_{36} \\ R_{41} & R_{42} & R_{43} & R_{44} & R_{45} & R_{46} \\ R_{51} & R_{52} & R_{53} & R_{54} & R_{55} & R_{56} \\ R_{61} & R_{62} & R_{63} & R_{64} & R_{65} & R_{66} \end{bmatrix} \begin{bmatrix} x_0 \\ \theta_0 \\ y_0 \\ \phi_0 \\ l_0 \\ \delta \end{bmatrix} \quad (2.28)$$

Comparing equation (2.27) with equation (2.23) we find that the following elements of the transfer matrix in equation (2.28) equal to zero, namely:

$$R_{13} = R_{14} = R_{23} = R_{24} = R_{31} = R_{32} = R_{41} = R_{42} = R_{36} = R_{46} = 0$$

These zero elements are direct consequences of the midplane symmetry. The elements in fifth column are also equal to zero, because the variables  $x, \theta, y, \phi$  and  $\delta$  are independent of the path length difference  $l$ , namely:

$$R_{15} = R_{25} = R_{35} = R_{45} = R_{65} = 0.$$

And, for the elements in the sixth column:

$$R_{61} = R_{62} = R_{63} = R_{64} = R_{65} = 0 ,$$

because we have restricted the problem to static magnetic fields, where the scalar momentum is a constant of motion. Expanding and retaining only the first-order terms of  $(dR)^2 = dx^2 + dy^2 + (1 + hx)^2 ds^2$  (see Appendix A) we obtain the first-order path length difference as:

$$l - l_0 = (S - s) = \int_0^s x(\tau) h(\tau) d\tau + \text{Higher order terms}$$

Just for the mathematical convenience, we use parameters  $\tau$  to express a point on  $s$  in the path integral formulae.

Using equations (2.16) and (2.17), we obtain:

$$l = l_0 + x_0 \int_0^s c_x(\tau) h(\tau) d\tau + \theta_0 \int_0^s s_x(\tau) h(\tau) d\tau + \delta \int_0^s \eta_x(\tau) h(\tau) d\tau \quad (2.29)$$

From equation (2.29) we may write:

$$l = l_0 - R_{51} x_0 - R_{52} \theta_0 - R_{56} \delta \quad (2.30)$$

where

$$\begin{aligned} R_{51} &= - \int_0^s c_x(\tau) h(\tau) d\tau \\ R_{52} &= - \int_0^s s_x(\tau) h(\tau) d\tau \\ R_{56} &= - \int_0^s \eta_x(\tau) h(\tau) d\tau \end{aligned} \quad (2.31)$$

Consider the case where both of the dispersion and its derivative are zero,  $\eta_x = 0, \eta'_x = 0$ . We define the system as *Achromaticity* (first-order) and the lattice is *Achromatic Lattice*. From equation (2.20) and (2.31) we find that  $R_{51} = R_{52} = 0$ . Substitute them into equation (2.30) we note that if a system is achromatic, all particles with the same momentum have equal path lengths through the system. If the path length of all particles is independent of their initial momenta,  $R_{51} = R_{52} = R_{56} = 0$ , the path length is the same through the system. We define this system as *Isochronous System*.

Let us find the elements given in (2.31) for the ideal orbit for which the curvature of ideal orbit,  $(h(s))$ , is constant. For positive  $k_x$ , we obtain:

$$R_{51} = - \frac{h}{k_x} \text{sink}_x s, R_{52} = - \frac{h}{k_x^2} [1 - \cos k_x s] R_{56} = - \frac{h^2}{k_x^3} [k_x s - \text{sink}_x s] \quad (2.32)$$

From Taylor's expansion, equations (2.23), (2.24) and (2.32) with zero elements we find that:

$$R_{11} = (x|x_0) = c_x = \cos k_x s$$

$$R_{12} = (x|\theta_0) = s_x = \frac{1}{k_x} \sin k_x s$$

$$R_{16} = (x|\delta) = \eta_x = \frac{h}{k_x^2} [1 - \cos k_x s]$$

$$R_{21} = (\theta|x_0) = c'_x = -k_x \sin k_x s$$

$$R_{22} = (\theta|\theta_0) = s'_x = \cos k_x s$$

$$R_{26} = (\theta|\delta) = \eta'_x = \frac{h}{k_x} \sin k_x s$$

$$R_{33} = (y|y_0) = c_y = \cos k_y s$$

$$R_{34} = (y|\phi_0) = s_y = \frac{1}{k_y} \sin k_y s$$

$$R_{43} = (\phi|\phi_0) = c'_y = -k_y \sin k_y s$$

$$R_{51} = (l|x_0) = -\frac{h}{k_x} \sin k_x s$$

$$R_{52} = (l|\theta_0) = -\frac{h}{k_x^2} [1 - \cos k_x s]$$

$$R_{55} = (l|l) = 1$$

$$R_{56} = (l|\delta) = -\frac{h^2}{k_x^3} [k_x s - \sin k_x s]$$

$$R_{66} = (\delta|\delta) = 1$$

The other elements equal to zero.

From the results described above we conclude that the first-order matrix for the ideal magnets with path length  $L$ , as follow:

The transfer matrix for the general ideal magnet,  $M$  :

$$M(L/0) = \begin{bmatrix} \cos k_x L & \frac{1}{k_x} \sin k_x L & 0 & 0 & 0 & \frac{h}{k_x^2} (1 - \cos k_x L) \\ -k_x \sin k_x L & \cos k_x L & 0 & 0 & 0 & \frac{h}{k_x} \sin k_x L \\ 0 & 0 & \cos k_y L & \frac{1}{k_y} \sin k_y L & 0 & 0 \\ 0 & 0 & -k_y \sin k_y L & \cos k_y L & 0 & 0 \\ -\frac{h}{k_x} \sin k_x L & -\frac{h}{k_x^2} (1 - \cos k_x L) & 0 & 0 & 1 & -\frac{h^2}{k_x^3} (k_x L - \sin k_x L) \\ 0 & 0 & 0 & 0 & 0 & 1 \end{bmatrix} \quad (2.33)$$

where  $h : \frac{1}{\rho_0}, k_x^2 : (1-n)h^2, k_y^2 : nh^2$

$n$  : Dimensionless quantity defined by

$$n = - \left[ \frac{1}{hB_y} \left( \frac{\partial B_y}{\partial x} \right) \right]_{x=0, y=0}$$

$L$  : The field length of the bending magnet along the trajectory

For a pure quadrupole magnet, the matrix is evaluated by taking the limiting case  $h \rightarrow 0$  and letting: (see equation (2.15))

$$k_x^2 = k_q^2 \quad k_y^2 = -k_q^2$$

we obtain the first-order transfer matrix,  $M_q$ , as:

$$M_q(L/0) = \begin{bmatrix} \cos k_q L & \frac{1}{k_q} \sin k_q L & 0 & 0 & 0 & 0 \\ -k_q \sin k_q L & \cos k_q L & 0 & 0 & 0 & 0 \\ 0 & 0 & \cosh k_q L & \frac{1}{k_y} \sinh k_q L & 0 & 0 \\ 0 & 0 & -k_q \sinh k_q L & \cosh k_q L & 0 & 0 \\ 0 & 0 & 0 & 0 & 1 & 0 \\ 0 & 0 & 0 & 0 & 0 & 1 \end{bmatrix} \quad (2.34)$$

where  $k_q^2 : \left( \frac{B_0}{a} \right) \left( \frac{1}{B\rho_0} \right)$

$B\rho_0$  : The magnetic rigidity of the central trajectory.

$a$  : The radius of the aperture.

$B_0$  : Field which is positive for focusing in the horizontal direction ( $x$ ) and negative for defocusing in the vertical direction ( $y$ ).

$L$  : The effective field length of the quadrupole magnet.

In case of drift space,  $k_x = k_y = 0$ . Using equation (C.7) and the initial boundary conditions (C.8) in Appendix C, we obtain the first-order transfer matrix for drift space,  $M_{drift}$  as:

$$M_{drif}(L/0) = \begin{bmatrix} 0 & L & 0 & 0 & 0 & 0 \\ 0 & 0 & 0 & 0 & 0 & 0 \\ 0 & 0 & 0 & L & 0 & 0 \\ 0 & 0 & 0 & 0 & 0 & 0 \\ 0 & 0 & 0 & 0 & 1 & 0 \\ 0 & 0 & 0 & 0 & 0 & 1 \end{bmatrix} \quad (2.35)$$

where  $L$  : The length of the drift space

For the first-order transfer matrices for the fringing fields at both entrance and exit faces of bending magnets, we use impulse approximation. In this thesis such matrices are presented without derivation as a function of two new variables. They are the angle of inclination  $\beta_1$  of the entrance face, the angle of inclination  $\beta_2$  of the exit face, see Fig.2.4:

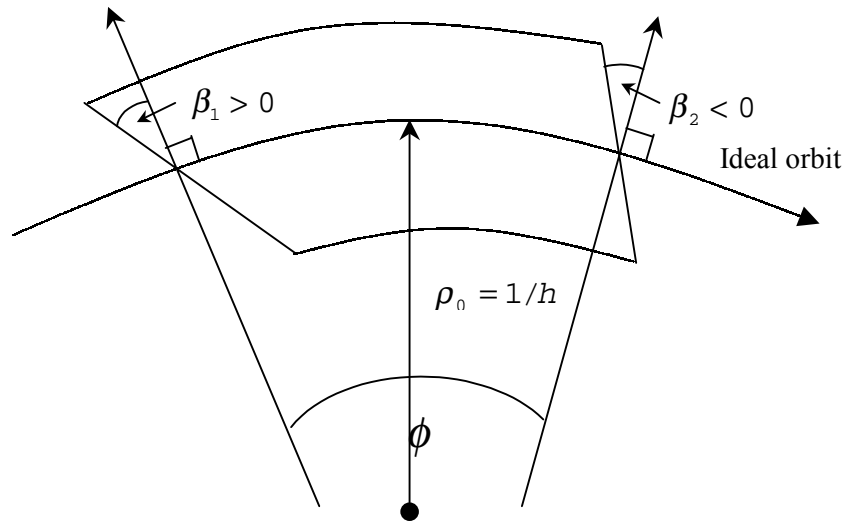


**Fig. 2.4** Field boundary for bending magnets

If the finite focusing terms of the fringing field is not included, the first-order transfer matrix for the fringing fields of the entrance face of bending magnet is expressed by:

$$\begin{bmatrix} 1 & 0 & 0 & 0 & 0 & 0 \\ h \tan \beta_{1,2} & 1 & 0 & 0 & 0 & 0 \\ 0 & 0 & 1 & 0 & 0 & 0 \\ 0 & 0 & -h \tan \beta_{1,2} & 1 & 0 & 0 \\ 0 & 0 & 0 & 0 & 1 & 0 \\ 0 & 0 & 0 & 0 & 0 & 1 \end{bmatrix} \quad (2.36)$$



## 2.2 The Betatron Oscillation

### 2.2.1 Betatron Functions

We have already studied the beam transport system in the forms of multiplication of transfer matrices. Although the transfer matrices are convenient, especially for computations on computer, They do not reveal characteristic properties of the particle trajectories. To deeper insight, the betatron functions are used and the motions are expressed by the Courant-Snyder invariant and Twiss parameters. Now, we start to solve the equation of motion analytically. The homogeneous differential equation of motion is:

$$u'' + k(s)u = 0 \quad (2.37)$$

where  $u$  stands for  $x$  or  $y$  and  $k(s)$  stands for  $k_x$  or  $k_y$ ,  $k(s)$  arises the results from the magnetic focusing as an arbitrary function of  $s$ . All constants and variables appearing here stand for their  $x$  or  $y$  components. The general solution of equation (2.37) is simply expressed by:

$$u(s) = \sqrt{\varepsilon\beta(s)} \cos[\psi(s) - \psi_0] \quad (2.38)$$

where the quantities  $\varepsilon$  and  $\psi_0$  are integration constants. The function amplitude  $\beta(s)$  is a function of the path length  $s$  and the *phase function*  $\psi(s)$  is given as (see Appendix D for details):

$$\psi(s) = \int_0^s \frac{d\tau}{\beta(\tau)} + \psi_0 \quad (2.39)$$

Since the phase function must satisfy the periodic boundary conditions, we can write:

$$\psi(s_2 + L) - \psi(s_1) = \Phi \quad (2.40)$$

where  $L = s_2 - s_1$ . The *betatron phase advance* is given as:

$$\Phi = \int_0^L \frac{ds}{\beta(s)} \quad (2.41)$$

We note that the amplitude function  $\beta(s)$  is also the local wave number of betatron oscillations. The betatron solution may be expressed in the form of the *Courant-Snyder invariant*  $C(u, u')$  (see Appendix D):

$$C(u, u') = \varepsilon = \gamma u^2 + 2\alpha uu' + \beta u'^2 \quad (2.42)$$

where

$$\begin{aligned}\alpha &= -\frac{1}{2}\beta' \\ \gamma &= \frac{(1+\alpha^2)}{\beta}\end{aligned}\tag{2.43}$$

The Courant-Snyder invariant is the function of *twice the action*. It is independent of  $s$  and has the form of the equation of an ellipse. The area of phase space enclosed by  $(u, u')$  of equation (2.42) is equaled to  $\pi\varepsilon$ . The constant  $\varepsilon$  is called the *beam emittance*. Sometimes the product  $\pi\varepsilon$  is also called the beam emittance. The ellipse parameters  $\beta, \alpha$  and  $\gamma$  are called the *Twiss parameters*. Particularly,  $\beta$  is called the *betatron function* or *beta function*.

### 2.2.2 Phase Ellipse

The Twiss parameters  $\beta, \alpha$  and  $\gamma$  are dependent on  $t$ . As a charged particle move always its trajectory in the real space, point  $(u, u')$  in the phase space move along the contour of an ellipse. Figure 2.5 shows the ellipse given by the Courant-Snyder invariant for a beam emittance  $\varepsilon$ . Sometimes, this ellipse is called the phase ellipse.

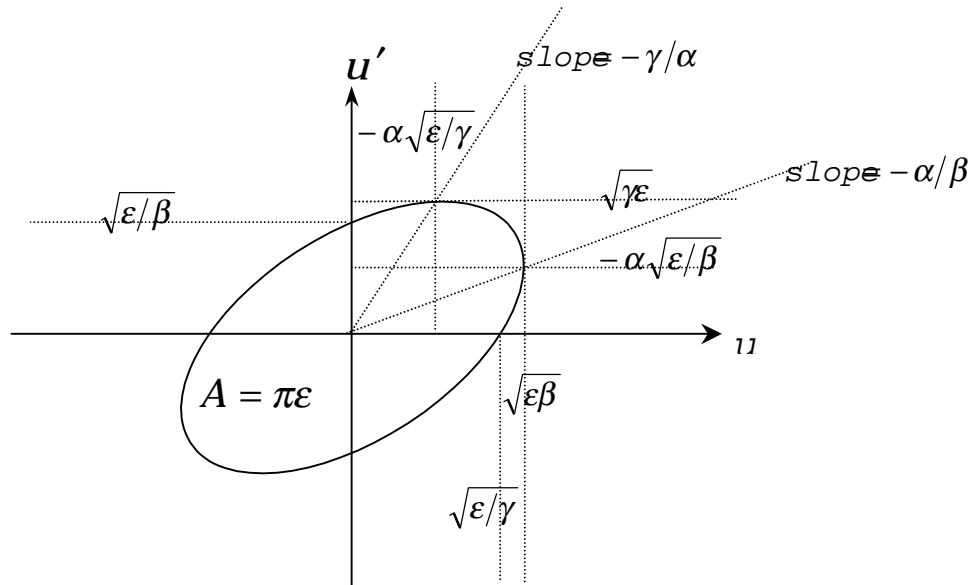


**Fig. 2.5** The Phase ellipse due to the Courant-Snyder invariant.  $\varepsilon$  is the beam emittance,  $\beta, \alpha$  and  $\gamma$  are the Twiss parameters.  $\beta' > 0$  is assumed.

The rms beam width is  $\sqrt{\varepsilon\beta(s)}$  and the rms beam divergence  $u'$  is  $\sqrt{\varepsilon\gamma(s)}$ . Since  $\gamma = (1+\alpha^2)/\beta$ , the rms beam divergence is smaller at the location with a large  $\beta$  value. The form of the ellipse changes constantly depending on the

focusing properties at particular point on  $s$ . However, the area surrounded the phase space ellipse is not changed and equal to  $\pi\varepsilon$ . This leads owing to Liouville's theorem:  $u \cdot u'$  is constant independent of  $s$  (see Liouville's theorem, H. Wiedemann, Particle Accelerator Physics Vol. 1, (1993)).

So far we know that any particle starting on the phase ellipse will stay on it. Now, we want to be able to describe how the phase ellipse transforms along the beam trajectories. We consider the Courant-Snyder invariant at the starting point  $s=0$ , equation (2.42) becomes:

$$\gamma_0 u_0^2 + 2\alpha_0 u_0 u'_0 + \beta u_0'^2 = \varepsilon \quad (2.44)$$

Using the transformation, the solution of the homogeneous equation of motion are:

$$\begin{aligned} u_i &= c_i u_0 + s_i u'_0 \\ u'_i &= c'_i u_0 + s'_i u'_0 \end{aligned} \quad (2.45)$$

where the subscript  $i$  stands for  $x$  and  $y$ . Insert (2.45) into (2.44) then compare the coefficients of  $u^2, u'^2$  and  $uu'$  with those of equation (2.42) we may write the results in the form of the ellipse transfer matrix (see also H. Wiedemann, (1993)) as:

$$\begin{bmatrix} \beta \\ \alpha \\ \gamma \end{bmatrix} = \begin{bmatrix} c_i^2 & -2c_i s_i & s_i^2 \\ -c_i c'_i & (s'_i c_i + s_i c'_i) & -s_i s'_i \\ c_i'^2 & -2s'_i c'_i & s_i'^2 \end{bmatrix} \begin{bmatrix} \beta_0 \\ \alpha_0 \\ \gamma_0 \end{bmatrix} \quad (2.46)$$

Parameters  $\beta, \alpha$  and  $\gamma$  are called the *Twiss parameters*. Consider the simplest case, for example, the phase ellipse in the drift space of length  $s$ , equation (2.46) becomes:

$$\begin{bmatrix} \beta \\ \alpha \\ \gamma \end{bmatrix} = \begin{bmatrix} 1 & -2s & s^2 \\ 0 & 1 & s \\ 0 & 0 & 1 \end{bmatrix} \begin{bmatrix} \beta_0 \\ \alpha_0 \\ \gamma_0 \end{bmatrix} \quad (2.47)$$

In equation (2.47), the parameter  $\gamma = \gamma_0$  is constant, i.e., the beam divergence,  $\sqrt{\varepsilon\gamma}$ , stays constant. This is obvious, since no force acts on the charged particles and they make constant linear motions. The parameters  $\alpha = \alpha_0 - \gamma_0 s$  and  $\beta = \beta_0 - 2s\alpha_0 + s^2\gamma_0$  are changed when the observation point  $s$  changes. Since we describe the transverse motion of a particle with equation (2.38), the amplitude function  $\sqrt{\varepsilon\beta(s)}$  and the phase function  $\psi(s)$  must changes so that

equation (2.38) expresses the constant linear motion. The phase ellipses are those shown in Fig. 2.6:

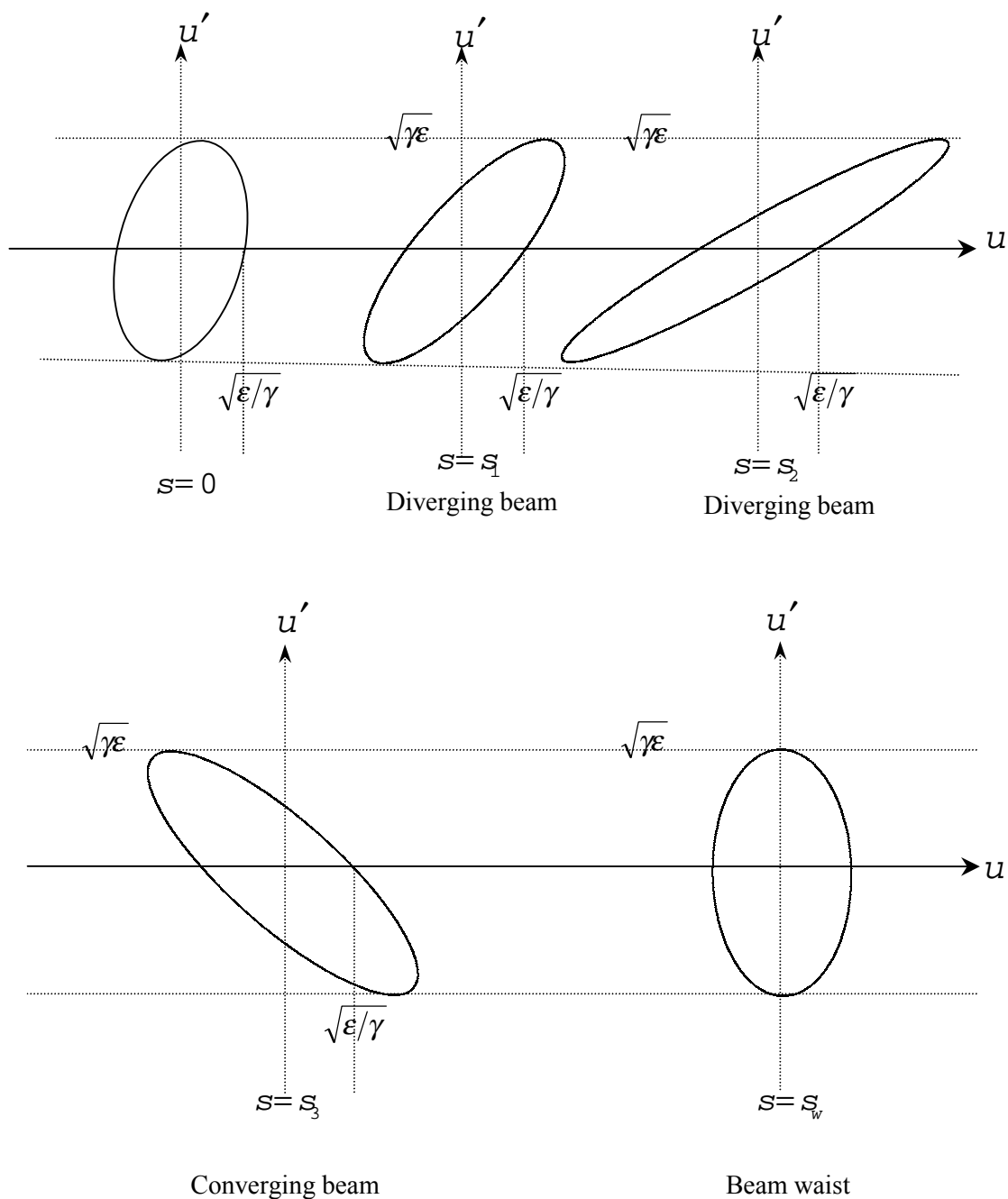


**Fig. 2.6** Transformation of a phase ellipse along drift space at different locations. (Wiedemann, H. 1993)

For obtaining the result shown in Fig.2.6 we assume  $\alpha_0 \neq 0$  at a location  $s=0$ . The orientation of the phase ellipse immediately tells us the characteristics of particles behavior. The divergent beam is such that  $u' > 0$  for  $u > 0$  or  $u' < 0$  for  $u < 0$ . On the other hand, the convergent beam has signs of

$u$  and  $u'$  as  $u' > 0$  for  $u < 0$  or  $u' < 0$  for  $u > 0$ . In Fig.2.6, the majority of  $(u, u')$  points satisfies the condition of divergence for  $s = s_1$  and  $s_2$ . Similarly the majority of point  $(u, u')$  satisfies the condition of the convergence for  $s = s_3$ . Suppose the minimum beam signed occurs at  $s = s_w$ . We assume that the betatron function takes the minimum value at the point where the beam size is minimum. Since  $\beta(s)$  and  $\alpha(s)$  are given as

$$\begin{aligned}\beta(s) &= \beta_0 - 2s\alpha_0 + s^2\gamma_0 \\ &= \gamma_0 \left( s - \frac{\alpha_0}{\gamma_0} \right)^2 + \left( \beta_0 - \frac{\alpha_0^2}{\gamma_0} \right)\end{aligned}$$

and

$$\alpha(s) = \alpha_0 - \gamma_0 s,$$

$\beta(s)$  is minimum for:

$$s_w = \frac{\alpha_0}{\gamma_0} \quad (2.48)$$

At  $s_w$ ,  $\alpha(s_w) = 0$ . So far, we did not take the phase function  $\psi(s)$  into account explicitly. Thus, that the occurrence of the beam waist at  $s_w$  in the drift space holds only approximately.

We transform the equation of motion by letting  $w(\varphi) = u(s)/\sqrt{\beta(s)}$  where the phase is defined as:

$$\varphi(s) = \frac{\psi}{\nu} = \frac{1}{\nu} \int_0^s \frac{d\tau}{\beta(\tau)} \quad (2.49)$$

where  $\nu$  is the constant which is called betatron tune. This shall be discussed in next section. The form of the equation of motion becomes (see Appendix D for detail):

$$\frac{d^2 w}{d\varphi^2} + \nu^2 w = 0 \quad (2.50)$$

These coordinates  $(w, \varphi)$ , are called the *normalized coordinates*. Obviously, the linear betatron motion is a simple harmonic motion with the frequency  $\nu$  which is called *betatron oscillations*.

### 2.2.3 Betatron Tune or Betatron Wave Number; $\nu_x, \nu_y$

We consider the phase  $\varphi$  in equation (2.49) for a full turn around a circular accelerator of the circumference  $L$ . For the full turn  $\varphi = 2\pi$  obviously. Then, the quantity  $\nu$  become:

$$v = \frac{1}{2\pi} \int_s^{s+L} \frac{d\tau}{\beta(\tau)} \quad (2.51)$$

The quantity  $v$  stands for the transverse  $v_x$ , and the vertical  $v_y$ . These are called *betatron tune wave numbers* or the *operating points* of the circular accelerator. We note that the betatron tunes are equal to the number of oscillations per revolution.

## 2.3 Beam Parameters

### 2.3.1 Momentum Compaction Factor $\alpha_c$

The first-order solutions for  $x$  in equation (2.12) can be written as the sum of two parts:

$$x = x_\beta + x_E \quad (2.52)$$

The solution of equation (2.12) is not periodic although  $nh^2$  is a periodic function. In equation (2.52), we take the solution  $x_\beta$  to be non-periodic and  $x_E$  periodic. For a solution of the form shown in equation (2.16),  $x_\beta = c_x x + s_x x'$  is the betatron displacement and  $x_E$  is a displacement which depends only on the energy of the particle. In this section we focus only on the energy displacement:

$$x_E = \eta_x(s) \delta = \eta_x(s) \frac{\Delta E}{E_0} \quad (2.53)$$

where  $\eta_x(s)$  is the dispersion function which is shown in section 2.1.4. Now we wish to study various quantities and some effects caused by deviations. So, an important consequence of the energy deviation is the associated change in the circumference of the closed orbit.

An electron of the nominal energy  $E_0$  circulates around the ideal orbit in one revolution for distance  $L_0$ , the circumference of the ideal orbit. For any other trajectory the path length is expressed by:

$$\begin{aligned} L &= \int_0^{L_0} dS = \int_0^{L_0} \sqrt{dx^2 + dy^2 + (1+hx)^2 ds^2} \\ &= L_0 + \int_0^{L_0} hxdst \dots \end{aligned} \quad (2.54)$$

We are only interested in the first-order terms. From the solution according to equation (2.52), equation (2.54) becomes:

$$L = L_0 + \int_0^{L_0} h x_{\beta} ds + \int_0^{L_0} h \eta_x \delta ds .$$

Because of the oscillatory character of the betatron motion  $\int_0^{L_0} h x_{\beta} ds = 0$ . If higher-order terms associated with betatron motion are neglected, we obtain:

$$\Delta L = L - L_0 = \delta \int_0^{L_0} h \eta_x ds \quad (2.55)$$

We note that the change of the circumference depends on the dispersion function  $\eta_x$ , which is normally positive, i.e., the total path length  $L$  for a higher momentum particle is longer than the ideal path length  $L_0$ . Since the dispersion is generated by the dipole magnet (bending magnet), the strong change of the circumference is dependent on a dipole field error. From equation (2.55) we obtain:

$$\begin{aligned} \frac{\Delta L}{L_0 \delta} &= \frac{1}{L_0} \int_0^{L_0} h \eta_x ds \\ \frac{\Delta L / L_0}{\Delta P / P_0} &= \langle h \eta_x \rangle = \alpha_c \\ \alpha_c &= \langle h \eta_x \rangle = \frac{1}{L_0} \oint \frac{\eta_x}{\rho} ds \end{aligned} \quad (2.56)$$

The *momentum compaction factor*  $\alpha_c$  depends on the average dispersion function. If the particle momentum is larger or smaller than that of the particle on the ideal orbit,  $\alpha_c$  is positive this means according to that  $L$  is longer or shorter than  $L_0$ . This arises from  $\alpha_c$  increases only in curved sections where  $\rho$  is finite. As a consequence,  $\alpha_c = 0$  means that the trajectory is a straight line and the length does not depend on the momentum.

In an isomagnetic field, the same radius of curvature of the orbit is equal along the orbit. The characteristic of  $h$  is as follows:

$$h(t) = \begin{cases} h_0 = 1/\rho_0, & \text{in magnets} \\ 0, & \text{elsewhere} \end{cases} \quad (\text{isomag}) \quad (2.57)$$

Equation (2.56) becomes:

$$\alpha_c = \frac{h_0}{L_0} \oint \eta_x ds \quad (\text{isomag}) \quad (2.58)$$

### 2.3.2 Closed Orbit

In a storage ring, each successive trajectory of an electron making the betatron and synchrotron oscillations is not completely closed. As we mentioned already concerning equation (2.52),  $x$  is non-periodic. Thus, the electron starting at a point in a storage ring does not return to the start point after one turn. In addition to this, there is additional reason of the non-periodic nature of  $x$ , if we discuss the phenomenon more rigorously. The emission of photons giving rise to excitations and damping of electron oscillations occurs randomly and the total process of the radiation damping is stochastic. This causes the energy spread of the electron beam mentioned below. However, the bundle of the trajectories oscillating transversely betatron oscillation and forming the electron beam as a result of a many turns makes a close beam with a finite cross-sectional size simply called the beam size. The trace of the center of the beam cross section forms an orbit closed completely. This average orbit is called the *closed orbit*. The location of the closed orbit differs if the average electron energy is different. Since the electron beam energy is decided by the balance of the radiation energy loss and its restoration by the RF acceleration, the closed orbit is often referred to as the equilibrium orbit. Although the betatron and synchrotron oscillations are nominally caused by restoring force acting toward the ideal orbit, the closed orbit is different from the ideal orbit and shifted from it. This is not only caused by the beam energy difference but by various errors existing in the storage ring, such as magnet misalignment, the field strength error, fringing field, the structure error of the RF cavity, the error in the RF frequency, the scattering of electrons by molecules in the residual, etc. The ideal orbit in a storage ring with drift spaces is often called the *designed orbit*. The phenomenon that the closed orbit is shifted from the designed orbit is called the *closed orbit distortion (COD)*. Obviously, the closed orbit distortion does not occur uniformly along the designed orbit. Thus, the location of the closed orbit must be measured precisely and correction of the closed orbit must be made. This is implemented by adjusting the magnetic field strengths and the RF frequency. The misalignment of magnet locations must be corrected in some case. Such correction of the closed orbit distortion is usually called the COD correction.

### 2.3.3 Transition Energy $\gamma_T$

Consider the revolution period of a particle in individual trajectory. Then, we have  $T = L/v$ , where  $L$  is the orbit length and  $v$  is the velocity of the particle. The fractional change of the revolution period is:

$$\begin{aligned} \frac{\Delta T}{T} &= \frac{\Delta L}{L} - \frac{\Delta v}{v} \\ &= \left( \frac{\Delta L/L}{\Delta P/P} - \frac{\Delta v/v}{\Delta P/P} \right) \frac{\Delta P}{P} \end{aligned}$$



Using the simple relation  $P = m\gamma v$ , where  $\gamma = 1/\sqrt{1-v^2/c^2}$ , and equation (2.56), we obtain:

$$\frac{\Delta T}{T} = (\alpha_c - \frac{1}{\gamma^2})\delta = \eta\delta \quad (2.59)$$

Where the *phase-slip factor*  $\eta$  is:

$$\mu = \alpha_c - \frac{1}{\gamma^2} \quad (2.60)$$

The more important case is that the phase-slip  $\mu = 0$ . We obtain:

$$\gamma_T = \sqrt{1/\alpha_c} \quad (2.61)$$

where  $\gamma_T$  is called *transition energy*. On the other hand, we write equation (2.60) in the form of:

$$\mu = \frac{1}{\gamma_T^2} - \frac{1}{\gamma^2} \quad (2.62)$$

If the phase-slip is zero, the revolution period is independent of the particle momentum (see equation (2.59)). All particles at different momentum travel rigidly around the orbit with equal revolution frequencies. This is the isochronous condition. For  $\gamma < \gamma_T$ ,  $\mu < 0$ , the revolution period is shorter than a synchronous particle for a higher momentum particle. Although a higher energy particle has the orbit length  $L$  longer than an synchronous particle  $L_0$ , in this case it travels faster, its speed exceeds the effect of its longer orbit length. Thus, the higher energy particle will arrive at a fixed location earlier than an synchronous particle. Another case is  $\gamma > \gamma_T$  the converse is true.

### 2.3.4 Energy Loss per Turn $U_0$

The energy loss per turn due to synchrotron radiation is expressed by (see Appendix E, (E.70) for details):

$$U_0 = \frac{C_\gamma E_0^4}{2\pi} I_2 \quad (2.63)$$

where  $C_\gamma = 8.85 \times 10^{-5} \text{ m / GeV}^3$  and  $I_2$  is radiation integral defined by equation (E.64) in Appendix E. For isomagnetic ring, the bending radius the same for all bending magnets  $\rho = \rho_0$ , the energy loss per turn is:

$$U_0 = \frac{C_\gamma E_0^4}{\rho_0} \quad (\text{isomorph}) \quad (2.64)$$

### 2.3.5 Damping Partition Numbers $J_x, J_y, J_E$

Higher energy electrons lose more energy into synchrotron radiation than lower energy electrons (see equation 2.63). This lost energy is compensated by longitudinal electric field of the RF cavity. The energy loss into synchrotron radiation causes the radiation damping of the beam oscillation to occur in longitudinal phase space with the damping coefficient  $\alpha_E$ . This oscillation damping is understandable, because the loss of the beam energy results in the shrinkage of the orbit. The energy gain from RF cavity occurs in the way that the acceleration toward longitudinal direction is enhanced. This causes the damping in the transverse direction. The damping coefficients are designated as  $\alpha_x$  for the horizontal damping and  $\alpha_y$  for the vertical damping. These damping coefficients for the betatron and *synchrotron oscillations* (see Appendix E, (E.22)) can be expressed by the three degrees of freedom in a bunch, namely:

$$\alpha_i = J_i \alpha_0 = J_i \frac{\langle P_\gamma \rangle}{2E_0} \quad (2.65)$$

where  $i$  stands for  $x, y$  and  $E$ .  $\alpha_0 = \langle P_\gamma \rangle / 2E_0$ . The **damping partition numbers** are:

$$J_x = (1 - D), \quad J_y = 1, \quad J_E = 2 + D \quad (2.66)$$

or

$$J_x = 1 - \frac{I_4}{I_2}, \quad J_y = 1, \quad J_E = 2 + \frac{I_4}{I_2} \quad (2.67)$$

where  $I_2, I_4$  are defined by equations (E.64) and (E.66) and  $D$  is defined by equation (E.33) in Appendix E. Specifically consider a strong focusing gradient,  $k > 0$ , with beam deflection,  $\rho \neq 0$ . For  $D = 1$  all damping in horizontal plane is lost and turn to excitation for  $D > 1$ . However, the beam is still stable owing to adiabatic damping. Conversely, strong defocusing, vertical focusing,  $k < 0$ , that is  $D < 1$ , the horizontal damping increases actually. There is a limit for the stability of synchrotron oscillations for  $D = 2$ . These damping partition numbers satisfy the Robinson's damping theorem:

$$\sum J_i = J_x + J_y + J_E = 4 \quad (2.68)$$

This indicates that no vertical bend occurs, since  $J_x + J_E = 3$ ,  $J_x \leq 3$ . In practice, the maximum tolerable value is  $J_x \leq 2$ , which we note that the synchrotron oscillation damping is twice as strong as the transverse damping.

### 2.3.6 Damping Times $\tau_x, \tau_y, \tau_E$

Damping time constants are expressed as (see Appendix E, E.62):

$$\begin{aligned}\tau_x &= \frac{2E_0}{J_x \langle P_\gamma \rangle} = \frac{4\pi}{C_\gamma} \frac{R\rho_0}{J_x E_0^3} = \frac{2E_0}{J_x U_0} T_0 \\ \tau_y &= \frac{2E_0}{J_y \langle P_\gamma \rangle} = \frac{4\pi}{C_\gamma} \frac{R\rho_0}{J_y E_0^3} = \frac{2E_0}{J_y U_0} T_0 \\ \tau_E &= \frac{2E_0}{J_E \langle P_\gamma \rangle} = \frac{4\pi}{C_\gamma} \frac{R\rho_0}{J_E E_0^3} = \frac{2E_0}{J_E U_0} T_0\end{aligned}\quad (2.69)$$

We note that for the isomagnetic field the damping time is inversely proportional to the cube of the power of energy. For a fixed  $B$ , it is inversely proportional to the square of the energy (see equation E.2 in Appendix E).

### 2.3.7 Energy Spread $\sigma_E$

So far, we have only considered the total energy loss due to synchrotron radiation. But electromagnetic radiation occurs in quanta of discrete energies, photon emission. When a photon is emitted, the electron energy makes a small discontinuous jump. The energy of electron is suddenly decreased by an amount  $\hbar\omega$ . Emission of many photons causes a changes in the electron energy leading to the spread energy within the beam. The relative energy spread  $\sigma_E/E_0$  is expressed by (see Appendix E, (E.82), for details):

$$\left(\frac{\sigma_E}{E_0}\right)^2 = C_q \frac{\gamma^2}{J_E \langle 1/\rho^2 \rangle} \langle 1/\rho^3 \rangle \quad (2.70)$$

or

$$\left(\frac{\sigma_E}{E_0}\right)^2 = C_q \gamma^2 \frac{I_3}{(2I_2 + I_4)} \quad (2.71)$$

where  $I_3$  is defined by equation (E.65) in Appendix E;  $C_q = 3.84 \times 10^{-13} \text{ m e t e}$ . is called the *quantum constant*. We note that the energy spread is independent of the RF voltage.

### 2.3.8 Bunch Length $\sigma_z$

Electron in a synchrotron and a storage ring is bunched. The bunching is brought about the RF acceleration. Electrons reading the RF cavity when voltage across the electrodes is toward the acceleration mode cannot pass through it. More precisely, only electrons making stable synchrotron oscillations can pass the RF electrode. The acceleration voltage range that traps electrons in the stable synchrotron oscillations is called the bucket existing in the accelerator is equal to the harmonic number mentioned later. The bunch length is expressed by (see Appendix E, (E.129), for details):

$$\sigma_z = 2c\gamma \sqrt{C_q \frac{\alpha_c T_0 E_0}{e\dot{V}} \frac{I_3}{(2I_2 + I_4)}} \quad (2.72)$$

where  $\dot{V}$  is the slope of RF voltage,  $C_q$  is equal to  $3.84 \times 10^{-13} \text{met}e$  and  $I_i$  is radiation integral. We note that the bunch length can be varied by varying the RF voltage and  $\sigma_z \propto 1/\sqrt{\dot{V}}$ . The bunch length is shorter for higher RF voltage; the resulting phase-space area is smaller for lower RF voltage the phase-space area is larger.

### 2.3.9 Beam Size $\sigma_x, \sigma_y$

The beam size or the distribution of the positions of electrons in the storage ring is determined by the damping effect due to synchrotron radiation. and the quantum excitation effect due to the photon emission. Since the damping effect causing by the quantum excitation a stochastic or random process, it leads to electron in equilibrium where the distribution of well approximated by the beam is Gaussian form in six degrees of freedom,  $x, x', y, y', z, \delta$ .  $z$  is longitudinal displacement from center of the bunch. The beam size or beam width in horizontal direction is expressed as (see also Appendix E for details):

$$\sigma_x^2 = C_q \gamma^2 \left( \frac{\beta_x \langle H(s) / \rho^3 \rangle}{J_x \langle 1/\rho^2 \rangle} + \eta_x^2 \frac{\langle 1/\rho^3 \rangle}{J_E \langle 1/\rho^2 \rangle} \right) \quad (2.73)$$

For an isomagnetic ring is:

$$\sigma_x^2 = \frac{C_q \gamma_0^2}{\rho_0} \left( \frac{\beta_x \langle H(s) \rangle_{isomag}}{J_x} + \frac{\eta_x^2(s)}{J_E} \right), \quad (isomag) \quad (2.74)$$

where  $H(s)$  is defined by equation (E.89) in Appendix E. The vertical beam size is expressed as (see Appendix E):

$$\sigma_y^2 \approx C_q \frac{\langle \beta_y^2 / \rho^3 \rangle}{J_y \langle 1 / \rho^2 \rangle} \quad (2.75)$$

For flat designed orbit,  $J_y$  is roughly equal to 1. For an isomagnetic ring, the vertical beam size may be written as:

$$\sigma_y^2 \approx C_q \frac{\langle \beta_y^2 \rangle}{\rho_0}, \quad (\text{isomag}) \quad (2.76)$$

where  $\langle . \rangle$  is the average over one revolution of the betatron oscillations.

### 2.3.10 Natural Emittance $\epsilon_x^0$

In section 2.2 we have already discussed the basic of the beam emittance. The emittance determines the beam size along with the betatron function: For the horizontal emittance:

$$\sigma_x = \sqrt{\epsilon_x \beta_x} \quad (2.77)$$

and for the vertical emittance:

$$\sigma_y = \sqrt{\epsilon_y \beta_y} \quad (2.78)$$

Natural rms emittance  $\epsilon_x^0$  is defined as (see equation (E.100) in Appendix E):

$$\epsilon_x^0 = \frac{\sigma_{x\beta}^2}{\beta_x} = C_q \gamma^2 \frac{\langle H(s) / \rho^3 \rangle}{J_x \langle 1 / \rho^2 \rangle} \quad (2.79)$$

For an isomagnetic ring:

$$\epsilon_x^0 = C_q \gamma_0^2 \frac{\langle H(s) \rangle_{\text{isomag}}}{J_x \rho_0}, \quad (\text{isomag}) \quad (2.80)$$

### 2.3.11 Chromaticity, $\xi_x, \xi_y$

So far, we have not taken any structural and other error into account. However, errors do exist in practice. For a storage ring, we will consider a first-order error arising from the deviation of electron energies from the ideal designed energy. The focusing (or defocusing) power of a quadrupole magnet is inversely proportional to the electron energy and causes the focal length of the

quadrupole magnet,  $f$ , to vary (see Fig.2.7). The Fig.2.7 shows that the focal length is shorter or longer when the energy of the electron is smaller or longer than the energy of the synchronous electron, respectively. This effect is called *chromatic effect*. It leads to the dependence of the tunes on energy. The dependence is different in the horizontal and vertical direction. In order to indicate the chromatic effect quantitatively, we define the quantity called the *chromaticity* as:

$$\xi_x = \frac{\Delta\nu_x}{\Delta E/E_0}, \quad \xi_y = \frac{\Delta\nu_y}{\Delta E/E_0} \quad (2.81)$$

where  $\Delta\nu_{x,y}$  are the shifts of tune from those of the synchronous electrons.

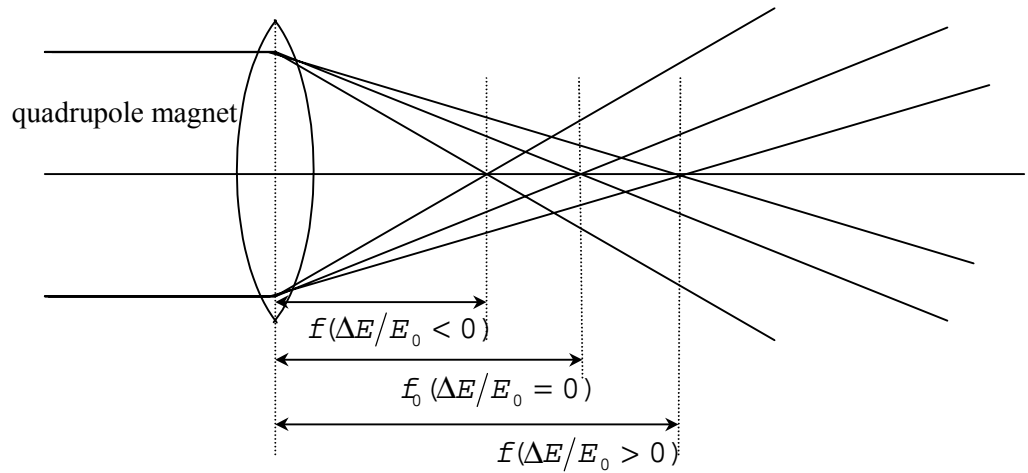


**Fig. 2.7** Chromatic focusing errors

Because the focusing action decreases with increasing energy, the tune decreases with increasing energy. Thus, the uncorrected chromaticities are negative numbers. Equation (2.81) implies that the spread in energy corresponds to the spread of tune within an electron beam. To correct the chromaticities, sextupole magnets are used. The nonlinear field of the sextupole magnet is utilized for the chromaticity correction. Most accelerators operate with zero or slightly positive chromaticities.

### 2.3.12 Harmonic Number $k$

The synchronous RF phase angle is presented in equation (E.18) in Appendix E. It is given as:

$$\begin{aligned} \omega_{rf} &= k \frac{2\pi}{T_0} \\ 2\pi f_{rf} &= 2\pi k f_{rev} \\ f_{rf} &= k f_{rev} \end{aligned} \quad (2.82)$$

This equation means the *RF frequency*  $f_{rf}$  is an integer multiple of *the revolution frequency*  $f_{rev}$  ( $f_{rev} = 1/T_0$ ). The integer wave number  $k$  is called *harmonic number*. The harmonic number is the maximum number of bunches that can exist in the storage ring.

### 2.3.13 Dynamic Aperture

Suppose we inject the electron beam in a storage ring. The obstacles exist in the vacuum chamber including the chamber walls. If the electron beam hit an obstacle, it cannot be stored in the storage ring. The clearance through the obstacles is called the physical aperture.

Suppose the physical aperture of the storage ring is wide enough. Even in a case like this, we cannot necessarily store the electrons in the storage ring. The reason is as follows: The electron motion in the storage ring is so complicated that an electron cannot make many turns in the storage ring and is lost away to infinity unless its initial condition is appropriate. The complicated electron motion is brought about by the structure of the betatron function in the unit magnet lattice and the random change in the motion by the emission of photons. So we have to investigate the initial condition of the electron,  $x_0, y_0, x'_0, y'_0$  etc, that keeps the electron on the closed orbit for many turns. This can be implemented only by the computer simulation of the electron motion. In this simulation, we have the electron beam consecutively for many turns. If we set up an initial condition, and find the location the electron after  $N$  turns, where  $N$  is sufficiently large. If the location is in the finite range, we change the initial condition and seek the location of the electron after  $N$  turns. We repeat this until we find the initial position  $(x_0, y_0)$  at which the electron is lost to infinity after  $N$  turns. By finding many points  $(x_0, y_0)$  we can draw a borderline. If an electron occurs outside this border, it cannot be held in the finite area after  $N$  turns. If the electron occurs inside the border, it is kept in the finite area after  $N$  turns. The area surrounded this border line is called the dynamic aperture.

For the simulation of the dynamic aperture, the computer code specially written for the purpose is available. Figure 2.8 shows the dynamic aperture for 7,500 turns in the Siam Photon Source, which is simulated by Prof. Goro Ioyama. We note that the dynamic aperture is reduced when magnet misalignments and field imperfection are included in the computation.

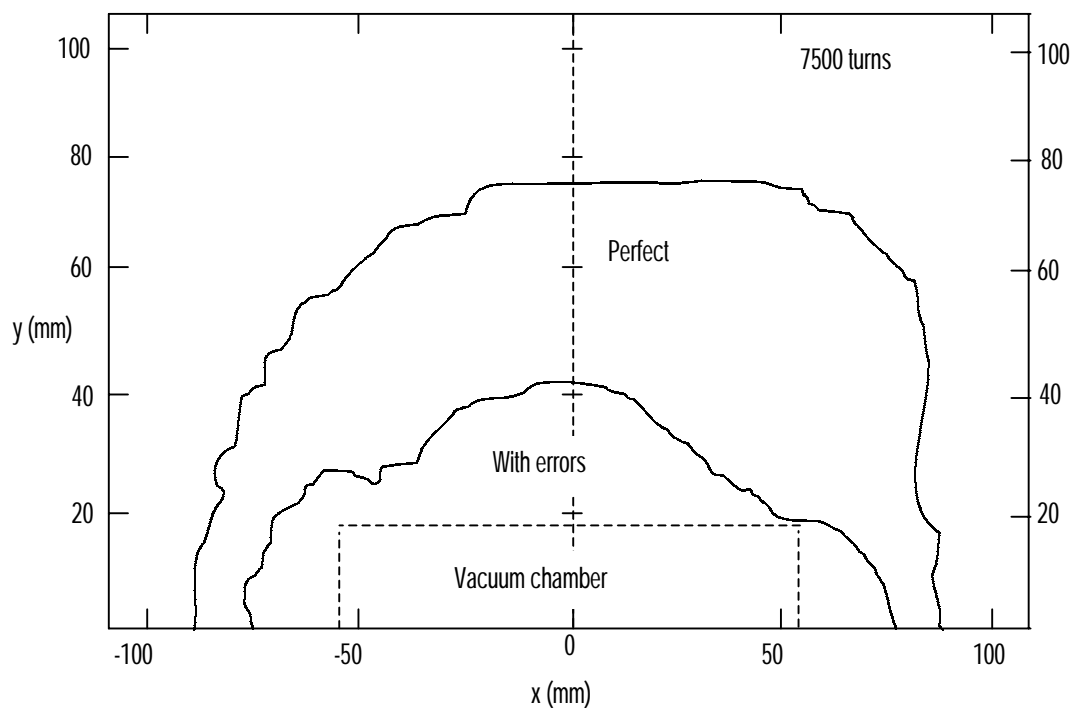


**Fig. 2.8** Dynamic apertures for a perfect machine and a realistic Machine with error (Isoyama, G. 1998)

Note that the dynamic aperture is larger than the physical aperture. In this thesis, we will only simulate the dynamic aperture for a perfect and machine with only error of nonlinear sextupole field.



# Chapter III

## Beam Dynamics Calculation

### 3.1 Data Collection

We deal with four paths of the Siam Photon Source, shown in Fig.1.1, which include LBT, SYN, HBT and STR. Dipole magnets and quadrupoles magnets, for guiding and focusing form the field give rise to only the linear effect on the electrons. Sextupole magnets used for the correction of chromatic aberrations caused by the quadrupole magnets give rise to the nonlinear effect. The real magnet lattice with alignment and other errors includes small corrector dipole magnets: Horizontal (STH) and vertical (STV) steering magnets. In addition to these, SYN and STR are equipped injection devices including bump (kicker) magnets and septum magnets and a RF cavity for acceleration and longitudinal focusing. We will briefly discuss the component magnets.

**Bending magnets (BM)** are used for bending electron beams. In the storage ring of the Siam Photon Source, sector type bending magnets are employed. The radius of curvature of the ideal orbit inside it is reference radius  $\rho_0$ , its arc length  $L$  and deflection type angle  $\phi = L/\rho_0 = Lh_0$ , where  $h_0$  is the curvature of the ideal orbit. Figure 3.1 shows the rectangular bending magnet of SYN.



**Fig. 3.1** Bending magnet of SYN

The dipole field is  $A_{10} = B(0,0,s) = hP_0/e$  (see Appendix B). In a pure *sector bend* the ideal path of the electrons enters and exits normal to the magnet. In general cases, the edges may be rotated by angles  $\beta_1, \beta_2$  (see Fig.2.3) and the rotation is included in the coordinate transformation along the direction normal to the eadg. If the magnet has parallel entrance and exit face with  $\beta_1 = \beta_2 = -\phi/2$ , it is called *rectangular bend*. If  $\beta_1 \neq \beta_2$ , it is called *wedge bend*.

**Quadrupole magnets (Q)** are used for focusing (QF) and defocusing (QD). The field gradient is given by (see Appendix B):

$$A_{11} = \left. \frac{\partial B_y}{\partial x} \right|_{x=0, y=0} = -nh^2 \left( \frac{P_0}{e} \right)$$

Figure 3.2 shows quadrupole magnets in STR of the Siam Photon Source.

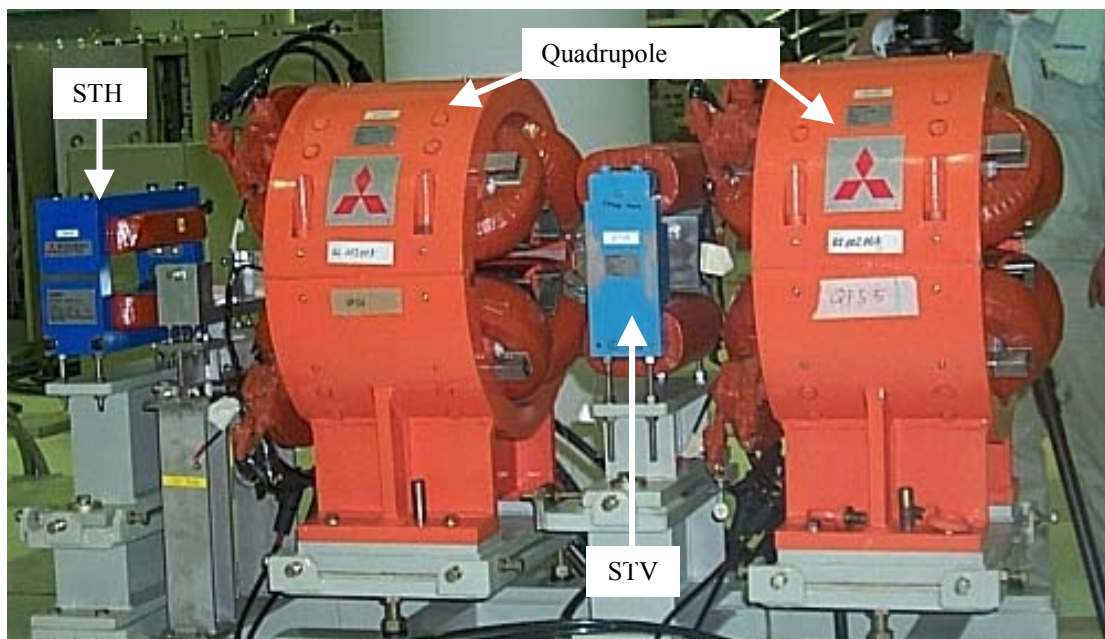


**Fig.3.2** Quadrupole magnets and steering magnets

**Sextupole magnets (SX)** are used for the correction of quadrupole chromatic errors (see section 2.3.11). The storage ring requires both sextupole focus (SXF) and sextupole defocus (SXD). The field gradient is given by (see Appendix B):

$$\frac{1}{2!} A_{12} = \left. \frac{1}{2!} \frac{\partial^2 B_y}{\partial x^2} \right|_{x=0, y=0} = 2\beta h^3 \left( \frac{P_0}{e} \right)$$

Figure 3.3 shows a sextupole magnet in SYN of the Siam Photon Source.



**Fig.3.3** Sextupole magnet

**RF cavity (RF)** is used to provide a source of electric field for beam acceleration and longitudinal focusing. Figure 3.4 shows the RF cavity in STR of the Siam Photon Source.



**Fig.3.4** The RF cavity in STR

**Correction or Steering magnets (ST)** are used for correction of close orbit locations. The example is shown in Fig.3.2. However, in this thesis, calculation does not include the steering magnets.

**Septum magnets (SM)** are used for the injection or for the beam separation in collider. A septum magnet is a copper sheet of high current attached to a dipole magnet in order to provide a sharp cut-off the field.

**Kickers or bump magnets (BM)** are used for injection, SYN and STR require either fast kickers to bend the injected beam toward the axis or slower kickers for multiturn injection. This device is not considered in the calculation of this thesis.

For the calculation and simulation, we have to collect some data to input in the computer software. We will consider the data in each path as following.

### 3.1.1 Low-Energy Beam Transport Line (LBT)

Descriptions of the transfer magnets are shown in Fig 3.5. For details of the data such as the distance between the magnets, angles of bending magnets, pole lengths etc. are listed in Appendix F.

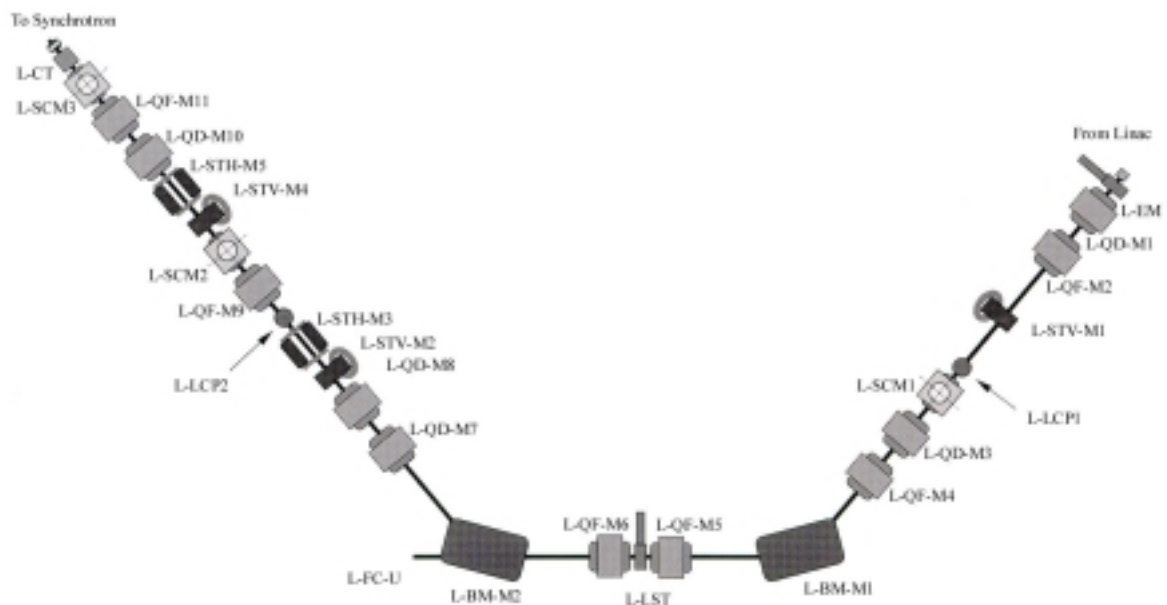


Fig. 3.5 Transfer magnet elements of LBT

Table 3.1 Magnet parameters of LBT

Magnet parameters of the magnets	
Bending magnets, B	
Type of magnets	wedge bend
Numbers of magnets	2
Radius, $\rho_0$	0.5 m
Bending angle	50.5°
Pole face rotation angle, $\beta_1 = \beta_2$	13.87°
Maximum magnetic field, $B$	0.267 T
Quadrupole magnets: q1-q10	
Number of magnets	11
Pole length	0.1 M
Maximum field gradient, $dB_y/dx$	3 T/m

### 3.1.2 Booster Synchrotron (SYN)

The magnet structure of SYN is shown in Fig. 3.6. For details of data, see in Appendix F.2.

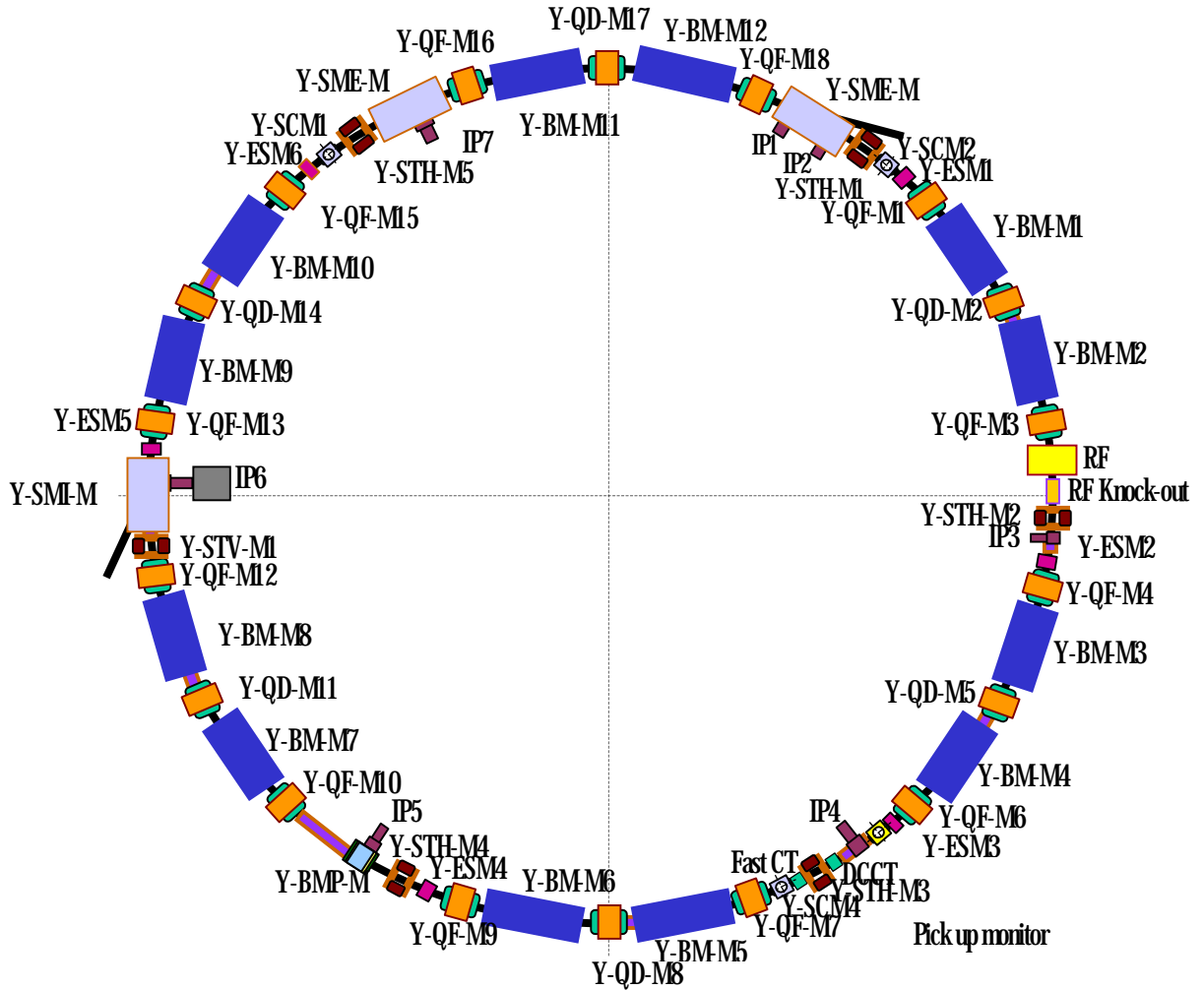


Fig.3.6 Magnet structure of SYN

Table 3.2 Parameters of SYN

Parameters of SYN	
Bending magnets, B	
Type of magnets	Rectangular bend
Numbers of magnets	2(6) = 12
Radius, $\rho_0$	3.030 m
Bending angle	30°
Pole face rotation angle, $\beta_1 = \beta_2$	15°
Maximum magnetic field, $B$	1.1 T

Quadrupole magnets, Q		
Number of magnets: q1, q2		2(6),1(6) = 18
Pole length		0.25 m
Maximum field gradient, $dB_y/dx$		4.8 T/m
Injection energy		40 MeV
Maximum energy		1 GeV
Lattice structure		FODO
RF frequency		118 MHz
Maximum RF voltage		60 kV
Chamber pressure (with beam)		$< 1 \times 10^{-6}$ Torr

### 3.1.3 High-Energy Transport Line (HBT)

The magnet structure of HBT is shown in Fig. 3.7. For details of data is shown in Appendix F3.

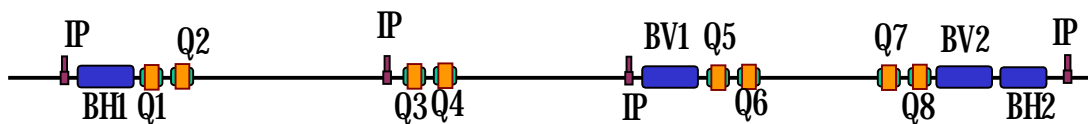


Fig.3.7 Magnet structure of HBT (Top view)

Table 3.3 Magnet parameters HBT

Parameters of magnets		
Bending magnets, B		
Type of magnets: bh, bv		wedge bend, rectangular bend
Numbers of magnets: bh1, bh2, bv1, bv2		4
Radius, $\rho_0$ : bh1, bh2, bv1, bv2		7.162, 7.162, 3.3356, 3.3356 m
Bending angle : bh1, bh2, bv1, bv2		4.0°, 2.0°, 17.5°, 17.5°
Pole face rotation angle		
bh1, $\beta_1 = \beta_2$ :eh1		2°
bh2, $\beta_1 = \beta_2$ :eh2		1°
Maximum magnetic field, $B$ : bv, bh		1, 0.47 T
Quadrupole magnets, Q		
Number of magnets: q1- q8		8
Pole length:		
q1 q6		0.4 m
q2 q3 q7 q8		0.3 m
q5		0.6 m
Maximum field gradient, $dB_y/dx$		
q1,q2,q3,q4,q5,		-8.01,6.34,-7.64,6.31,8.84,
q6,q7,q8		-2.87,5.07,-2.24

### 3.1.4 Storage Ring (STR)

#### Lattice Description

The storage ring has a double bend achromat lattice (DBA) and fourfold symmetry with four straight sections (see Fig. 3.8). The achromat lattice consists of two dispersion free straight and family of quadrupoles between. The magnet parameters and some designed parameters of the STR are listed in Table 3.

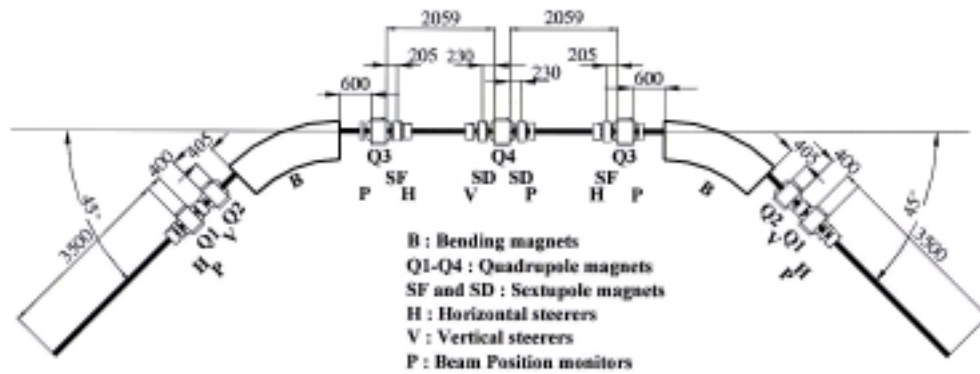


Fig. 3.8 Unit cell of magnet lattice

Table 3.4 Parameters of STR

Parameters of STR	
Bending magnets, B	
Type of magnets	sector bend
Numbers of magnets	2(4) = 8
Radius, $\rho_0$	2.78 m
Bending angle	45°
Maximum magnetic field, $B$	1.2 T
Quadrupole magnets, Q	
Number of magnets: q1-q4	7(4) = 28
Pole length	0.29 m
Maximum field gradient, $dB_y/dx$ : q1,q2,q3,q4	10,10,12,12 T/m
SExtupole magnets, SX	
Number of magnets: sf, sd	8,8
Pole length: sf, sd	0.15, 0.2 m
Maximum field gradient, $ d^2B_y/dx^2 (1/B\rho_0)$	3.6 m <sup>-2</sup>
Maximum energy	1 GeV
Lattice structure	DBA
Superperiodicity	4
RF frequency	118 MHz
Maximum RF voltage	120 kV





## 3.2 Software

In the calculation of electron beams, computer programs LATTICE and BETA are used to obtain the positions and characteristic etc. of an electron in the system.

**LATTICE** is a computer program that calculates the first-order characteristics of synchrotrons and beam transport systems. John Staples developed the program in Lawrence Berkeley Laboratory, University of California Berkeley in 1987. Though program LATTICE is a first-order program, the effect of sextupoles on the chromaticity of a synchrotron lattice is included, and the optimizer sets up the sextupole field strength for zero chromaticity. The program uses matrix algebra to calculate the progression of the betatron parameters and twiss parameters along the beam line. LATTICE has two distinct modes which are the *lattice mode* and the *transport mode*. In this thesis, we use the lattice mode to find the matching functions of SYN and STR, while transport mode is used to propagate a predefined beam through LBT and HBT. The result of calculations will be displayed in both numerically and graphically.

**BETA** is a computer program for using in the analysis of the synchrotron and storage ring, In this thesis, we use BETA to analyse only STR. Most of the output data are displayed in the form of plots. With this program we can perform the following calculations:

- 1) Linear lattice parameters calculations: BETA computes fully coupled motion of the synchrotron oscillation and the betatron oscillation of electrons. Although the cause of the betatron oscillation and that of the synchrotron oscillation are coupled. This is easily understandable because the synchrotron oscillation is accompanied by the change in the orbit length and the oscillatory change in the orbit length contains the transversal oscillation components. The relevant parameters of STR such as first-order matrix elements, twiss parameters, dispersion functions, betatron and synchrotron tunes, tune shifts as a function of betatron amplitudes, damping partition numbers, damping times, beam emittances, the bunch length and the energy spread are displayed.
- 2) Linear lattice matching.
- 3) Calculation of the second-order transfer matrix.
- 4) Calculation of the horizontal and vertical chromaticities and the adjustment of any values.
- 5) The dynamic aperture simulation. The simulation is also performed in the presence of errors.
- 6) Simulation of multipole field errors.
- 7) Simulation of the close orbit distortion.
- 8) Treatment of the linear and non-linear effects of wigglers and undulators on the beam dynamics.

However, in this thesis we use BETA to deal with only items 1) and 5).

### 3.3 Twiss Parameters

To help clear understanding, we will show the locations of the magnets with the schematic layout of each path before showing its twiss parameters.

#### 3.3.1 Twiss Parameters of LBT

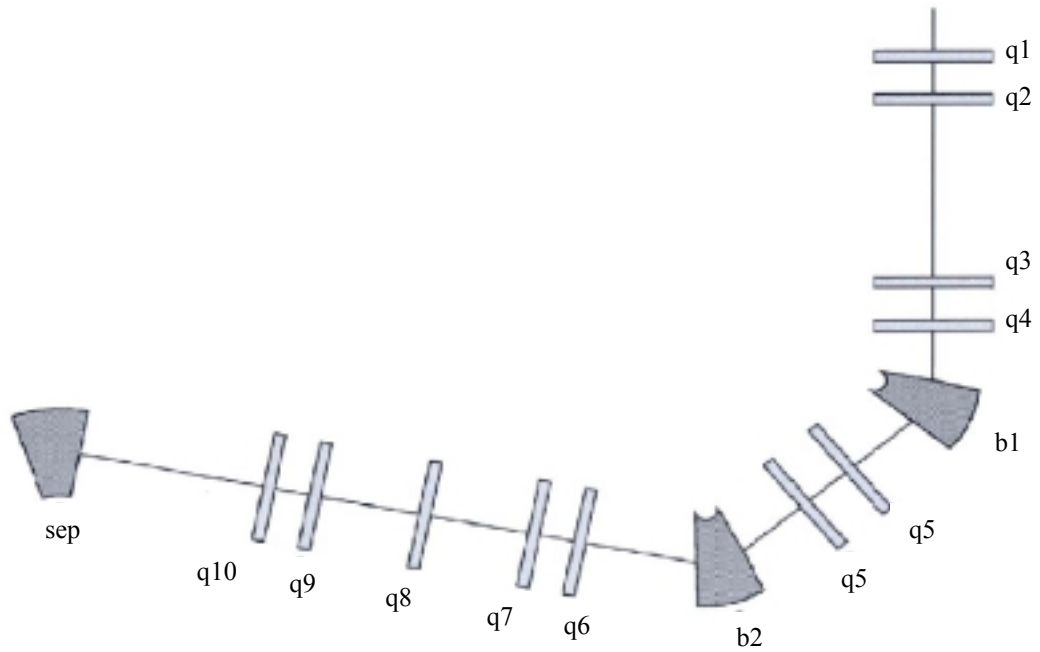


**Fig. 3.10** The schematic layout of LBT

**Table 3.5** Twiss parameters of LBT

Elements	$\beta_x$ (m)	$\alpha_x$ (rad)	$\beta_y$ (m)	$\alpha_y$ (rad)	$\eta_x$ (m)	$\eta'_x$ (rad)
	4.38	0.00	4.38	0.00	0.00	0.00
d1	4.41	-0.09	4.41	-0.09	0.00	0.00
q1	4.57	-1.56	4.29	1.27	0.00	0.00
d2	5.58	-1.78	3.58	1.09	0.00	0.00
q2	5.61	1.44	3.58	-1.00	0.00	0.00
d3	2.40	0.56	8.19	-1.89	0.00	0.00
q3	2.51	-1.64	7.85	5.19	0.00	0.00
d4	3.62	-2.08	5.06	4.12	0.00	0.00
q4	3.73	1.01	4.66	-0.05	0.00	0.00
d5	2.92	0.76	4.75	-0.14	0.00	0.00
e	2.92	-0.68	4.75	1.66	0.00	0.00
b	1.59	2.88	3.44	1.31	0.18	0.77
e	1.59	2.09	3.44	2.62	0.18	0.86
d6	0.30	-0.05	1.04	1.17	0.73	0.86
q5	0.31	-0.04	0.93	-0.07	0.77	-0.00
d7	0.45	-0.69	1.01	-0.29	0.77	-0.00
d7	0.86	-1.34	1.16	-0.50	0.77	-0.00
q5	1.04	-0.45	1.42	-2.17	0.73	-0.86
d8	2.08	-1.18	5.78	-4.71	0.18	-0.86
e	2.08	-2.20	5.78	-2.51	0.18	-0.77
b	2.34	1.77	8.24	-3.07	-0.00	0.00
e	2.34	0.61	8.24	0.06	0.00	0.00
d9	1.71	0.06	8.24	-0.06	0.00	0.00
q6	1.71	-0.02	8.24	0.02	0.00	0.00
d10	1.77	-0.20	8.23	-0.01	0.00	0.00
q7	1.97	-1.78	7.60	6.18	-0.00	-0.00
d11	6.52	-3.58	0.82	1.80	-0.00	-0.00
q8	6.59	2.88	0.57	0.75	0.00	0.00
d12	2.71	1.68	1.27	-1.57	0.00	0.00
q9	2.21	3.23	1.72	-3.10	0.00	0.00
d13	0.73	1.68	4.13	-4.94	0.00	0.00
q10	0.52	0.53	4.59	0.61	0.00	0.00
d14	5.11	-3.40	3.39	0.13	0.00	0.00
sep	6.77	-0.00	3.33	0.00	-0.50	-0.50

### 3.3.2 Twiss Parameters of SYN

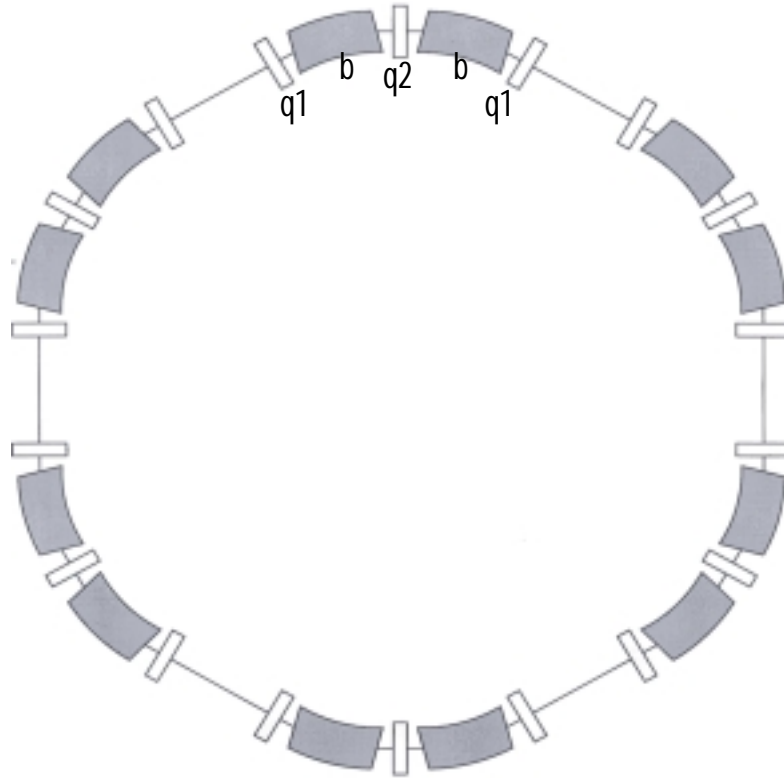


**Fig. 3.11** The schematic layout of SYN

**Table 3.6** Twiss parameters of SYN

Elements	$\beta_x$ (m)	$\alpha_x$ (rad)	$\beta_y$ (m)	$\alpha_y$ (rad)	$\eta_x$ (m)	$\eta'_x$ (rad)
	6.77	-0.00	3.33	0.00	1.86	0.00
d1	6.93	-0.15	3.66	-0.31	1.86	0.00
q1	6.40	2.20	4.18	-1.86	1.78	-0.66
d2	5.16	1.93	5.39	-2.17	1.58	-0.66
e	5.16	1.47	5.39	-1.72	1.58	-0.52
b	1.42	0.67	12.68	-2.88	0.98	-0.22
e	1.42	0.54	12.68	-1.80	0.98	-0.13
d2	1.18	0.27	13.79	-1.90	0.94	-0.13
q2	1.18	-0.27	13.79	1.90	0.94	0.13
d2	1.42	-0.54	12.68	1.80	0.98	0.13
e	1.42	-0.67	12.68	2.88	0.98	0.22
b	5.16	-1.47	5.39	1.72	1.58	0.52
e	5.16	-1.93	5.39	2.17	1.58	0.66
d2	6.40	-2.20	4.18	1.86	1.78	0.66
q1	6.93	0.15	3.66	0.31	1.86	0.00
d1	6.77	0.00	3.33	-0.00	1.86	0.00

### 3.3.3 Twiss Parameters of HBT

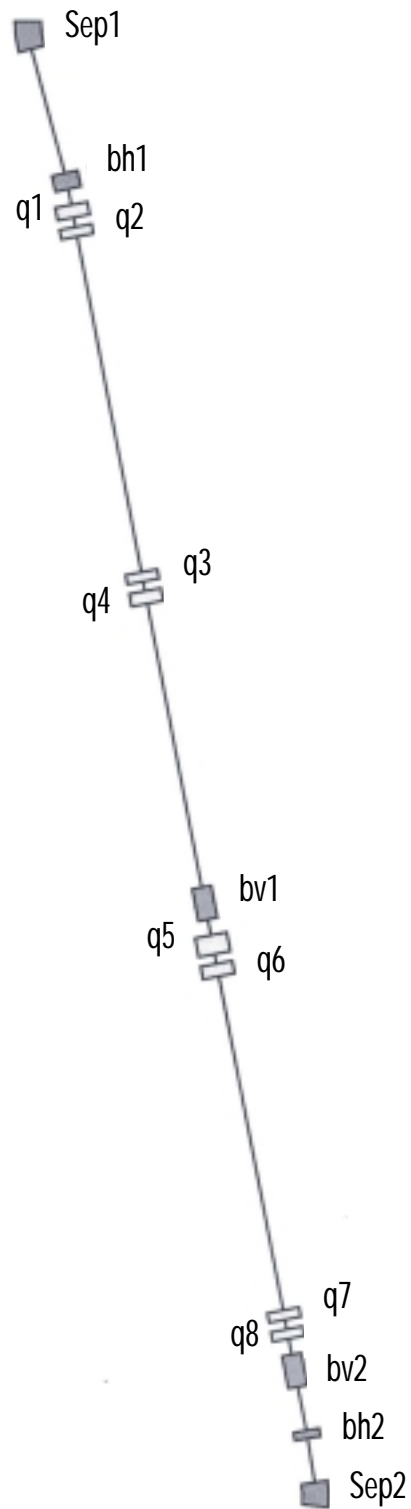


**Fig. 3.12** The schematic layout of HBT

**Table 3.7** Twiss parameters of HBT

Elements	$\beta_x$ (m)	$\alpha_x$ (rad)	$\beta_y$ (m)	$\alpha_y$ (rad)	$\eta_x$ (m)	$\eta'_x$ (rad)
	6.77	0.00	3.33	0.00	1.86	0.00
Sep1	6.42	0.39	3.56	-0.26	1.68	-0.40
d1	6.20	-0.33	10.45	-1.46	0.07	-0.40
eh1	6.20	-0.36	10.45	-1.41	0.07	-0.40
bh1	6.58	-0.39	11.94	-1.56	-0.12	-0.33
eh1	6.58	-0.42	11.94	-1.50	-0.12	-0.33
d2	7.04	-0.51	13.51	-1.64	-0.28	-0.33
q1	9.72	-6.80	11.19	6.89	-0.46	-0.59
d	14.24	-8.26	7.45	5.59	-0.64	-0.59
q2	16.35	1.69	5.62	0.90	-0.75	-0.13
d3	6.99	-0.80	22.75	-2.52	-2.07	-0.13
q3	9.07	-6.58	19.81	11.64	-2.33	-1.58
d	13.45	-8.04	13.45	9.58	-2.80	-1.58
q4	15.86	2.62	9.74	0.58	-3.00	0.59
d4a	11.55	2.17	8.81	0.46	-2.47	0.59
d4b	8.05	1.73	8.09	0.33	-1.94	0.59
d4c	5.34	1.28	7.61	0.21	-1.42	0.59
d4d	3.44	0.84	7.34	0.09	-0.89	0.59
d4e	2.33	0.39	7.29	-0.04	-0.36	0.59
d4f	2.02	-0.05	7.47	-0.16	0.17	0.59
d4g	2.52	-0.50	7.86	-0.28	0.70	0.59
d4h	3.81	-0.94	8.48	-0.41	1.22	0.59
d4i	5.90	-1.39	9.32	-0.53	1.75	0.59
d4j	8.79	-1.83	10.38	-0.65	2.28	0.59
bv1	13.04	-2.34	10.83	0.23	2.88	0.59
d5	15.50	-2.58	10.63	0.18	3.17	0.59
q5	13.15	6.02	14.68	-7.72	2.96	-1.30
d	9.79	5.17	19.69	-8.96	2.57	-1.30
q6	7.72	0.35	22.70	1.96	2.30	-0.05
d6	16.58	-1.19	5.11	-0.29	1.72	-0.05
q7	15.20	5.60	6.01	-2.83	1.59	-0.77
d	12.03	4.96	7.85	-3.29	1.36	-0.77
q8	10.64	-0.10	8.80	0.26	1.21	-0.22
d7	10.76	-0.15	8.57	0.20	1.10	-0.22
bv2	11.17	-0.25	7.54	0.78	0.88	-0.22
d8	12.02	-0.38	5.78	0.49	0.58	-0.22
eh2	12.02	-0.41	5.78	0.50	0.58	-0.22
bh2	12.22	-0.37	5.55	0.45	0.53	-0.19
eh2	12.22	-0.40	5.55	0.46	0.53	-0.18
d8	13.50	-0.53	4.70	0.16	0.28	-0.18
Sep2	13.39	0.69	4.58	-0.00	0.23	0.06

### 3.3.4 Twiss Parameters of STR

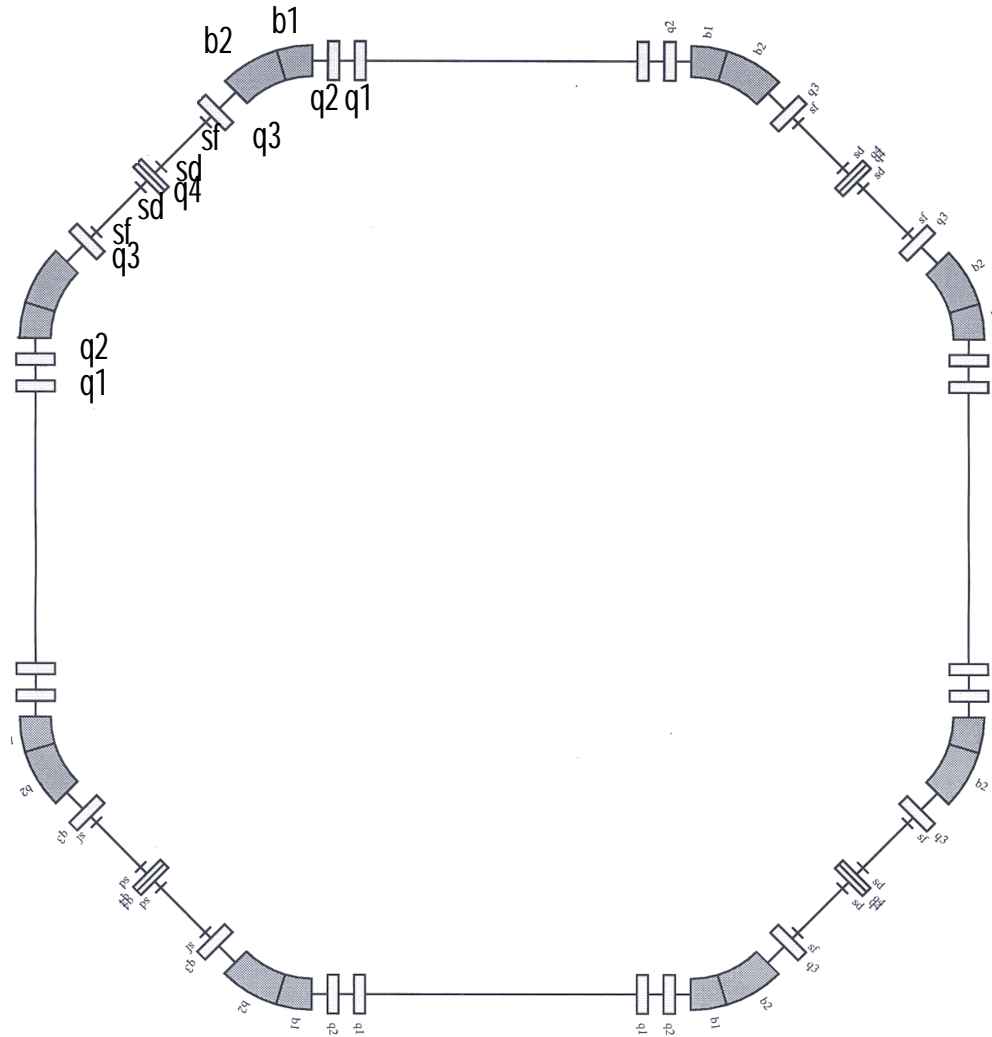


**Fig.3.13** The schematic layout of STR

**Table 3.8** Twiss parameters of STR

Elements	$\beta_x$ (m)	$\alpha_x$ (rad)	$\beta_y$ (m)	$\alpha_y$ (rad)	$\eta_x$ (m)	$\eta'_x$ (rad)
	13.38	-0.00	4.58	-0.00	-0.00	-0.00
d1	14.30	-0.26	7.25	-0.76	-0.00	-0.00
q1	11.37	9.58	9.61	-7.96	-0.00	0.00
d2	5.01	6.31	17.04	-10.64	-0.00	0.00
q2	2.78	1.98	18.99	4.46	-0.00	0.00
d3	1.47	1.26	15.56	4.01	-0.00	0.00
b1	0.55	-0.16	9.73	3.11	0.12	0.29
b2	4.03	-2.18	3.28	1.61	0.81	0.71
d4	7.17	-3.04	1.74	0.95	1.24	0.71
q3	7.39	2.33	1.60	-0.44	1.31	-0.24
dsf	6.47	2.15	1.81	-0.59	1.26	-0.24
sf	6.47	2.15	1.81	-0.59	1.26	-0.24
d5	1.78	0.74	5.68	-1.80	0.87	-0.24 -
sd	1.78	0.74	5.68	-1.80	0.87	0.24
dsd	1.48	0.54	6.55	-1.97	0.81	-0.24
q4	1.41	-0.00	6.84	0.00	0.80	-0.00
q4	1.48	-0.54	6.55	1.97	0.81	0.24
dsd	1.78	-0.74	5.68	1.80	0.87	0.24
sd	1.78	-0.74	5.68	1.80	0.87	0.24
d5	6.47	-2.15	1.81	0.59	1.26	0.24
sf	6.47	-2.15	1.81	0.59	1.26	0.24
dsf	7.39	-2.33	1.60	0.44	1.31	0.24
q3	7.17	3.04	1.74	-0.95	1.24	-0.71
d4	4.03	2.18	3.28	-1.61	0.81	-0.71
b2	0.55	0.16	9.73	-3.11	0.12	-0.29
b1	1.47	-1.26	15.56	-4.01	-0.00	-0.00
d3	2.78	-1.98	18.99	-4.46	-0.00	-0.00
q2	5.01	-6.31	17.04	10.64	-0.00	-0.00
d2	11.37	-9.58	9.61	7.96	-0.00	-0.00
q1	14.30	0.26	7.25	0.76	-0.00	-0.00
d1	13.38	0.00	4.58	-0.00	-0.00	-0.00



### 3.4 Result of Calculations and Discussion

In this section will show important parameters such as beam sizes and betatron functions and dispersion functions and discuss about them. betatron functions. The complete results are shown in Appendix F.

#### 3.4.1 LBT

We will only show the beam sizes, betatron functions and dispersion function of the beam through the elements of the lattice, because in transfer line the other characteristics are not important. (see Appendix F.1)

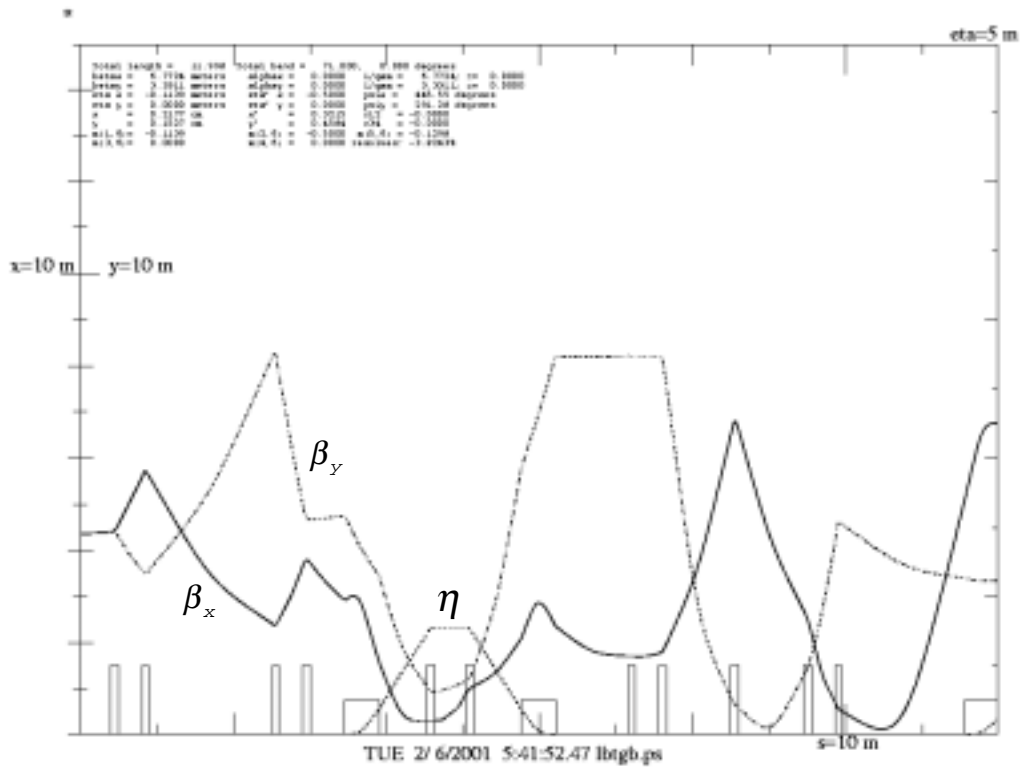


**Fig.3.14** Betatron functions and dispersion function in LBT

Figure 3.14 shows how the beam from LINAC change in LBT. The betatron functions are  $\beta_x = 4.375\text{cm}$ ,  $\beta_y = 4.375\text{cm}$  and the dispersion is equal to zero at the entrance to LBT. At the end of LBT, where a septum magnet is located, the betatron functions are  $\beta_x = 6.7724\text{m}$ ,  $\beta_y = 3.3311\text{m}$ . However, the dispersion is not equal to zero but  $\eta_x = -0.1139\text{ m}$  (see the results in Appendix F.1 for details). This implies that the beam is bent at the septum location,

Figure 3.15 shows the beam sizes in both horizontal and vertical directions are  $\sigma_x = 0.22\text{cm}$  and  $\sigma_y = 0.15\text{cm}$  at the end of LBT. (see the results in Appendix F.1 for details)

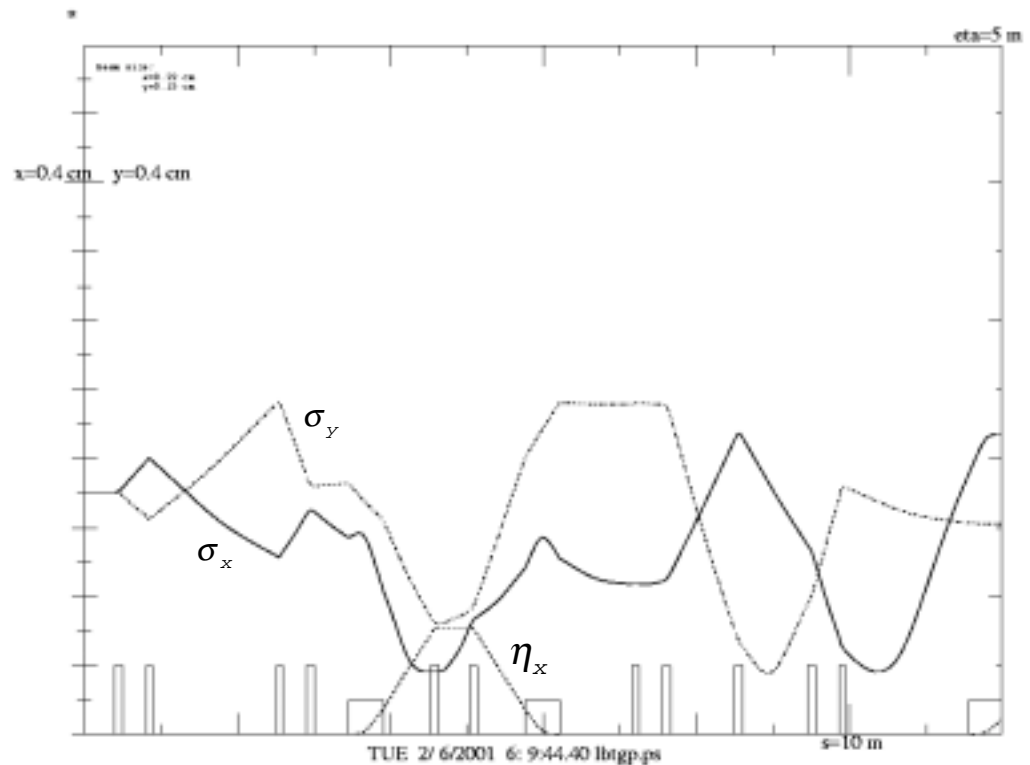


Fig 3.15 Beam sizes in LBT, electron energy 40 MeV.

### 3.4.2 SYN

The important parameters of SYN are listed in Table 3.9. (see Appendix F.2)

Table 3.9 Main parameters of SYN

Parameters of SYN	
Minimum electron energy	40 MeV
Maximum electron energy	1 GeV
Circumference, $C$	43.188 m
Superperiodicity	6
Natural rms horizontal emittance, $\epsilon_x^0$	$273.562 \pi$ nm rad
Betatron wave numbers or tune numbers, $\nu_x, \nu_y$	2.25, 1.25
Damping partition numbers, $D, J_x, J_y, J_E$	0.09996, 0.9004, 1.00, 2.0996
Damping times, $\tau_x, \tau_y, \tau_E$	18.893, 17.011, 8.1021 ms
Synchrotron radiation (energy loss per turn), $U_0$	0.029349 MeV/turn

The septum magnet located at the entrance of the synchrotron injects electrons of 40 MeV. Then, they are accelerated by the synchrotron acceleration mechanism (the betatron acceleration plus the compensation of the energy lost to synchrotron radiation) until its energy increase to 1 GeV. The natural emittance is  $273.562 \pi \cdot \text{nm} \cdot \text{rad}$ . In one revolution, the electron loses energy as 0.029349 MeV. The horizontal and vertical tunes are 2.25 and 1.25, respectively. This indicates that the electron oscillates 2.25 times per turn in the horizontal direction and 1.25 times per turn in the vertical direction.

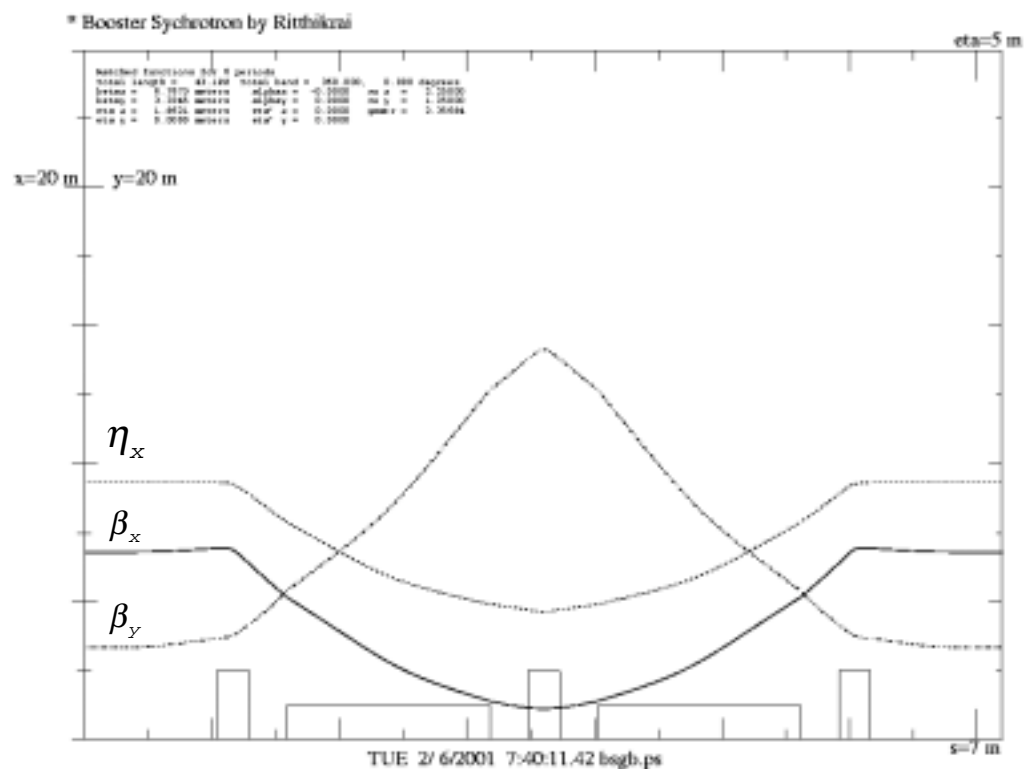


**Fig. 3.16** Betatron functions and dispersion function in SYN

Figure 3.16 shows the betatron functions and the dispersion function in the unit cell of the lattice. At the straight section  $\eta_x = 1.8621\text{m}$ ,  $\beta_x = 6.7673\text{m}$  and  $\beta_y = 3.3345\text{m}$ . The maximum betatron values are  $\beta_{x \text{ max}} = 6.9260\text{m}$  and  $\beta_{y \text{ max}} = 13.791\text{m}$ .

Figure 3.17 shows the beam sizes,  $\sigma_x = 0.13\text{cm}$  and  $\sigma_y = 0.03\text{cm}$ , at the end of the unit cell. The maximum beam sizes are  $\sigma_{x \text{ max}} = 0.13\text{cm}$  and  $\sigma_{y \text{ max}} = 0.06\text{cm}$ . The details of the results of the calculations are shown in Appendix F.2.

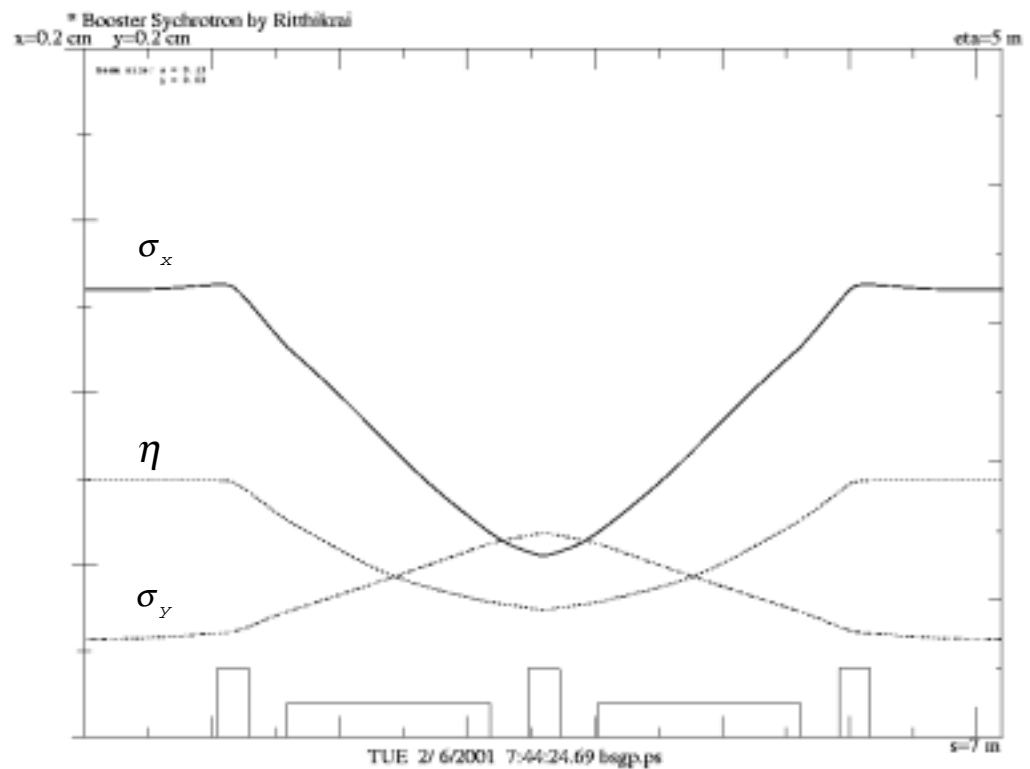


Fig. 3.17 Beam sizes for SYN in a unit cell of Lattice.

### 3.4.3 HBT

The betatron functions and the dispersion function are shown in Fig. 3.18. The beams are injected from SYN with  $\beta_x = 6.77\text{m}$ ,  $\beta_y = 3.33\text{m}$  and  $\eta_x = 1.86\text{m}$ . At the exit of the lattice,  $\beta_x = 13.385\text{m}$ ,  $\beta_y = 4.5825\text{m}$  and  $\eta_x = 0.2286\text{m}$ . The detail of results of the calculations is shown in Appendix F.3.

Figure 3.19 shows the horizontal and vertical beam sizes in HBT. At the end point, the horizontal and vertical beam sizes are 1.8 mm and 0.3 mm, respectively.

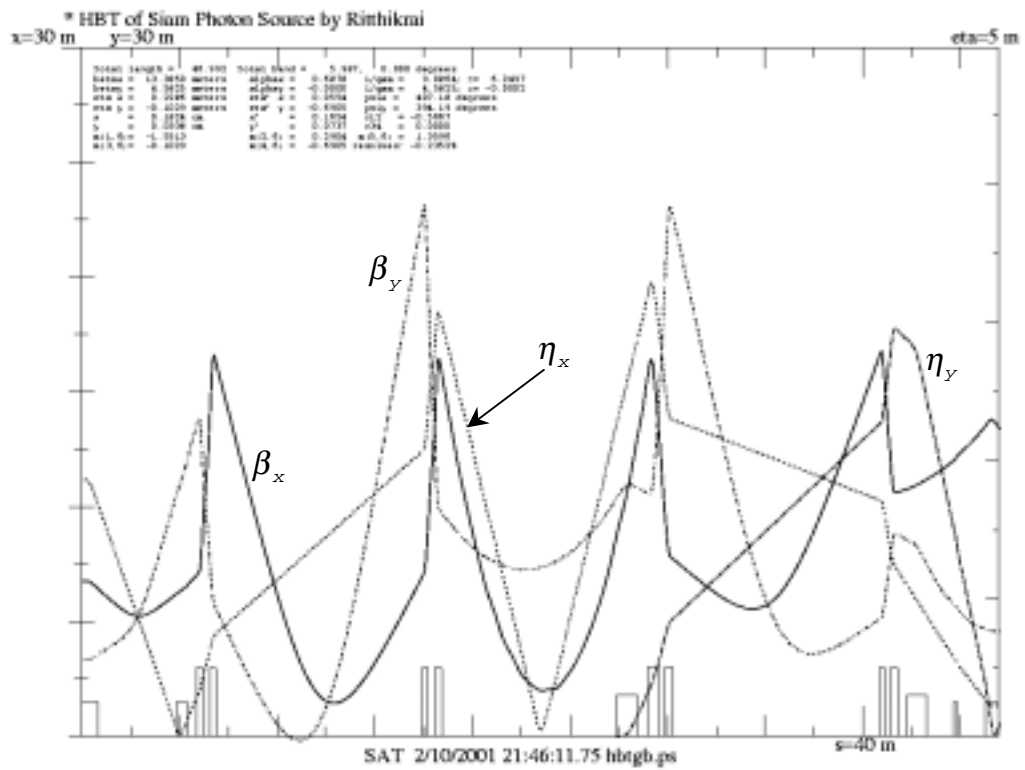


Fig. 3.18 Betatron functions and dispersion function in HBT

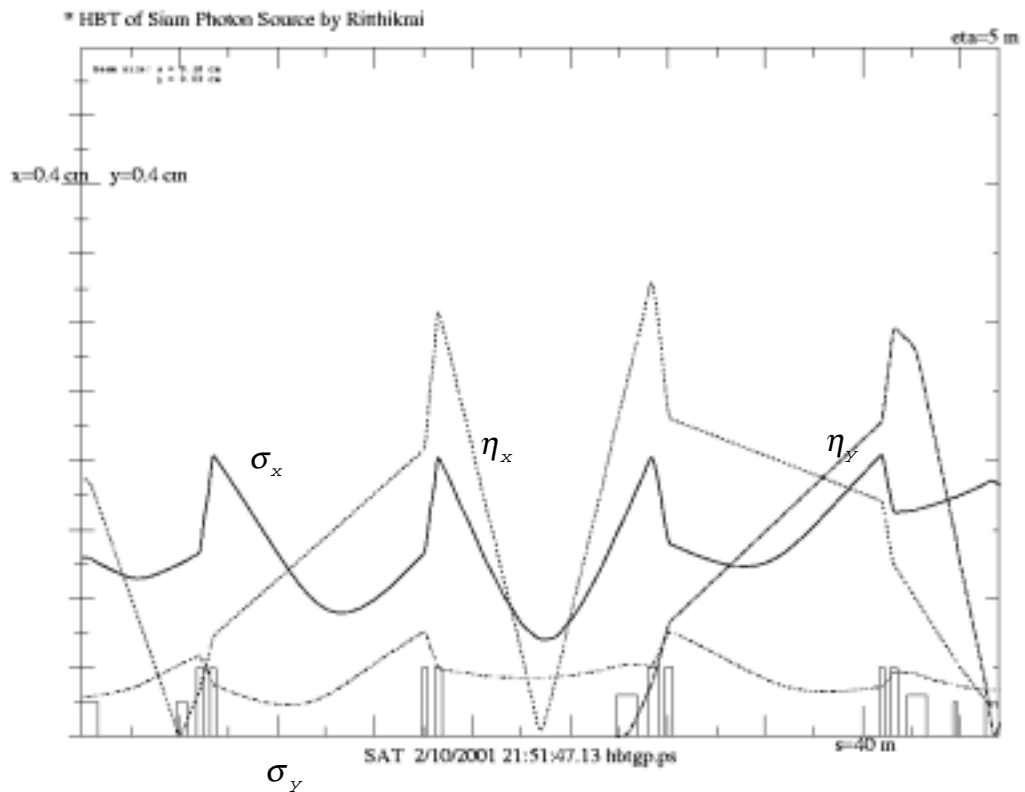


Fig. 3.19 Beam sizes in HBT

### 3.4.4 STR

The 1 GeV electrons injected from HBT are stored in the storage ring. The storage ring of the Siam Photon Source has a circumference of 81.3 m. It has a four 7 m long-straight sections and fourfold symmetry with Double Bend Achromat (DBA) cells. The natural emittance is  $73.411 \pi \cdot \text{nm}\cdot\text{rad}$ . This is 7 times smaller than that of the original ring of SORTEC,  $500 \pi \cdot \text{nm}\cdot\text{rad}$ . The reduction in the emittance implies that the beam size is also small. Therefore, the synchrotron light acquires more brilliance.

Without chromaticity compensations, the chromaticities in the horizontal and vertical directions are  $-7.648$  and  $-6.727$ , respectively. These values imply that the chromatic errors occur in both horizontal and vertical directions. The details of results of the calculations without chromaticity corrections are shown in Appendix F.4. In this thesis, the chromaticities are corrected to be zero. For this case, both program LATTICE and program BETA are used. The details of results from program LATTICE and program BETA are shown in Appendix F.5 and Appendix F.6, respectively. The main parameters of STR are shown in Table 3.10.

**Table 3.10 Main parameters of STR**

Parameters of STR	
Electron energy, $E_0$	1.0 GeV
Circumference, $C$	81.3 m
Magnet lattice	DBA
Superperiodicity	4
Long straight sections	7 m $\times$ 4
Natural rms horizontal emittance, $\epsilon_x^0$	$73.411 \pi \text{ nm rad}$
Natural chromaticities, $\xi_x, \xi_y$	-7.648, -6.727
Beam sizes, $\sigma_x, \sigma_y$	0.95, 0.18 mm
Betatron wave numbers or tune numbers, $\nu_x, \nu_y$	4.76, 2.82
Damping partition numbers, $D, J_x, J_y, J_E$	0.09996, 0.9004, 1.00, 2.0996
Damping times, $\tau_x, \tau_y, \tau_E$	18.893, 17.011, 8.1021 ms
Synchrotron radiation (energy loss per turn), $U_0$	0.031900 MeV/turn
Energy spread, $\sigma_E/E_0$	$5.0220 \times 10^{-4}$

An electron loses energy of 31.9 eV per revolution into synchrotron radiation. In the revolution, electrons have the horizontal damping and the energy damping with damping partition numbers of 0.9004 and 2.0996,

respectively. However, the balance between the damping and the quantum fluctuation (random change in the beam energy by emitting photons) of the beam energy occurs an equilibrium distribution of electrons in the beam is attained. It determines the equilibrium values of the beam emittance and the energy spread. The value of the energy spread is  $5.0220 \times 10^{-4}$ . The operating points in the horizontal and vertical directions are 4.76 and 2.82, respectively.

Figure 3.20 shows the betatron ( $\beta_x, \beta_y$ ) functions and the dispersion function ( $\eta_x$ ) in a unit cell of STR at the operating point,  $\nu_x = 4.76$ ,  $\nu_y = 2.82$ . In section 3.3, Table 3.8 shows the slope of the betatron functions equal to zero,  $\alpha_x = \alpha_y = 0$ , at the end of lattice. This indicates that the beam is parallel to the ideal orbit. The maximum values of the betatron functions are  $\beta_{x \max} = 14.30\text{m}$  at the location of the defocusing quadrupole magnet and  $\beta_{y \max} = 19.36\text{m}$  at the location of the focusing quadrupole magnet. The minimum value of the horizontal betatron is  $\beta_{x \min} = 0.55\text{m}$  at the location of end of b1. This is 0.82 m away from the dispersion free straight section side.

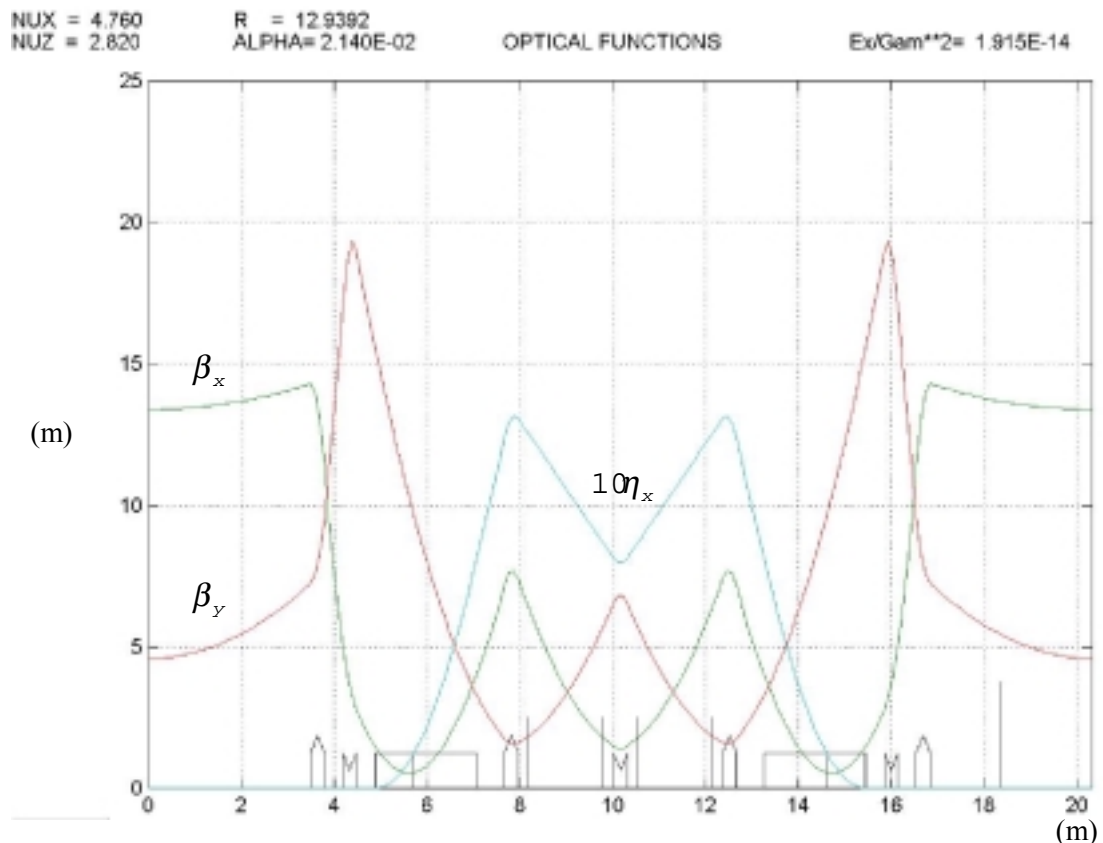


**Fig. 3.20** Betatron functions and dispersion function in a unit cell of STR

We notice that the horizontal betatron function is focused at the locations of q1 and q3, and it is defocused at the locations of q2 and q4. Inversely, the vertical betatron function is focused at the locations of q2 and q4, and it is

defocused at the locations of q1 and q3. In order to obtain the betatron functions as shown in Fig.3.20, we used the field gradient of the quadrupole magnets as shown in Table 3.11.

**Table 3.11** The field gradient of the quadrupoles in STR

Quadrupole	Field gradient	Type
q1	9.198045	Focusing
q2	-9.573124	Defocusing
q3	8.410067	Focusing
q4	-6.888579	Defocusing

Figure 3.21 shows the beam sizes for the horizontal and vertical directions in a unit cell where 10% coupling is assumed. The horizontal beam size is  $\sigma_x = 0.95$  mm and the vertical beam size is  $\sigma_y = 0.18$  mm. The maximum horizontal and vertical beam sizes are  $\sigma_{x \max} = 0.98$  mm and  $\sigma_{y \max} = 0.36$  mm, respectively (see the results in Appendix F.5 and F.6 for details).

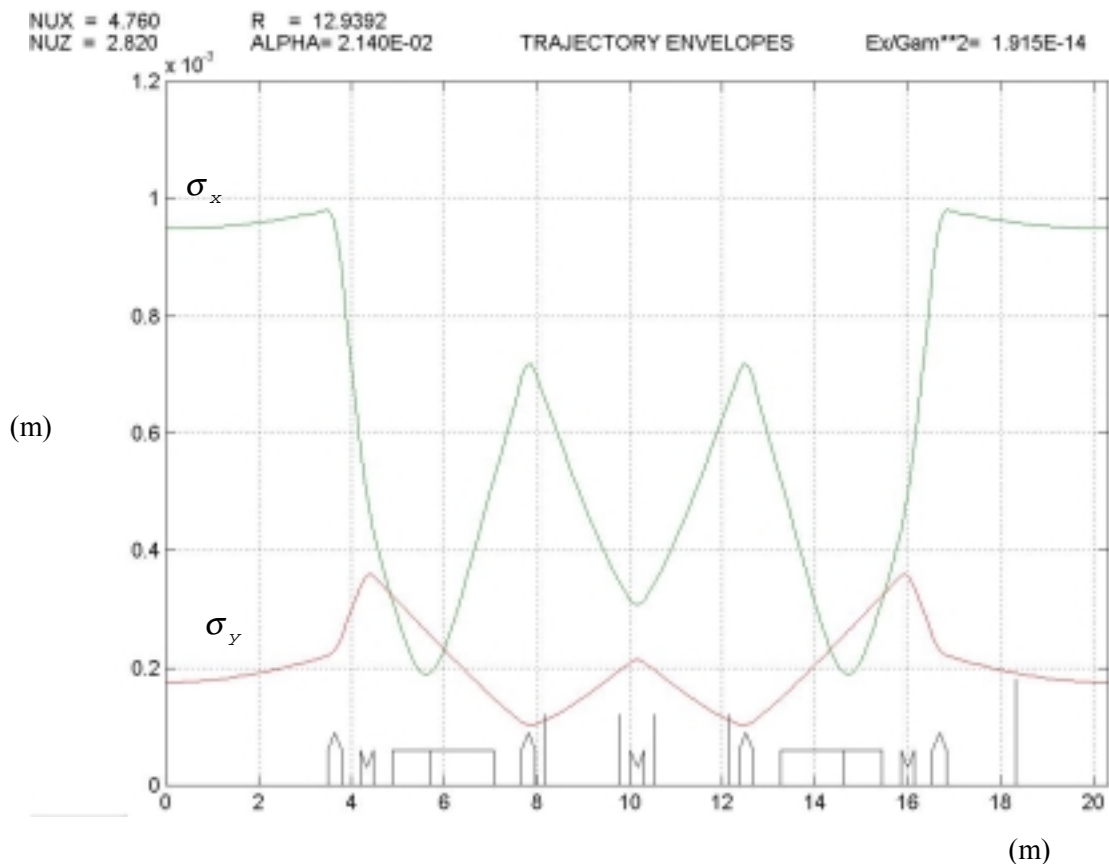


**Fig. 3.21** Beam sizes in a unit cell of lattice of STR



Figure 3.22 shows the dynamic aperture for the perfect machine simulated at the center of the long straight section by tracking a electron for 4,000 turns. It is much larger than the physical aperture of the vacuum chamber. Therefore, the horizontal and vertical phase spaces of the electron for many oscillation amplitudes within the physical aperture are not distorted very much.

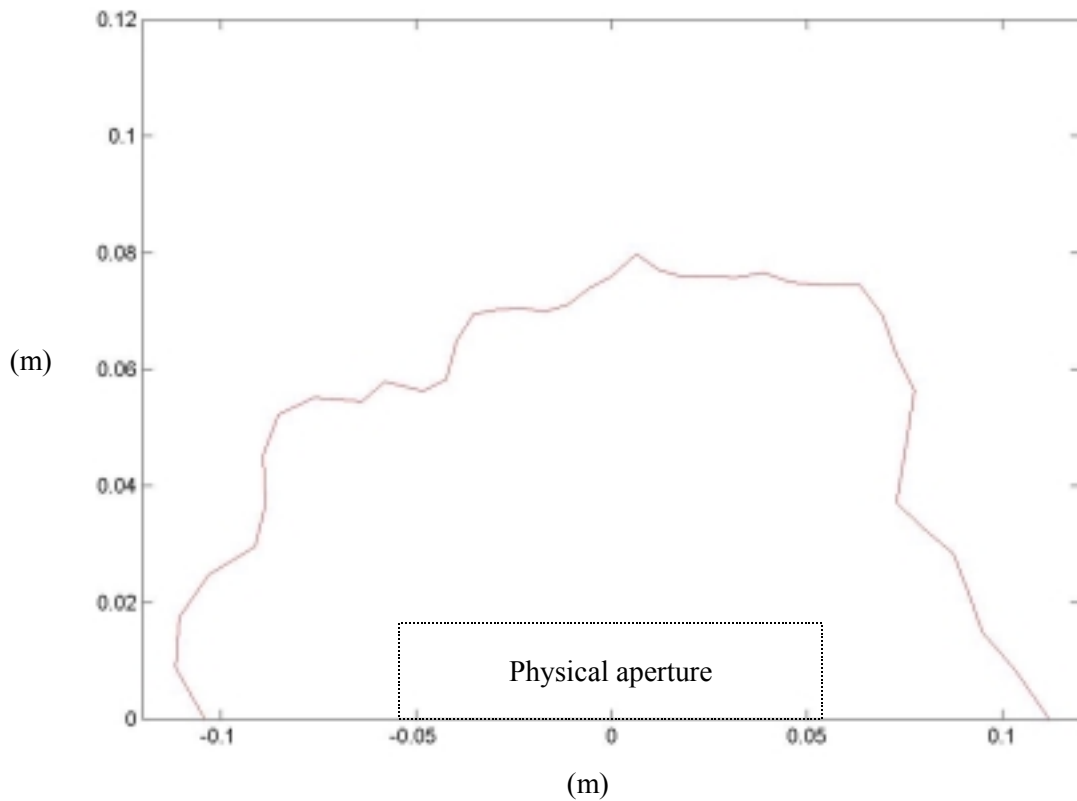


**Fig.3.22** The dynamic aperture for perfect machine at the center of the long straight section. The dashed line is the physical aperture of the vacuum chamber

# Chapter IV

## Conclusion

The purposes of this work are to explain the analytical part of the electron motion in a storage ring and calculate the important beam parameters. I started by studying the basic theory of the beam dynamics in the storage ring. Then, I studied the usage and performance of program LATTICE and program BETA. After that, I collected the various data such as the structure of the lattice, parameters of the magnets, etc. These input data are used to calculate the Twiss parameters and the important beam parameters with program LATTICE. From plotting the Twiss parameters, I have the betatron functions and the dispersion function in graphs in both horizontal and vertical directions. The horizontal and vertical beam sizes are also plotted. Moreover, the program BETA is used for the simulations of the dynamic aperture, here the field gradient of the magnets from program LATTICE are used as the input data for program BETA.

### 4.1 Beam Dynamics

The 1 GeV electrons in the storage ring are relativistic, traveling with a velocity very close to the speed of light. The trajectories of these electrons are kept close to the ideal orbit by focusing and bending electron orbit by the magnetic fields. These linear magnetic fields, produced in dipole and quadrupole magnets, determine the single particle behaviour in the storage ring in the linear approximation. The electrons execute transverse betatron oscillation around the ideal orbit (see Fig. 3.20). The electron beam contains electrons with energies that differ from the designed ring energy. These off-momentum electrons have a new ideal orbit that depend on the momentum deviation and is described by dispersion function. They execute betatron oscillations around this new momentum-dependent closed orbit. Furthermore, by the process of synchrotron radiation and acceleration in RF cavity, synchrotron oscillations result.

### 4.2 Beam Characteristics

As mentioned in section 3.4, the important characteristics of the beam are concluded here. The natural emittance of the beam is  $73.4 \pi \cdot \text{nm} \cdot \text{rad}$ . At the mid-point of the long straight section, the horizontal and vertical beam sizes are 0.95 mm and 0.18 mm, respectively. The minimum value of the horizontal beam size is 0.2 mm at a position about  $(3/8)L$  away from the edge on the dispersion free straight section, where  $L$  is the bending magnet length (see Fig. 3.21). In a revolution, the electron oscillates about 4.76 times and 2.82 times in horizontal and vertical directions, respectively. The number of bunches in the storage ring are about 32.

### 4.3 Future Perspective

The calculations of various parameters using program LATTICE in this thesis have been carried out only first-order matrix transport. This implies that the Twiss parameters and various beam parameters are of the first-order, too. In future, the BETA program should be considered more in detail, because with program BETA we can calculate parameters to the higher-order and take various errors of the beam into account.

At the time when this thesis was written, the assembly of the Siam Photon Source was not yet completed. However, when the machine is ready to run, the results of this work should be examined experimentally.

In the near future, the insertion devices, undulators and wigglers, will be installed in the storage ring. So, beam dynamics studies including the effect of these devices will be necessary. The beam dynamics studies of the undulators and wigglers are interesting to work out.

## **References**

## References

- Brown, K. L. (1982). A First–second-order matrix theory for the design of beam transport systems and charged particle spectrometers. **SLAC Report No.75**: 71-134.
- Brown, K. L. and Rothacker, F. (1977). A Computer program designing charged particle beam transport systems, **SLAC Report-91, Rev.2**: 41- 49.
- Brown, K. L. (n.d.). Optics and lattices. In Chao, A. W. and Tigner, M. (eds.). **Handbook of accelerator physics and engineering** (pp 55-62). Singapore: World Scientific.
- Dibartolo, B. (1991). **Classical theory of electromagnetism**. Singapore: Simon & Schuster.
- Edwards, A. D. and Syphers, M. . (n.d.). Phas space, Longitudinal motion, and Linear coupled systems. In Chao, A. W. and Tigner, M. (eds.). **Handbook of accelerator physics and engineering** (pp 49-53). Singapore: World Scientific.
- Farvacque, L., Laclare, J., and Ropert, A. (1989, February). BETA: Beta user's guide [Computer software], **ESRF-SR/LAT-88-08**. Eropean Synchrotron Radiation Facility.
- Irwin, J. and Yan, T. Y. (n.d.) Dynamic Aperture. In Chao, A. W. and Tigner, M. (eds.). **Handbook of accelerator physics and engineering** (pp 87-91). Singapore: World Scientific.
- Jackson, J. D. (1998). **Classical electrodynamics** (3<sup>rd</sup> ed.). New York: John Wiley & Sons.
- Lee, S. Y. (1999). **Accelerator physics**. Singapore: World scientific.
- Heald, M. A. and Marion, J. B. (1995). **Classical electromagnetic radiation** (3<sup>rd</sup> ed.). United States of America: Saunders College.
- Matthew, S. (1970). **The physics of electron storage rings and introduction**. California, Santa Cruz: University of California.
- Pairsuwan, W. and Ishii, T. (1998). The Siam photon laboratory. **J. Synchrotron Rad.** 5: 1173 – 1175.

- Pairsuwan, W., Songsiriritthigul, P., Yamakawa, T., Isoyama, G., and Ishii, T. (1998). Present status of synchrotron radiation research in Thailand –The Siam photon project. **International Meeting on Frontiers of Physics**. (2). Kuala Lumpur: Malaysia.
- Staples, J. (1987, June). LATTICE: a beam transport program [Computer software], **LBL-23939**. University of California Berkeley: Lawrence Berkeley Laboratory.
- Wiedemann, H. (1993). **Particle accelerator physics** (Vols 1-2). New York: Springer – Verlag.
- Winnick, H. (1995). **Synchrotron radiation sources a primer**. Singapore: World Scientific.

# **Appendices**

# Appendix A

## Equation of Motion

We derive the equation of motion of the charged particle in the static magnetic field.

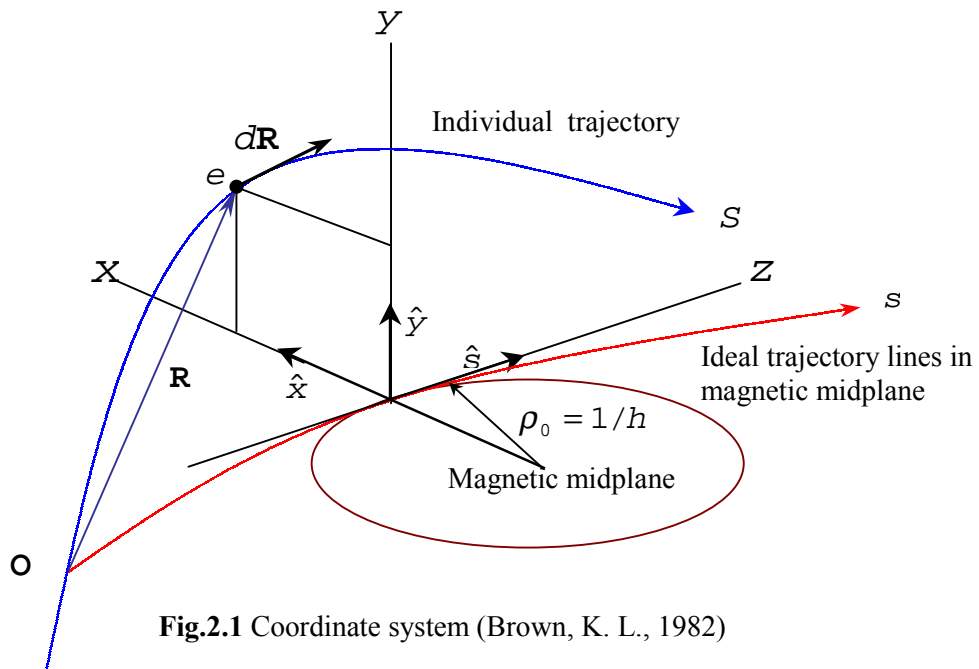


**Fig.2.1** Coordinate system (Brown, K. L., 1982)

We define three mutually perpendicular unit vectors,  $(\hat{x}, \hat{y}, \hat{s})$ . The direction of motion of the particle is tangent to the ideal trajectory and in positive direction of  $\hat{s}$ .  $\hat{x}$  is perpendicular to the  $\hat{s}$  direction and parallel to the magnetic midplane.  $\hat{y}$  is perpendicular to the magnetic midplane. We write the relations of the unit vectors as:

$$\begin{aligned}
 \hat{x} &= \hat{y} \times \hat{s} \\
 \hat{y} &= \hat{s} \times \hat{x} \\
 \hat{s} &= \hat{x} \times \hat{y}
 \end{aligned}
 \tag{A.1}$$

Consider the ideal trajectory, unit vectors depend only on the coordinate  $s$ . We use the prime to indicate the operation  $d/ds$ . We may write as:



$$\begin{aligned}
\hat{x}' &= h\hat{s} \\
\hat{y}' &= 0 \\
\hat{z}' &= -h\hat{x}
\end{aligned} \tag{A.2}$$

$h=1/\rho_0$  where  $\rho_0$  is the radius of curvature of the ideal trajectory defined as positive as shown in Fig.2.1. To facilitate the equation of motion, we rewrite the equation of motion in terms of the expressions  $d\mathbf{R}/dR$  (the unit tangent vector of the trajectory) and  $d^2\mathbf{R}/dR^2$  (the deviation of the unit tangent vector), where  $\mathbf{R}$  is the coordinate vector and  $R$  is the the absolute value of  $R$ , namely:

$$\begin{aligned}
\frac{d\mathbf{R}}{dR} &= \frac{d\mathbf{R}}{ds} \frac{ds}{dR} = \frac{\mathbf{R}'}{R'} \\
\frac{d^2\mathbf{R}}{dR^2} &= \frac{1}{R'} \frac{d}{ds} \left( \frac{\mathbf{R}'}{R'} \right) \\
(R')^2 \frac{d^2\mathbf{R}}{dR^2} &= \mathbf{R}'' - \frac{1}{2} \frac{\mathbf{R}'}{(R')^2} \frac{d}{ds} (R')^2
\end{aligned} \tag{A.3}$$

Consider the equation of motion for a particle in a static magnetic field. Let  $e$  be the charged particle,  $\mathbf{B}$  the static magnetic field and  $\mathbf{v}$  the velocity of the particle. We write the relation of the time rate of the change of the momentum according to the *Lorentz force*:

$$\frac{d\mathbf{P}}{dt} = e(\mathbf{v} \times \mathbf{B}) \tag{A.4}$$

We write the velocity  $\mathbf{v}$  in terms of the tangent unit vector of trajectory as  $\left( \frac{d\mathbf{R}}{dR} \right) v$  and the momentum  $\mathbf{P}$  as  $\left( \frac{d\mathbf{R}}{dR} \right) P$ . Equation (4) becomes:

$$\begin{aligned}
v \frac{d}{dR} \left( \frac{d\mathbf{R}}{dR} P \right) &= e v \left( \frac{d\mathbf{R}}{dR} \times \mathbf{B} \right) \\
P \frac{d^2\mathbf{R}}{dR^2} + \frac{d\mathbf{R}}{dR} \left( \frac{dP}{dR} \right) &= e \left( \frac{d\mathbf{R}}{dR} \times \mathbf{B} \right)
\end{aligned}$$

Since the static magnetic force is always perpendicular to the velocity of the particle, the momentum  $P$  is expected as constant.  $dP/dR$  is, therefore, vanished. The final result is:

$$\frac{d^2\mathbf{R}}{dR^2} = \frac{e}{P} \left( \frac{d\mathbf{R}}{dR} \times \mathbf{B} \right)$$

Substituting this equation into equation (A.3) and after simplification we obtain:

$$\mathbf{R}'' - \frac{1}{2} \frac{\mathbf{R}'}{(R')^2} \frac{d}{ds} (R')^2 = \frac{e}{P} R' (\mathbf{R}' \times \mathbf{B}) \quad (\text{A.5})$$

Consider the coordinate system, the three dimensions is illustrated by Fig. A.1

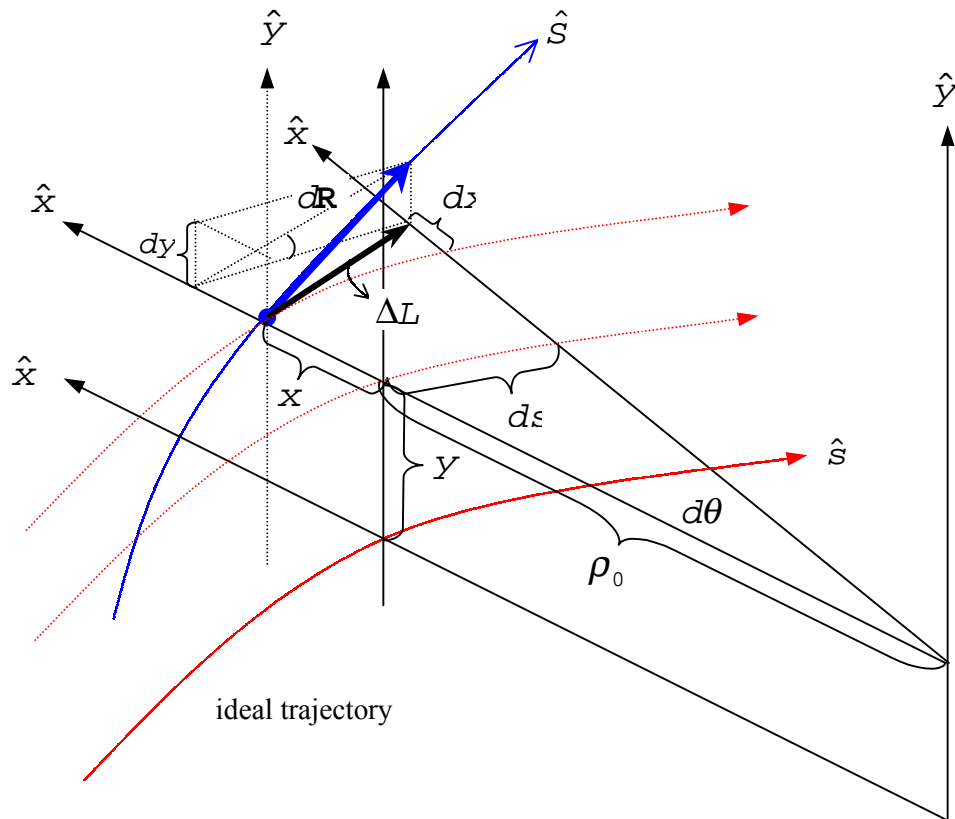


**Fig. A.1** Deflecting of a particle trajectory, ideal trajectory  $\hat{S}$  and individual trajectory  $\hat{S}$ .

where  $d\theta$  is the deflection angle. From the Fig.A.1 the deflection angle for the ideal trajectory is  $d\theta = \rho_0 ds$  (see Fig.A.1), so when  $d\theta$  is small, we can approximately calculate the path length element for individual trajectory as:

$$\begin{aligned} d\mathbf{R} &= \hat{y}dy + \hat{x}dx + \hat{z}\Delta L \\ &= \hat{y}dy + \hat{x}dx + \hat{z}(\rho_0 + x)d\theta \\ d\mathbf{R} &= \hat{x}dx + \hat{y}dy + (1 + hx)\hat{z}ds \end{aligned} \quad (\text{A.6})$$

and we obtain:

$$(dR)^2 = d\mathbf{R} \cdot d\mathbf{R} = dx^2 + dy^2 + (1+hx)^2 ds^2$$

Differentiating equation (A.6) with respect to  $s$ . From equation (A.2), we obtain:

$$\begin{aligned}\mathbf{R}' &= x'\hat{x} + y'\hat{y} + (1+hx)\hat{s} \\ (R')^2 &= x'^2 + y'^2 + (1+hx)^2 \\ \frac{1}{2} \frac{d}{dR} (R')^2 &= x'x'' + y'y'' + (1+hx)(hx' + h'x)\end{aligned}$$

and

$$\mathbf{R}'' = (x'' - h(1+hx))\hat{x} + y''\hat{y} + (2hx' + h'x)\hat{s}$$

Substituting these equations into equation (A.5), we obtain the equation of motion as:

$$\begin{aligned}& \left( x'' - h(1+hx) - \frac{x'}{(R')^2} (x'x'' + y'y'' + (1+hx)(hx' + h'x)) \right) \hat{x} \\ & + \left( y'' - \frac{y'}{(R')^2} (x'x'' + y'y'' + (1+hx)(hx' + h'x)) \right) \hat{y} \\ & + \left( (2hx' + h'x) - \frac{(1+hx)}{(R')^2} (x'x'' + y'y'' + (1+hx)(hx' + h'x)) \right) \hat{s} \quad (\text{A.7}) \\ & = \left( \frac{e}{P} R' (y'B_t - (1+hx)B_y) \right) \hat{x} + \left( \frac{e}{P} R' (1+hx)B_x - x'B_t \right) \hat{y} \\ & + \left( \frac{e}{P} R' (x'B_y - y'B_x) \right) \hat{s}\end{aligned}$$

If now we retain only terms to second-order in  $x$ ,  $y$  and their derivatives and note that  $(R')^2 = 1 + 2hx + \dots$ , that is  $1/(R')^2 = 1 - 2hx + \dots$ . The components of the equation of motion,  $x$  and  $y$  as:

$$\begin{aligned}x'' - h(1+hx) - x'(hx' + h'x) &= \frac{e}{P} R' (y'B_s - (1+hx)B_y) \\ y'' - y'(hx' + h'x) &= \frac{e}{P} R' (1+hx)B_x - x'B_s\end{aligned} \quad (\text{A.8})$$

# Appendix B

## Magnetic Field Expansion to Second-Order Only

For the particle in vacuum, we may express the relation of the static magnetic and the scalar magnetic potential as: (since we are restricting the problem to static magnetic fields, we can omit the minus sign, for convenience)

$$\mathbf{B} = \nabla\phi \quad (\text{B.1})$$

The scalar magnetic potential  $\phi$  will be expanded in the curvilinear coordinate about the ideal trajectory on the midplane which is already shown in Fig.1.1. And the Laplace equation is used:

$$\nabla^2\phi = 0 \quad (\text{B.2})$$

In appendix A we have:

$$d\mathbf{R} = \hat{x}dx + \hat{y}dy + (1 + hx)\hat{s}ds$$

therefore, the Laplace equation has the form of:

$$\nabla^2\phi = \frac{1}{(1 + hx)} \frac{\partial}{\partial x} \left[ (1 + hx) \frac{\partial\phi}{\partial x} \right] + \frac{\partial^2\phi}{\partial y^2} + \frac{1}{(1 + hx)} \frac{\partial}{\partial s} \left[ \frac{1}{(1 + hx)} \frac{\partial\phi}{\partial s} \right] = 0 \quad (\text{B.3})$$

Since the scalar magnetic potential  $\phi$  is an odd function,  $\phi(x, y, s) = -\phi(x, -y, s)$ . This is equivalent to say that:

$$\begin{aligned} B_x(x, y, s) &= -B_x(x, -y, s) \\ B_y(x, y, s) &= B_y(x, -y, s) \\ B_s(x, y, s) &= -B_s(x, -y, s) \end{aligned} \quad (\text{B.4})$$

For the ideal trajectory, on midplane  $y = 0$ , equation (B.4) gives  $B_x = B_s = 0$ . Only  $B_y$  remains nonzero, therefore, generally we make an answer of the Laplace equation, with equation (B.1), in the form of a power expansion with respect to the ideal trajectory:

$$\phi(x, y, s) = (A_{10} + A_{11}x + A_{12} \frac{x^2}{2!} + \dots y) + (A_{30} + A_{31}x + A_{32} \frac{x^2}{2!} + \dots \frac{y^3}{3!}) + \dots \quad (\text{B.5})$$

where (see equation (B.4), only  $B_y$  is nonzero on the midplane)

$$A_{1n} = \left. \frac{\partial^n B_y}{\partial x^n} \right|_{\substack{x=0 \\ y=0}} = \text{Function of } s \text{ only} \quad (\text{B.6})$$

Substituting equation (B.5) into equation (B.3). Give the recursion formula, but instead we shall only be interested in the first- and second-order, namely we shall find that:

$$A_{30} = -(A_{10}'' + hA_{11} + A_{12})$$

Inserting equation (B.5) in to (B.1), we obtain:

$$\begin{aligned} B_x(x, y, s) &= A_{11}y + A_{12}xy + \dots \\ B_y(x, y, s) &= A_{10} + A_{11}x + \frac{1}{2!} A_{12}x^2 + \frac{1}{2!} A_{30}y^2 + \dots \\ B_s(x, y, s) &= \frac{1}{(1+hx)} (A_{10}'y + A_{11}'xy + \dots) \end{aligned} \quad (\text{B.7})$$

Inspection, consider the ideal trajectory particle,  $y=0$ . Equation (B.7) becomes:

$$\begin{aligned} B_x(x, 0, s) &= 0 \\ B_y(x, 0, s) &= A_{10} + A_{11}x + \frac{1}{2!} A_{12}x^2 + \dots \\ B_s(x, 0, s) &= 0 \end{aligned} \quad (\text{B.8})$$

Considering only  $B_y$ , using equation (B.6) we obtain:

$$B_y(x, 0, s) = B_y \Big|_{\substack{x=0 \\ y=0}} + \left. \frac{\partial B_y}{\partial x} \right|_{\substack{x=0 \\ y=0}} + \frac{1}{2!} \left. \frac{\partial^2 B_y}{\partial x^2} \right|_{\substack{x=0 \\ y=0}} + \dots \quad (\text{B.9})$$

If we write  $B_y$  in terms of dimensionless quantities  $n(s)$   $\beta(s)$  etc., we shall obtain:

$$B_y(x, 0, s) = B_y(0, 0, s) \{ 1 - nhx + \beta h^2 x^2 + \dots \} \quad (\text{B.10})$$

Direct comparison of equation (B.9) and (B.10) yields:

$$n = - \left( \frac{1}{hB_y} \left( \frac{\partial B_y}{\partial x} \right) \right) \Bigg|_{\substack{x=0 \\ y=0}} \quad \text{and} \quad \beta = \frac{1}{2!h^2B_y} \left( \frac{\partial^2 B_y}{\partial x^2} \right) \Bigg|_{\substack{x=0 \\ y=0}} \quad (\text{B.11})$$

From the beam rigidity in equation (2.6) and equation (B.10), we obtain the coefficients of the field expansions as:

$$\begin{aligned} A_{10} &= B_y(0,0,s) = h \left( \frac{P_0}{e} \right) \\ A_{11} &= \frac{\partial B_y}{\partial x} \Bigg|_{\substack{x=0 \\ y=0}} = -nh^2 \left( \frac{P_0}{e} \right) \\ \frac{1}{2!} A_{12} &= \frac{1}{2!} \frac{\partial^2 B_y}{\partial x^2} \Bigg|_{\substack{x=0 \\ y=0}} = 2\beta h^3 \left( \frac{P_0}{e} \right) \\ A_{30}'' &= -[h'' - nh^3 + 2\beta h^3] \left( \frac{P_0}{e} \right) \\ A_{10}' &= h \left( \frac{P_0}{e} \right) \\ A_{11}' &= -[2nhh' + n'h^2] \left( \frac{P_0}{e} \right) \end{aligned} \quad (\text{B.12})$$

Substituting this equation into equation (B.7), we obtain:

$$\begin{aligned} B_x(x,y,s) &= \left( \frac{P_0}{e} \right) [-nh^2y + 2\beta h^3xy + \dots] \\ B_y(x,y,s) &= \left( \frac{P_0}{e} \right) [h + -nh^2x + \beta h^3x^2 - \frac{1}{2}(h'' - nh^3 + 2\beta h^3)y^2 + \dots] \quad (\text{B.13}) \\ B_s(x,y,s) &= \left( \frac{P_0}{e} \right) [(h'y - (n'h^2 + 2nhh' + hh')xy + \dots)]. \end{aligned}$$

# Appendix C

## The First-Order Solutions of the Equation of Motion

We express the specific position of an arbitrary particle with respect to the ideal trajectory at  $s=0$  as  $x_0, y_0, x'_0, y'_0$  and  $\delta$ . These five boundary values are equal to zero for the ideal trajectory. The fivefold Taylor expansion shall be considered in a general way using these boundary values and detailed formulas only first-order shall be developed. The expressions are written as:

$$\begin{aligned} x &= \sum (x|_{x_0^{\kappa} y_0^{\lambda} x'_0{}^{\mu} y'_0{}^{\nu} \delta^{\chi}}) x_0^{\kappa} y_0^{\lambda} x'_0{}^{\mu} y'_0{}^{\nu} \delta^{\chi} \\ y &= \sum (y|_{x_0^{\kappa} y_0^{\lambda} x'_0{}^{\mu} y'_0{}^{\nu} \delta^{\chi}}) x_0^{\kappa} y_0^{\lambda} x'_0{}^{\mu} y'_0{}^{\nu} \delta^{\chi} \end{aligned} \quad (C.1)$$

Where  $\sum$  indicates the summation over zero and all-positive integer values of the exponents  $\kappa, \lambda, \mu, \nu$  and  $\chi$ .  $x$  and  $y$  are the deviations of an arbitrary trajectory with respect to the ideal trajectory as function of  $s$ . The parentheses are the symbol for the Taylor coefficients, these coefficients are function of  $s$ . The detailed calculations involve only the terms of first-order, namely:

$$\begin{aligned} x &= (x|_1) + (x|x_0) x_0 + (x|y_0) y_0 + (x|x'_0) x'_0 + (x|y'_0) y'_0 + (x|\delta) \delta + \text{Higher order} \\ y &= (y|_1) + (y|x_0) x_0 + (y|y_0) y_0 + (y|x'_0) x'_0 + (y|y'_0) y'_0 + \text{Higher order} \end{aligned} \quad (C.2)$$

The terms which indicate a coupling between the coordinates  $x$  and  $y$  would be zero, and the constant terms are zero also, namely: (results from the midplane symmetry.)

$$\begin{aligned} (x|y_0) &= (y|x_0) = 0 \\ (x|y'_0) &= (y|x'_0) = 0 \\ (x|_1) &= (y|_1) = 0 \end{aligned} \quad (C.3)$$

Equation (C.2) becomes:

$$\begin{aligned} x &= (x|x_0) x_0 + (x|x'_0) x'_0 + (x|\delta) \delta \\ y &= (y|y_0) y_0 + (y|y'_0) y'_0 \end{aligned} \quad (C.4)$$

It is convenient to introduce the following abbreviations:

$$\begin{aligned} (x|x_0) &= c_x & (x|x'_0) &= s_x & (x|\delta) &= \eta_x \\ (y|y_0) &= c_y & (y|y'_0) &= s_y \end{aligned} \quad (C.5)$$

The equation (C.4) becomes:

$$\begin{aligned} x &= c_x x_0 + s_x x'_0 + \eta_x \delta \\ y &= c_y y_0 + s_y y'_0 \end{aligned} \quad (C.6)$$

Substituting equation (C.6) into equation (2.12), By comparing the coefficients of  $x_0, x'_0, y_0, y'_0$  and  $\delta$ , we obtain:

$$\begin{aligned} c_x'' + k_x^2 c_x &= 0 \\ s_x'' + k_x^2 s_x &= 0 \\ c_y'' + k_y^2 c_y &= 0 \\ s_y'' + k_y^2 s_y &= 0 \\ \eta_x'' + k_x^2 \eta_x &= h \end{aligned} \quad (C.7)$$

where  $k_x^2 = (1-n)h^2$  and  $k_y^2 = nh^2$ . Equation (C.7) indicates that the solutions of the first-order equations of motion (equation (2.12)) are  $c_x, s_x, \eta_x$  for the  $x$  motion and  $c_y, s_y$  for the  $y$  motion. At  $s=0$  the coefficients in equation (C.5) satisfy the following boundary conditions:

$$\begin{aligned} c(0) &= 1 & c'(0) &= 0 \\ s(0) &= 0 & s'(0) &= 1 \\ \eta_x(0) &= 0 & \eta_x'(0) &= 0 \end{aligned} \quad (C.8)$$

Now we shall calculate the solutions of equation (C.7) both the homogeneous and inhomogeneous equation.

### Solutions of the homogeneous equation of motion

It is very convenient to approximate  $h$ ,  $n$ , and  $k^2$  in the equation of motions as uniform piecewise. With these restrictions and the boundary conditions (equation (C.8)), the solutions of the homogeneous equations of motion (C.7) are the simple trigonometric functions, namely:

$$\begin{aligned} c_x(s) &= \cos k_x s & s_x(s) &= \left(\frac{1}{k_x}\right) \sin k_x s \\ c_y(s) &= \cos k_y s & s_y(s) &= \left(\frac{1}{k_y}\right) \sin k_y s \end{aligned} \quad (C.9)$$



And for  $k_x, k_y$  are negative values:

$$\begin{aligned} c_x(s) &= \cos|k_x|s & s_x(s) &= \left(\frac{1}{|k_x|}\right) \sin|k_x|s \\ c_y(s) &= \cos|k_y|s & s_y(s) &= \left(\frac{1}{|k_y|}\right) \sin|k_y|s \end{aligned} \quad (\text{C.10})$$

where  $k_x^2 = (1-n)h^2$  and  $k_y^2 = nh^2$ .  $h = 1/\rho_0$  is constant where  $\rho_0$  is the radius of the ideal trajectory.  $c_i$  stands for  $c_x, c_y$ , and  $s_i$  stands for  $s_x, s_y$ . They are represented in each interval of uniformity by a sinusoidal function, hyperbolic function, linear function of  $s$ , or a simply constant. The  $c_i$  and  $s_i$  are called cosine like solutions and sine like solutions, respectively. Using equation (C.7), we may write the interested relation as:

$$\frac{d}{ds}(c_i s'_i - c'_i s_i) = 0$$

Integrate this equation, use the boundary conditions (C.8), we find:

$$(c_i s'_i - c'_i s_i) = 1 \quad (\text{C.9})$$

This expression is the determinant of the first-order transport matrix representing either  $x$  or  $y$  equations of motion (see Wronskian determinant), namely:

$$\begin{vmatrix} c_i & s_i \\ c'_i & s'_i \end{vmatrix} = 1: \text{Constant} \quad (\text{C.10})$$

This equation is equivalent to Liouville's theorem (see Wiedemann, H. (1993). Particle Accelerator Physics (Vol. 1)) which states that phase areas are conserved throughout the system in either  $x$  and  $y$  plane motions.

### First-Order solutions of the inhomogeneous equation of motion

In equation (C.7) an inhomogeneous equation is shown as:

$$\eta''_x + k_x^2 \eta_x = h \quad (\text{C.11})$$

From equation (C.5) we have  $\eta_x = (x|\delta)$  where  $\delta = \Delta P/P$ . This indicates that the beam is not monochromatic but has a finite spread of energies. The variation in the deflection is caused by such a *chromatic error*  $\Delta E$  in the bending magnets. The function  $\eta_x$  is called *dispersion function*. We use Green's function method to solve this perturbation equation by obtaining:

$$\eta_x = \int_0^s h(\tau) G(s, \tau) d\tau \quad (\text{C.12})$$

where  $\tau$  is just the variable of integration and:

$$G(s, \tau) = s_x(s)c_x(\tau) - c_x(\tau)s_x(s) \quad (\text{C.13})$$

After inserting equation (C.13) into equation (C.12), we obtain:

$$\eta_x = s_x(s) \int_0^s h(\tau) c_x(\tau) d\tau - c_x(s) \int_0^s h(\tau) s_x(\tau) d\tau \quad (\text{C.14})$$

The first derivative of equation (C.14) respects to  $s$  as:

$$\begin{aligned} \eta'_x &= s'_x(s) \int_0^s h(\tau) c_x(\tau) d\tau + c_x(s) s_x(s) h(s) - c'_x(s) \int_0^s h(\tau) s_x(\tau) d\tau - c_x(s) s_x(s) h(s) \\ &= s'_x(s) \int_0^s h(\tau) c_x(\tau) d\tau - c'_x(s) \int_0^s h(\tau) s_x(\tau) d\tau \end{aligned}$$

And the second derivative respects to  $s$ :

$$\eta''_x = s''_x(s) \int_0^s h(\tau) c_x(\tau) d\tau - c''_x(s) \int_0^s h(\tau) s_x(\tau) d\tau + s'_x(s) c_x(s) h(s) - c'_x(s) s_x(s) h(s)$$

Using the relation  $(c_x s'_x - c'_x s_x) = 1$ , (C.9) we obtain:

$$\eta''_x = s''_x(s) \int_0^s h(\tau) c_x(\tau) d\tau - c''_x(s) \int_0^s h(\tau) s_x(\tau) d\tau + h(s)$$

Substituting them into equation (2.11), we obtain:

$$\eta''_x + k_x^2 \eta_x = h(s)$$

which is the identical to equation (C.11). Therefore, equation (C.14) is indeed a particular solution of the inhomogeneous equation. That is:

$$\eta_x = s_x(s) \int_0^s h(\tau) c_x(\tau) d\tau - c_x(s) \int_0^s h(\tau) s_x(\tau) d\tau$$

Using equations (C.9) and (C.10), we find that:

$$\eta_x = \frac{h}{k_x^2} [1 - \cos k_x s] = \frac{h}{k_x^2} [1 - c_x] \quad (\text{C.15})$$

# Appendix D

## Betatron Functions

The homogeneous differential equation of motion:

$$u'' + k(s)u = 0 \quad (D.1)$$

We apply the variation method of integration constants and use the try solutions with amplitude and phase as function of  $s$ , namely:

$$u(s) = \sqrt{\varepsilon\beta(s)} \cos(\psi(s) - \psi_0) \quad (D.2)$$

The first and second derivatives of equation (D.2),  $\beta \equiv \beta(s)$   $\psi \equiv \psi(s)$ , are:

$$u' = \frac{\beta'}{2} \sqrt{\frac{\varepsilon}{\beta}} \cos(\psi - \psi_0) - \sqrt{\varepsilon\beta} \sin(\psi - \psi_0) \psi' \quad (D.3)$$

$$u'' = \sqrt{\varepsilon} \frac{\beta\beta'' - \frac{1}{2}\beta'^2}{2\beta^{3/2}} \cos(\psi - \psi_0) - \sqrt{\frac{\varepsilon}{\beta}} \beta' \sin(\psi - \psi_0) \quad (D.4)$$

$$- \sqrt{\varepsilon\beta} \sin(\psi - \psi_0) \psi'' - \sqrt{\varepsilon\beta} \cos(\psi - \psi_0) \psi'^2$$

Substituting equations (D.4) and (D.2) into (D.1). Regard that equation (D.2) is the solution on the condition that the sum of all coefficients of the sine and cosine terms equal zero, namely:

$$\frac{1}{2} \left( \beta\beta'' - \frac{1}{2}\beta'^2 \right) - \beta^2 \psi'^2 + \beta^2 k = 0 \quad (D.5)$$

and

$$\begin{aligned} \beta'\psi' + \beta\psi'' &= 0 \\ (\beta\psi')' &= 0 \\ \beta\psi' &= \text{Constant} \\ \beta\psi' &= 1 \end{aligned} \quad (D.6)$$

Where the constant is chosen equal to the unity since the normalization of the *phase function*, after integration we obtain the phase function as:

$$\psi(s) = \int_0^s \frac{d\tau}{\beta(\tau)} + \psi_0 \quad (D.7)$$

Inserting equation (D.6) into (D.5), we obtain:

$$\frac{1}{2} \beta \beta'' - \frac{1}{4} \beta'^2 + \beta^2 k = 1 \quad (\text{D.8})$$

with

$$\begin{aligned} \alpha &= -\frac{1}{2} \beta' \\ \gamma &= \frac{(1 + \alpha^2)}{\beta} \end{aligned} \quad (\text{D.9})$$

Equation (D.8) becomes:

$$\beta'' + 2k\beta - 2\gamma = 0 \quad (\text{D.10})$$

Using the general solution  $u(s)$  of equation (D.2), its derivative  $u'(s)$  of equation (D.3) and the phase function, equation (D.7), we obtain:

$$C(u, u') = \varepsilon = \gamma u^2 + 2\alpha u u' + \beta u'^2 \quad (\text{D.11})$$

where  $C(u, u')$  is the *Courant-Snyder invariant*.  $\varepsilon$  is the emittance and the parameters  $\gamma, \alpha$  and  $\beta$  are called Twiss parameters. Particularly,  $\beta$  is called the betatron function or betafunction.

To normalize the coordinate  $(u, s)$  we define new variables as:

$$w(\varphi) = \frac{u(s)}{\sqrt{\beta(s)}} \quad (\text{D.12})$$

and

$$\varphi = \frac{\psi}{\nu} = \frac{1}{\nu} \int_0^s \frac{d\tau}{\beta(\tau)} \quad (\text{D.13})$$

where the *phase function*  $\varphi$  in coordinates  $(w, \varphi)$  stand for  $\varphi_x$  and  $\varphi_y$ . The *betatron tune*  $\nu$  stands for  $\nu_x$  and  $\nu_y$ . From equation (D.12),  $d\varphi/dt \equiv \varphi'$ , we obtain the derivatives:

$$\begin{aligned} u &= \sqrt{\beta} w \\ u' &= \frac{1}{\nu \sqrt{\beta}} \frac{dw}{d\varphi} + \frac{\beta'}{2\sqrt{\beta}} \quad ; \varphi' = \frac{1}{\nu \beta} \\ u'' &= \frac{1}{\nu^2 \beta^{3/2}} \frac{d^2 w}{d\varphi^2} + w \left( \frac{\beta''}{2\sqrt{\beta}} - \frac{\beta'^2}{4\beta^{3/2}} \right) \end{aligned}$$

Inserting these equations into equation (D.1), we obtain:

$$\frac{d^2 w}{d\varphi^2} + v^2 \left( \frac{\beta\beta''}{2} - \frac{\beta'^2}{4} + k\beta^2 \right) w = 0$$

Using equation (D.8) we obtain the final form of harmonic oscillation equation, these coordinates  $(w, \varphi)$  are called the *normalized coordinates*:

$$\frac{d^2 w}{d\varphi^2} + v^2 w = 0 \tag{D.14}$$

# Appendix E

## Radiation Damping and Excitations

### Synchrotron Radiation Power per Turn

The instantaneous power radiated by a relativistic electron at energy  $E$  depends on the angle between the force and the electron velocity, namely:

$$P_{\perp} = \gamma^2 P_{\parallel} \quad (\text{E.1})$$

where  $\gamma^2 = (E/mc^2)^2$ . Since, the power when the force is perpendicular to the velocity  $P_{\perp} \equiv P_{\gamma}$  is much larger than when the force is parallel to the velocity, we shall consider only  $P_{\gamma}$  which is defined by:

$$P_{\gamma} = C_{\gamma} \frac{e^2 c^3}{2\pi} E^2 B^2 \quad (\text{E.2})$$

where  $B$  is the magnetic field.  $E$  is the energy of the electron.  $C_{\gamma}$  is Sand's radiation constant defined as:

$$C_{\gamma} = 8.85 \times 10^{-5} \text{ m /GeV}^3$$

Sometimes we usefully express equation (E.2) in the form of:

$$P_{\gamma} = C_{\gamma} \frac{c}{2\pi} \frac{E^4}{\rho^2} \quad (\text{E.3})$$

If we integrate the power  $P_{\gamma}$  with respect to time  $t$  once around the ring, we shall get the *total energy radiation in one revolution*  $U_0$ . Since  $dt = ds/c$ , we obtain:

$$U_0 = \frac{C_{\gamma} E_0^4}{2\pi} \oint \frac{ds}{\rho^2} = \frac{C_{\gamma} E_0^4}{2\pi} \oint h^2(s) ds \quad (\text{E.4})$$

By using the distance around the ring  $L = 2\pi R$ , we can write equation (E.4) in the useful form as:

$$U_0 = C_\gamma E_0^4 R \oint \frac{1}{L} h^2 ds = C_\gamma E_0^4 R \langle h^2 \rangle \quad (\text{E.5})$$

For an isomagnetic ring,  $h = 1/\rho_0$  we obtain:

$$U_0 = \frac{C_\gamma E_0^4}{\rho_0} \quad (\text{isomagnetic}) \quad (\text{E.6})$$

Therefore, the total average of synchrotron radiation power per turn is:

$$\langle P_\gamma \rangle = \frac{U_0}{T_0} = \frac{c C_\gamma}{2\pi} E_0^4 \langle h^2 \rangle \quad (\text{E.7})$$

Here  $T_0 = c/2\pi R$  is the revolution period where  $R$  is the average radius of the storage ring. For an isomagnetic ring the total average of synchrotron radiation power per turn is:

$$\langle P_\gamma \rangle = \frac{c C_\gamma}{2\pi} \frac{E_0^4 h_0}{R} = \frac{c C_\gamma E_0^4}{L \rho_0} \quad (\text{isomagnetic}) \quad (\text{E.8})$$

## Damping of Synchrotron Motion

The variation of the synchrotron radiation power around synchronous energy  $E_0$  may be written as:

$$U_{rad}(E) = U_0 + W \Delta E \quad (\text{E.9})$$

where

$$W = \left. \frac{dU_{rad}}{dE} \right|_{E=E_0} \quad (\text{E.10})$$

Consider the moving position of the synchronous electron at the center of the bunch and any other electron position in the bunch by giving its longitudinal displacement  $z$  from the bunch center. The Figure E.1 shows the positions of two revolutions of the electron within a bunch. One revolution the electron is ahead of the synchronous electron by distance  $z_1$ . Next revolution the longitudinal displacement has decreased to  $z_2$ .

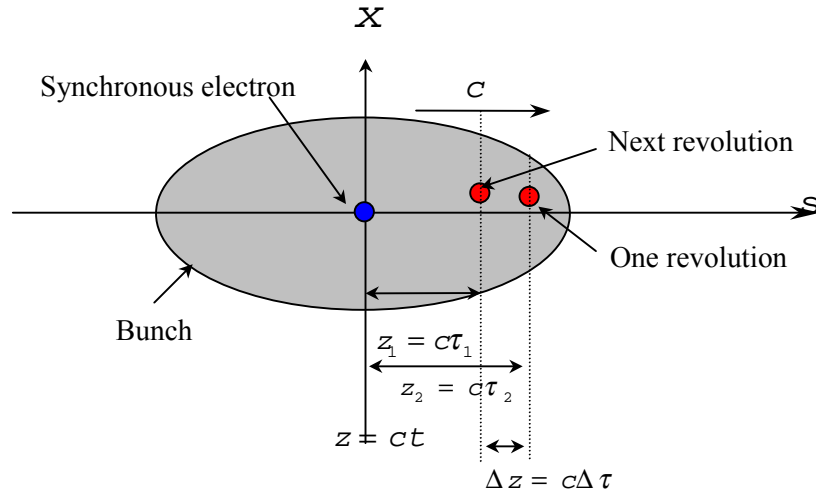


**Fig.E.1** Longitudinal motion of an electron within a bunch

We assume that the electron travel at the speed of light  $c$ . Therefore, the time displacement from the center of the bunch is:

$$\Delta\tau(t) = \frac{\Delta z(t)}{c} \quad (\text{E.11})$$

We note that the time displacement is positive when the electron arrives at each azimuth ahead of the synchronous electron. The path length difference between the any electron of energy  $E$  and the synchronous electron of energy  $E_0$  is (see section 2.3.1):

$$\Delta L = \alpha_c L_0 \frac{\Delta E}{E_0} \quad (\text{E.12})$$

where  $\alpha_c$  is the momentum compaction factor and  $L_0$  is the ideal trajectory path length. The electron fails to reach its previous azimuth distance  $\Delta z = -\Delta L$ . From equation (E.11-12), we obtain:

$$\Delta\tau = -\alpha_c T_0 \frac{\Delta E}{E_0} \quad (\text{E.13})$$

where  $T_0 = L_0/c$  is the period of the synchronous electron. Thus, the time rate of change (on average) of  $\tau$  is  $\Delta\tau/T_0$  or:

$$\frac{d\tau}{dt} = -\alpha_c \frac{\Delta E}{E_0} \quad (\text{E.14})$$



During the revolution, the electron loses energy  $U_{rad}$  into synchrotron radiation. This loss is compensated by the RF energy gain,  $eV(\tau)$ , in the RF cavity. Thus, the net changes in energy is (on average):

$$\frac{d(\Delta E)}{dt} = \frac{eV(\tau) - U_{rad}}{T_0} \quad (E.15)$$

We focus only on the small energy oscillations which is small time displacement. We retain only the linear part of the variation of  $V(\tau)$ . Then, we write the energy gain in the RF cavity  $U_{rf}$  to compensate the energy loss as:

$$U_{rf} = eV(\tau) = U_0 + e\dot{V}\tau \quad (E.16)$$

where  $U_0$  is the energy gain at  $\tau = 0$  and  $\dot{V} = dV/d\tau$ .

To simplicity, we assume that the RF voltage of the RF cavity in storage ring to have a sinusoidal variation with time, namely:

$$V(\tau) = V_0 \sin \omega_{rf}(\tau + \tau_s) \quad (E.17)$$

where  $\omega_{rf}\tau_s$  is called the *synchronous RF phase angle*. The RF angular frequency is:

$$\omega_{rf} = k \frac{2\pi}{T_0} = k\omega_0 \quad (E.18)$$

where  $k$  is the harmonic number and  $\omega_0$  is the *revolution angular frequency*.

From equation (E.17) and (E.16) at  $\tau = 0$  we obtain:

$$U_0 = eV_0 \sin \omega_{rf}\tau_s \quad (E.19)$$

and

$$\dot{V} = \omega_{rf} V_0 \cos \omega_{rf}\tau_s \quad (E.20)$$

Combining equations (E.15) and (E.16) and approximation for small  $\tau$  and  $\Delta E$ , using equation (E.9), we obtain:

$$\frac{d(\Delta E)}{dt} = \frac{e\dot{V}\tau - W \Delta E}{T_0} \quad (E.21)$$

Taking the time derivation of (E.14) and combining with (E.21) we obtain:

$$\frac{d^2\tau}{d\ell^2} + 2\alpha_E \frac{d\tau}{dt} + \omega_s^2 \tau = 0 \quad (\text{E.22})$$

with

$$\alpha_E = \frac{W}{2T_0} \quad (\text{E.23})$$

and

$$\omega_s^2 = \frac{\alpha_c \dot{\mathcal{V}}}{T_0 E_0} \quad (\text{E.24})$$

Equation (E.22) is the equation of the damped harmonic oscillator with synchrotron frequency  $\omega_s$  and the damping constant  $\alpha_E$ . This oscillations is simply called the *synchrotron oscillations*. Since the damping rate in storage ring is normally small,  $\alpha_E \ll \omega_s$ , the solution of (E.22) is:

$$\tau = A e^{-\alpha_E t} \cos(\omega_s t - \theta_0) \quad (\text{E.25})$$

## The Damping Partition

Consider equation (E.23), we have:

$$\alpha_E = \frac{W}{2T_0} = \frac{1}{2T_0} \left. \frac{dU_{rad}}{dE} \right|_{E=E_0} \quad (\text{E.26})$$

The radiation energy loss per revolution can be evaluated by:

$$U_{rad} = \oint P_\gamma dt = \oint P_\gamma \frac{dt}{ds} ds = \frac{1}{c} \oint P_\gamma (1 + hx) ds$$

We choose only the displacement due to energy deviation that is  $x = \eta_x \Delta E / E_0$ . Equation (E.26) becomes:

$$U_{rad} = \frac{1}{c} \oint P_\gamma \left( 1 + \eta_x h \frac{\Delta E}{E_0} \right) ds$$

Substituting into equation (E.10), we obtain:

$$W = \left. \frac{dU_{rad}}{dE} \right|_{E=E_0} = \frac{1}{c} \oint \left( \frac{dP_\gamma}{dE} + \eta_x h \frac{P_\gamma}{E_0} \right) ds \quad (\text{E.27})$$

Since  $P_\gamma$  is proportional to the product  $E^2 B^2$ , we obtain:

$$\frac{dP_\gamma}{dE} = 2 \frac{P_\gamma}{E_0} + 2 \frac{P_\gamma}{B_0} \frac{dB}{dE}$$

But

$$\frac{dB}{dE} = \frac{dx}{dE} \frac{dB}{dx} = \frac{\eta_x}{E_0} \frac{dB}{dx},$$

so that

$$\frac{dP_\gamma}{dE} = 2 \frac{P_\gamma}{E_0} + 2 \frac{P_\gamma}{B_0} \frac{\eta_x}{E_0} \frac{dB}{dx} \quad (\text{E.28})$$

Putting it into (E.27), we obtain:

$$W = \left. \frac{dU_{\text{rad}}}{dE} \right|_{E=E_0} = \frac{1}{c} \oint \left( 2 \frac{P_\gamma}{E_0} + 2 \frac{P_\gamma}{B_0} \frac{\eta_x}{E_0} \frac{dB}{dx} + \eta_x h \frac{P_\gamma}{E_0} \right) ds \quad (\text{E.29})$$

$$W = \frac{U_0}{E_0} \left( 2 + \frac{1}{cU_0} \oint \left( \eta_x P_\gamma \left( h + \frac{2}{B_0} \frac{dB}{dx} \right) \right)_{E=E_0} ds \right) \quad (\text{E.30})$$

We may write the damping coefficient in equation (E.26) in the form:

$$\alpha_E = \frac{W}{2T_0} = \frac{U_0}{2T_0 E_0} (2 + D) = (2 + D) \frac{\langle P_\gamma \rangle}{2E_0} \quad (\text{E.31})$$

with

$$D = \frac{1}{cU_0} \oint \left( \eta_x P_\gamma \left( h + \frac{2}{B_0} \frac{dB}{dx} \right) \right)_{E=E_0} ds \quad (\text{E.32})$$

Equation (E.32) be written in a more useful form by taking equations (E.4) and (E.5) and we defining the quadrupole field gradient,  $n(s) = -\frac{1}{hB} \frac{dB}{dx}$ , (see equation (B.11) in Appendix B.) Equation (E.32) becomes:

$$D = \frac{\oint (\eta_x(s) h^3 (1 - 2n(s))) ds}{\oint h^2 ds} \quad (\text{E.33})$$

This equation is called the *damping partition number*. For an isomagnetic ring,  $h = 1/\rho_0$ , we obtain:

$$D = \frac{h_0^2}{2\pi} \oint \eta_x(s) [1 - 2n(s)] ds \quad (\text{isomag}) \quad (\text{E.34})$$

## Damping of Betatron Oscillations

### Vertical Betatron Oscillations

We approximate the motion by ignoring the variation of  $\beta_y$  with  $s$ , then we write the betatron phase-space coordinates as:

$$\begin{aligned} y &= A \cos \phi \\ y' &= \frac{A}{\beta_y} \sin \phi \end{aligned} \quad (\text{E.35})$$

where  $\phi = s/\beta_y$ . The amplitude  $A$  can be obtained by:

$$A^2 = y^2 + (\beta_y y')^2 \quad (\text{E.36})$$

The energy gain  $\delta p$  from RF accelerating force on the average is parallel to the ideal orbit (See Fig.E.2). We write  $p_{\perp}$  for component of momentum  $\mathbf{p}$  that is perpendicular to the ideal orbit.

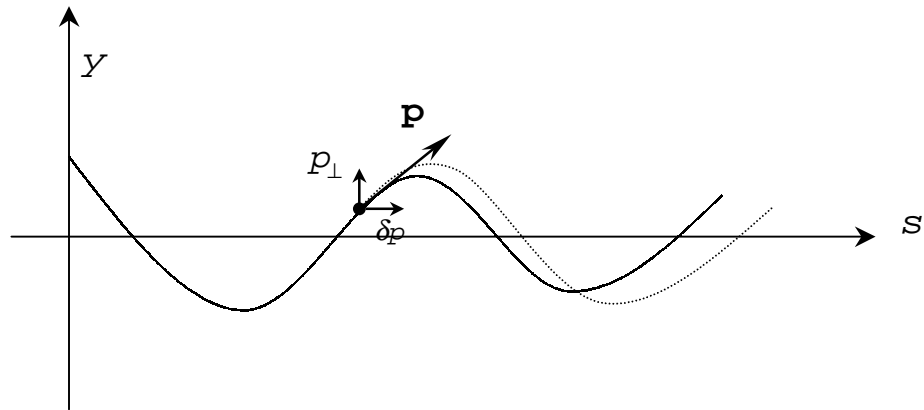


**Fig.E.2.** Effect of energy gain from RF accelerating system on the vertical betatron oscillations.

Since the angle are small, we can write the slope as:

$$y' = \frac{p_{\perp}}{p} \quad (\text{E.37})$$

The accelerating field from RF cavity does not changes  $y$ , but change  $y'$  which goes over to:

$$y' \rightarrow \frac{p_{\perp}}{p + \delta p} = \frac{p_{\perp}}{p} \left( 1 - \frac{\delta p}{p} \right) = y' \left( 1 - \frac{\delta p}{p} \right) \quad (\text{E.38})$$

where the change in  $y'$  is:

$$\Delta y' = -y' \frac{\delta p}{p} = -y' \frac{\delta E}{E} \quad (\text{E.39})$$

where  $\delta E = |c\delta p|$  is the amount of energy loss into synchrotron radiation. Using differentiation of equation (E.36), the corresponding change of amplitude  $A$  is:

$$A\delta A = \langle \beta^2 y' \Delta y' \rangle = -\langle (\beta_y y')^2 \rangle \frac{U_0}{E_0} \quad (\text{E.40})$$

where we now average over the betatron oscillations in one revolution. Since the motion is sinusoidal, we have  $\langle (\beta_y y')^2 \rangle = A^2/2$ . Equation (E.40) becomes:

$$\frac{\delta A}{A} = -\frac{U_0}{2E_0} \quad (\text{E.41})$$

Therefore, The derivation of amplitude can be obtained:

$$\frac{1}{A} \frac{dA}{dt} = \frac{1}{T_0} \frac{\delta A}{A} = -\frac{U_0}{2E_0 T_0} \quad (\text{E.42})$$

By integrating, we find that the motion is exponentially damped, namely  $A = A_0 e^{-\alpha_y t}$ , with the damping coefficient is:

$$\alpha_y = \frac{U_0}{2E_0 T_0} = \frac{\langle P_{\gamma} \rangle}{2E_0} \quad (\text{E.43})$$

We note that this damping does not occur from the synchrotron radiation process, but occurs from process of energy gain from RF system.

### Horizontal Betatron Oscillations

The horizontal displacement from the ideal orbit is:

$$x = x_{\beta} + x_E \quad (\text{E.44})$$

with

$$x_E = \eta_x(s) \frac{\delta E}{E_0} \quad (\text{E.45})$$

where  $x_\beta$  is the betatron displacement,  $x_E$  is the off-energy closed orbit,  $\eta_x$  is the dispersion function and  $\delta E$  is the amount of energy change in one revolution. Similarly, the position in space of the electron is not changed, i.e., the total displacement  $x$  does not change. Therefore, we obtain:

$$\begin{aligned} \delta x &= \delta x_\beta + \delta x_E = 0 \\ \delta x_\beta &= -\delta x_E = -\eta_x \frac{\delta E}{E_0} \end{aligned} \quad (\text{E.46})$$

The resulting change of betatron amplitude can be obtained by the change of the betatron slope (see Fig.E.3):

$$\delta x'_\beta = -\delta x'_E = -\eta'_x \frac{\delta E}{E_0} \quad (\text{E.47})$$

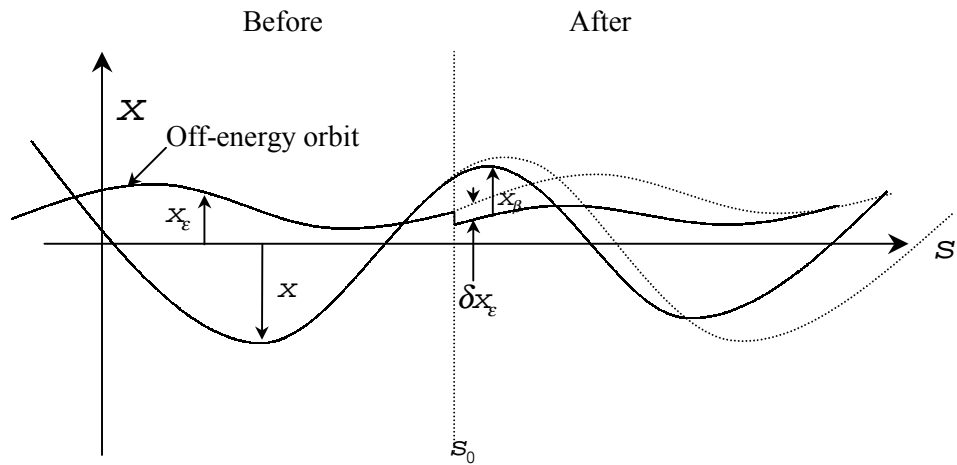


**Fig.E.3.** Effect of energy changes at  $s_0$  on the horizontal betatron displacement.

We may consider the horizontal betatron motion by:

$$\begin{aligned} x_\beta &= A \cos \phi \\ x'_\beta &= -\frac{A}{\beta_x} \sin \phi \end{aligned} \quad (\text{E.48})$$

and

$$A^2 = x_\beta^2 + (\beta_x x'_\beta)^2 \quad (\text{E.49})$$

where  $\phi = s/\beta_x$ , the change in the amplitude becomes:

$$A\delta A = x_\beta \delta x_\beta + \beta^2 x'_\beta \delta x'_\beta \quad (\text{E.50})$$

Using (E.47), we obtain:

$$A\delta A = -(\eta_x x_\beta + \beta^2 \eta'_x x'_\beta) \frac{\delta E}{E_0} \quad (\text{E.51})$$

To simplify the discussion of the damping, we restrict the consideration to separated function of function guide field, so we express the off-energy in an element length  $\delta l$  as:

$$\delta E = -\frac{P_\gamma(x_\beta)}{c} \delta l \quad (\text{E.52})$$

Expanding to first-order of this equation and using equation (E.2) and (A.6), we obtain:

$$\delta E = -\frac{1}{c} \left( P_\gamma + 2 \frac{P_\gamma}{B_0} \frac{dB}{dx_\beta} x_\beta \right) (1 + hx_\beta) ds \quad (\text{E.53})$$

Substituting equation (E.53) into (E.51) and neglecting all linear terms in  $x'_\beta$ . Since their average over the betatron phase is zero, we obtain:

$$A\delta A = x_\beta \eta_x \left( 1 + \frac{2}{B_0} \frac{dB}{dx_\beta} x_\beta + x_\beta h \right) \frac{P_\gamma}{cE_0} ds \quad (\text{E.54})$$

Averages over the betatron oscillations in one revolution, with  $\langle x_\beta \rangle = 0$  and from (E.48)  $\langle x_\beta^2 \rangle = A^2/2$ , we find that:

$$\frac{\langle \delta A \rangle}{A} = \frac{U_0}{2E_0} \frac{\oint \eta_x h^3 (1 - 2n(s)) ds}{\oint h^2 ds} = D \frac{U_0}{2E_0} \quad (\text{E.55})$$

Here we used equation (E.33). We note that the right side is positive, i.e., the rate change is increase in horizontal betatron amplitude due to synchrotron radiation. The contribution from the RF acceleration goes exactly the same as for the vertical

oscillations which is shown in equation (E.42). Thus, we obtain the total effect in one revolution as:

$$\frac{1}{T_0} \frac{\Delta A}{A} = -(1-D) \frac{U_0}{2T_0 E_0} \quad (\text{E.56})$$

therefore, we obtain the damping coefficient in horizontal oscillations as:

$$\alpha_x = (1-D) \frac{U_0}{2T_0 E_0} = (1-D) \frac{\langle P_\gamma \rangle}{2E_0} \quad (\text{E.57})$$

## Damping Partition Numbers

The damping coefficients in equations (E.31), (E.43) and (E.57) may be written in three degrees of freedom in a bunch, namely:

$$\alpha_i = J_i \alpha_0 = J_i \frac{\langle P_\gamma \rangle}{2E_0} \quad (\text{E.58})$$

where  $i$  stand for  $x, y$  and  $E$ .  $\alpha_0 = \langle P_\gamma \rangle / 2E_0$  and the *damping partition numbers* are:

$$J_x = (1-D), \quad J_y = 1, \quad J_E = 2+D \quad (\text{E.59})$$

Consider the summations:

$$\sum J_i = J_x + J_y + J_E = 4 \quad (\text{E.60})$$

Note that the results satisfy the Robinson's theorem (see Robinson's theorem, H. Wiedemann, Particle Accelerator Physics Vol. 1, (1993)).

## Damping Times

The *damping times* are defined by  $1/\alpha_i$ . From (E.58) we obtain:

$$\tau_i = \frac{2E_0}{J_i \langle P_\gamma \rangle} \quad (\text{E.61})$$

Using equation (E.4), we obtain:



$$\begin{aligned}
\tau_x &= \frac{2E_0}{J_x \langle P_\gamma \rangle} = \frac{4\pi}{C_\gamma} \frac{R\rho_0}{J_x E_0^3} = \frac{2E_0}{J_x U_0} T_0 \\
\tau_y &= \frac{2E_0}{J_y \langle P_\gamma \rangle} = \frac{4\pi}{C_\gamma} \frac{R\rho_0}{J_y E_0^3} = \frac{2E_0}{J_y U_0} T_0 \\
\tau_E &= \frac{2E_0}{J_E \langle P_\gamma \rangle} = \frac{4\pi}{C_\gamma} \frac{R\rho_0}{J_E E_0^3} = \frac{2E_0}{J_E U_0} T_0
\end{aligned} \tag{E.62}$$

## Radiation Integrals

In summary we list the radiation integrals as below:

$$I_1 = \oint \left( \frac{\eta_x}{\rho} \right) ds = \oint h \eta_x ds \tag{E.63}$$

$$I_2 = \oint \left( \frac{1}{\rho} \right)^2 ds = \oint h^2 ds \tag{E.64}$$

$$I_3 = \oint \left( \frac{1}{\rho} \right)^3 ds = \oint h^3 ds \tag{E.65}$$

$$I_4 = \oint \frac{\eta_x (1 - 2n)}{\rho^3} ds = \oint h^3 \eta_x (1 - 2n) ds \tag{E.66}$$

$$I_5 = \oint \frac{(\gamma \eta_x^2 + 2\alpha \eta_x \eta_x' + \beta \eta_x'^2)}{|\rho|^3} ds = \oint H |h|^3 ds \tag{E.67}$$

where  $h = 1/\rho$ ,  $n = -(1/Bh)(dB/dx)$ .  $\eta_x$  is the dispersion and

$$H = \gamma \eta_x^2 + 2\alpha \eta_x \eta_x' + \beta \eta_x'^2 \tag{E.68}$$

From equation (E.7) with  $T_0 = L_0/c$ , the *total average radiated power per revolution* becomes:

$$\langle P_\gamma \rangle = \frac{C_\gamma E_0^4}{2\pi} \frac{I_2}{T_0} \tag{E.69}$$

From equation (E.5) the *total energy radiation in one revolution* becomes:

$$U_0 = \frac{C_\gamma E_0^4}{2\pi} I_2 \quad (\text{E.70})$$

From equation (E.59) the *damping partition numbers* become:

$$J_x = 1 - \frac{I_4}{I_2}, \quad J_y = 1, \quad J_E = 2 + \frac{I_4}{I_2} \quad (\text{E.71})$$

## Energy Spread

To evaluate the effect due to emission of photon, quantum excitation, we express the energy deviation from the synchronous energy in complex form as:

$$\Delta E = A_0 e^{i\omega_s(t-t_0)} \quad (\text{E.72})$$

where  $A_0$  is amplitude of synchrotron motion, and  $\omega_s$  is the synchrotron frequency. Now we suppose that at some instant  $t_1$  the energy is suddenly decreased by an amount  $u$  via quantum emission. After  $t_1$  the energy oscillation is:

$$\Delta E = A_0 e^{i\omega_s(t-t_0)} - u e^{i\omega_s(t-t_1)} = A_1 e^{i\omega(t-t_1)} \quad (\text{E.73})$$

By multiplying the second equality with its imaginary conjugate, we obtain:

$$A_1^2 = A_0^2 + u^2 - 2uA_0 \cos\omega_s(t_1 - t_0) \quad (\text{E.74})$$

We note that the synchrotron oscillation has changed the amplitude. Since the time at which photon emission occurs is random, we average the amplitude as:

$$\langle \Delta A^2 \rangle = \langle A_1^2 - A_0^2 \rangle = u^2 \quad (\text{E.75})$$

The rate of change of the amplitude per unit time around the ring is obtained as:

$$\left\langle \frac{dA^2}{dt} \right\rangle_q = \frac{d\langle A^2 \rangle}{dt} \Big|_q = \int_0^\infty \dot{n}(u) u^2 du = \langle \dot{N}_{ph} \rangle_s \langle u^2 \rangle_s \quad (\text{E.76})$$

where subscripts  $q$  and  $s$  indicate the effect due to quantum excitation and an average over the ring, respectively.  $\dot{n}(u)$  is the number of photon of energy  $u$  emitted per unit time,  $\dot{N}_{ph}$  is the total flux of photon. Since, damping causes the reduction in amplitude of energy oscillations, we obtain:

$$\left. \frac{d\langle A^2 \rangle}{dt} \right|_d = -2\alpha_E \langle A^2 \rangle \quad (\text{E.77})$$

Since the growth of the effect is limited by damping, quantum fluctuation and damping lead to an equilibrium state, thus from (E.76, E.77) we obtain:

$$\begin{aligned} 2\alpha_E \langle A^2 \rangle &= \langle \dot{N}_{ph} \langle u^2 \rangle \rangle_s \\ \langle A^2 \rangle &= \frac{1}{2\alpha_E} \langle \dot{N}_{ph} \langle u^2 \rangle \rangle_s = \frac{1}{2} \tau_E \langle \dot{N}_{ph} \langle u^2 \rangle \rangle_s \end{aligned} \quad (\text{E.78})$$

where  $\tau_E = 1/\alpha_E$  is called the *synchrotron oscillation damping time*. We assume the energy distribution due to statistical emission of photon is as a gaussian distribution, therefore the mean square equilibrium energy width is expressed as:

$$\begin{aligned} \sigma_E^2 &= \frac{1}{2} \langle A^2 \rangle \\ \text{Using (E.78)} \quad \sigma_E^2 &= \frac{1}{4} \tau_E \langle \dot{N}_{ph} \langle u^2 \rangle \rangle_s \end{aligned} \quad (\text{E.79})$$

The expression of the mean square energy fluctuation rate over one revolution around the ideal orbit without proof as (Lee, S. Y., 1999):

$$\langle \dot{N}_{ph} \langle u^2 \rangle \rangle_s = \frac{3}{2} C_u \hbar c \gamma^3 \frac{\langle P_\gamma \rangle}{\langle 1/\rho^2 \rangle} \langle 1/\rho^3 \rangle \quad (\text{E.80})$$

where  $C_u = 55/24\sqrt{3}$ . Using equation (E.62) with  $E_0 = m\gamma c^2$ , equation (E.79) becomes:

$$\sigma_E^2 = \frac{3 C_u \hbar m c^3 \gamma^4}{4 J_E \langle 1/\rho^2 \rangle} \langle 1/\rho^3 \rangle \quad (\text{E.81})$$

and the *equilibrium energy spread* becomes :

$$\left( \frac{\sigma_E}{E_0} \right)^2 = C_q \frac{\gamma^2}{J_E \langle 1/\rho^2 \rangle} \langle 1/\rho^3 \rangle \quad (\text{E.82})$$

where

$$C_q = \frac{55}{32\sqrt{3}} \frac{\hbar}{mc} = 3.84 \times 10^{-13} \text{ m} . \quad (\text{E.83})$$

For an isomagnetic ring, we obtain:

$$\left( \frac{\sigma_E}{E_0} \right)^2 = C_q \frac{\gamma_0^2}{J_E \rho_0}, \quad (\text{isomag}) \quad (\text{E.84})$$

From equations (E.64), (E.65) and (E.71) we obtain the energy spread in the form of:

$$\left( \frac{\sigma_E}{E_0} \right)^2 = C_q \gamma^2 \frac{I_3}{(2I_2 + I_4)} \quad (\text{E.85})$$

## Beam Width and Emittance

### Horizontal Beam Width

The emission of photon also excites random betatron oscillations. However the position and direction of a electron with respect to ideal orbit is not change. The quantum fluctuation gives only a change in the magnitude of the momentum. So we may write the change of the betatron displacement and slope when a photon emits energy  $u$  as:

$$\begin{aligned} \delta x = 0 &= \delta x_\beta + \eta_x \frac{u}{E_0}, & \delta x_\beta &= -\eta_x \frac{u}{E_0} \\ \delta x' = 0 &= \delta x'_\beta + \eta'_x \frac{u}{E_0}, & \delta x'_\beta &= -\eta'_x \frac{u}{E_0} \end{aligned} \quad (\text{E.86})$$

To modify these equations, we substitute them into the Courant-Snyder invariant,  $\gamma x^2 + 2\alpha x x' + \beta x'^2 = \epsilon_x$ , we obtain:

$$\gamma (\delta x_\beta)^2 + 2\alpha \delta x_\beta \delta x'_\beta + \beta^2 (\delta x'_\beta)^2 = \delta \epsilon_x \quad (\text{E.87})$$

$$\delta \epsilon_x = \frac{u^2}{E_0^2} (\gamma \eta_x^2 + 2\alpha \eta_x \eta'_x + \beta \eta_x'^2)$$

$$\delta \epsilon_x = \frac{u^2}{E_0^2} H(s) \quad (\text{E.88})$$

where

$$H(s) = (\gamma \eta_x^2 + 2\alpha \eta_x \eta'_x + \beta \eta_x'^2) \quad (\text{E.89})$$

The result in equation (E.88) gives the amplitude produced when we start with zero amplitude. If we have an amplitude  $\sqrt{\epsilon_x}$  and the quantum emission is completely random the change in the probable value of  $\epsilon_x$  is just  $\delta \epsilon_x$ , namely:

$$\delta\langle\epsilon_x\rangle = \frac{u^2}{E_0^2} H(s) \quad (\text{E.90})$$

We average over all photon energies, multiply by the number of photons emitted per unit time and then integrate over once around the orbit, we obtain the resulting change which we may write  $\Delta\langle\epsilon_x\rangle$  as:

$$\Delta\langle\epsilon_x\rangle = \frac{1}{cE_0^2} \oint \dot{N}_{ph} \langle u^2 \rangle H(s) ds \quad (\text{E.91})$$

$$\Delta\langle\epsilon_x\rangle = \frac{2\pi R}{cE_0^2} \langle \dot{N}_{ph} \langle u^2 \rangle H(s) \rangle_s \quad (\text{E.92})$$

Here we take the time  $dt = ds/c$ . The rate of change of the oscillation amplitude due to the quantum fluctuation occurs in the time  $2\pi R/c$  of one revolution becomes:

$$\left. \frac{d\langle\epsilon_x\rangle}{dt} \right|_q = \frac{1}{E_0^2} \langle \dot{N}_{ph} \langle u^2 \rangle H(s) \rangle_s \quad (\text{E.93})$$

where the subscript  $s$  indicates averaging around the ring. We know that this excitation is compensated by damping, similarly to (E.77):

$$\left. \frac{d\langle\epsilon_x\rangle}{dt} \right|_d = -2\alpha_x \langle\epsilon\rangle = -\frac{2\langle\epsilon\rangle}{\tau_x} \quad (\text{E.94})$$

Using (E.93) and (E.94), we obtain:

$$\langle\epsilon_x\rangle = \frac{\tau_x}{2E_0^2} \langle \dot{N}_{ph} \langle u^2 \rangle H(s) \rangle_s \quad (\text{E.95})$$

Consider the simple solution of equation of motion, as:

$$x_\beta = \sqrt{\epsilon_x} \sqrt{\beta_x} \cos(\phi_x + \phi_0)$$

We expect the betatron displacement rms spread to:

$$\sigma_{x_\beta}^2 = \langle x_\beta^2(s) \rangle = \frac{1}{2} \langle\epsilon_x\rangle \beta_x \quad (\text{E.96})$$

From equation (E.95), we obtain:

$$\frac{\sigma_{x_\beta}^2}{\beta_x} = \frac{1}{4} \frac{\tau_x}{E_0^2} \left\langle \dot{N}_{ph} \langle u^2 \rangle H(s) \right\rangle_s \quad (\text{E.97})$$

Using equation (E.80):

$$\left\langle \dot{N}_{ph} \langle u^2 \rangle H(s) \right\rangle_s = \frac{3}{2} C_u \hbar c \gamma^3 \frac{\langle P_\gamma \rangle}{\langle 1/\rho^2 \rangle} \langle H(s)/\rho^3 \rangle \quad (\text{E.98})$$

where  $C_u = 55/24\sqrt{3}$ , and from (E.62) we obtain:

$$\frac{\sigma_{x_\beta}^2}{\beta_x} = C_q \gamma^2 \frac{\langle H(s)/\rho^3 \rangle}{J_x \langle 1/\rho^2 \rangle} \quad (\text{E.99})$$

where  $C_q$  is defined by equation (E.83), we define equation (E.99) as the *natural emittance*  $\varepsilon_x^0$ , namely:

$$\varepsilon_x^0 = \frac{\sigma_{x_\beta}^2}{\beta_x} = C_q \gamma^2 \frac{\langle H(s)/\rho^3 \rangle}{J_x \langle 1/\rho^2 \rangle} \quad (\text{E.100})$$

For an isomagnetic ring the natural emittance becomes:

$$\varepsilon_x^0 = \frac{\sigma_{x_\beta}^2}{\beta_x} = C_q \gamma_0^2 \frac{\langle H(s) \rangle_{isomag}}{J_x \rho_0}, \quad (isomag) \quad (\text{E.101})$$

Comparing this equation with equation (E.84), we obtain:

$$\varepsilon_x^0 = \frac{J_E}{J_x} \langle H(s) \rangle_{isomag} \left( \frac{\sigma_E}{E_0} \right)^2, \quad (isomag) \quad (\text{E.102})$$

Note that we have already considered the radial spread due to  $x_\beta$ , but not yet from the contribution from energy oscillation term,  $x_E = \eta_x(s)u/E_0$ . The mean-square radial spread due to the energy spread is expressed by:

$$\sigma_{x_E}^2 = \eta_x^2 \left( \frac{\sigma_E}{E_0} \right)^2 \quad (\text{E.103})$$

We may add both radial spread due to batatron and energy oscillations to the total radial spread as:

$$\sigma_x^2 = \sigma_{x_\beta}^2 + \sigma_{x_E}^2 \quad (\text{E.104})$$

Consider only the case of an isomagnetic field, from equations (E.84) and (E.101) we get the mean square *horizontal beam size* as:

$$\sigma_x^2 = \frac{C_q \gamma_0^2}{\rho_0} \left( \frac{\beta_x \langle H(s) \rangle_{\text{isomag}}}{J_x} + \frac{\eta_x^2(s)}{J_E} \right), \quad (\text{isomag}) \quad (\text{E.105})$$

### Vertical Beam Width

So far we have assumed that the emission of photon has not change the direction of motion of the electron, this is not strictly correct. Since, when the electron emits a photon at nonzero angle with respect to its direction of motion, it experiences the small transverse impulse. Consider a photon with momentum  $u/c$  is emitted at angle  $\phi_\gamma$  with respect to the electron's momentum, the transverse component kick is then equal to  $u\phi_\gamma/c$ . Since the position of electron is not changed, we may write the transverse angular kicks on phase-space coordinates as:

$$\delta x = 0, \delta x' = \frac{u}{E_0} \phi_x, \quad \delta y = 0, \delta y' = \frac{u}{E_0} \phi_y \quad (\text{E.106})$$

where  $\phi_x, \phi_y$  are the projections of  $\phi_\gamma$  onto  $x, y$  axes respectively. We consider only in the effect on vertical betatron motion, because  $\delta x'$  is very small compared to equation (E.85). Using equation (E.106), equation (E.90) becomes:

$$\delta \langle \varepsilon_y \rangle = \frac{u^2}{E_0^2} \phi_y^2 \beta_y \quad (\text{E.107})$$

where the phase ellipse invariant along  $y$  axis is  $\gamma^2 + 2\alpha\gamma\gamma' + \beta\gamma'^2 = \varepsilon_y$ . Similarly to the horizontal direction, we obtain the equilibrium *vertical beam width* as:

$$\frac{\sigma_y^2}{\beta_y} = \frac{1}{4} \frac{\tau_y}{E_0^2} \langle \dot{N}_{ph} \langle \phi_y^2 u^2 \rangle \beta_y \rangle_s \quad (\text{E.108})$$

Since we are dealing with the small effect case, we make the approximation:

$$\langle \phi_y^2 u^2 \rangle \approx \langle \phi_y^2 \rangle \langle u^2 \rangle \quad (\text{E.109})$$

and because the synchrotron radiation is emitted in the forward direction within a cone of angular  $1/\gamma$ , we then have:

$$\langle \phi_Y^2 \rangle \approx \frac{1}{\gamma^2} \quad (\text{E.110})$$

Equation (E.108) becomes:

$$\frac{\sigma_{y\beta}^2}{\beta_y} \approx \frac{1}{4} \frac{\tau_y}{E_0^2 \gamma^2} \langle \dot{N}_{ph} \langle u^2 \rangle \rangle_s \langle \beta_y \rangle \quad (\text{E.111})$$

Using equation (E.79), we obtain:

$$\frac{\sigma_y^2}{\sigma_E^2} \approx \frac{1}{E_0^2 \gamma^2} \frac{\tau_y}{\tau_E} \langle \beta_y^2 \rangle \quad (\text{E.112})$$

Using equation (E.62), we obtain:

$$\frac{\sigma_y^2}{\sigma_E^2} \approx \frac{1}{E_0^2 \gamma^2} \frac{J_E}{J_y} \langle \beta_y^2 \rangle \quad (\text{E.113})$$

For the flat designed orbit  $J_y$  roughly equal to 1. The vertical beam size in an isomagnetic ring is:

$$\sigma_y^2 \approx C_q \frac{\langle \beta_y^2 \rangle}{\rho_0}, \quad (\text{isomag}) \quad (\text{E.114})$$

The *vertical emittance* can be calculated from  $\varepsilon_y = \sigma_y^2 / \beta_y$ , we obtain:

$$\varepsilon_y \approx C_q \frac{\langle \beta_y^2 \rangle^{1/2}}{\rho_0}, \quad (\text{isomag}) \quad (\text{E.115})$$

## Linear Coupling Emittance

The horizontal emittance was defined by:

$$\varepsilon_x = \frac{\sigma_x^2}{\beta_x} \quad (\text{E.116})$$

The vertical emittance was defined by:

$$\varepsilon_y = \frac{\sigma_y^2}{\beta_y} \quad (\text{E.117})$$



The quantum excitation of the radial oscillations can be shared with the vertical oscillations in proportion up to equal division.

$$\varepsilon_x + \varepsilon_y = \varepsilon_x^0 \quad (\text{E.118})$$

where natural emittance  $\varepsilon_x^0$  is defined by equation (E.100). The horizontal and vertical emittances can be redistributed with appropriate linear betatron coupling, namely:

$$\varepsilon_x = \frac{1}{1 + \kappa} \varepsilon_x^0, \quad \varepsilon_y = \frac{\kappa}{1 + \kappa} \varepsilon_x^0 \quad (\text{E.119})$$

where  $\kappa$  is the *coupling constant*, is defined by:

$$\varepsilon_y = \kappa \varepsilon_x \quad (\text{E.120})$$

## Bunch Length

The distribution function for energy deviations is approximately Gaussian, when we assume the energy oscillations are linear, so called Gaussian distribution.

$$\psi(E) = \frac{1}{\sqrt{2\pi}\sigma_E} \exp\left(-\frac{u^2}{2\sigma_E^2}\right) \quad (\text{E.121})$$

where  $u$  is emission quantum energy and the parameter  $\sigma_E$  is often called the standard deviation. And we find that the time displacement is Gaussian distribution when we defined the time displacement  $\tau$  by:

$$\tau = \frac{\alpha_c}{\omega_s E_0} \theta \quad (\text{E.122})$$

where  $\omega_s$  is the angular frequency of the energy oscillation.  $\alpha_c$  is momentum compaction factor and  $\theta$  is just a scale equivalent of  $\tau$ . The distribution in the normalized time displacement  $\theta$  is: (Matthew Sands, SLAC 121, (1970))

$$\psi(\theta) = \frac{1}{\sqrt{2\pi}\sigma_E} \exp\left(-\frac{\theta^2}{2\sigma_E^2}\right) \quad (\text{E.123})$$

Equation (E.121) and (E.123) follow that there are associations between time displacement  $\tau$  and the standard deviation  $\sigma_E$ , from equation (E.122) we may write:

$$\sigma_\tau = \frac{\alpha_c}{\omega_s E_0} \sigma_E \quad (\text{E.124})$$

From equation (E.85) we obtain:

$$\sigma_{\tau}^2 = C_{\alpha} \frac{\alpha_c^2}{\omega_s^2} \frac{\gamma^2 I_3}{(2I_2 + I_4)} \quad (\text{E.125})$$

Taking  $\omega_s$  from equation (E.24), we obtain:

$$\sigma_{\tau}^2 = C_{\alpha} \frac{\alpha_c T_0 E_0}{e\dot{V}} \frac{\gamma^2 I_3}{(2I_2 + I_4)} \quad (\text{E.126})$$

For the case of an isomagnetic field, using equation (E.84), we obtain:

$$\sigma_{\tau}^2 = C_{\alpha} \frac{\alpha_c^2}{\omega_s^2} \frac{\gamma_0^2}{J_E \rho_0^2}, \quad (\text{isomag}) \quad (\text{E.127})$$

Taking  $\omega_s$  from equation (E.24), we obtain:

$$\sigma_{\tau}^2 = C_{\alpha} \frac{\alpha_c T_0 E_0}{e\dot{V}} \frac{\gamma_0^2}{J_E \rho_0^2}, \quad (\text{isomag}) \quad (\text{E.128})$$

when we multiply the spread of time displacement  $\sigma_{\tau}$  by the speed of electrons  $c$ , we obtain the spread of longitudinal displacement from the center of the bunch. This is called *bunch half length*, and we obtain *bunch length* as:

$$\sigma_1 = 2c\gamma \sqrt{C_{\alpha} \frac{\alpha_c T_0 E_0}{e\dot{V}} \frac{I_3}{(2I_2 + I_4)}} \quad (\text{E.129})$$

# Appendix F

## The Results of Calculations

### F.1 The Results of Calculations for the Low-Energy Beam Transport Line (LBT) by the Program LATTICE

Beam rigidity = 0.1351194 t-m  
x,y emittance = 0.070000 0.070000 cm-mrad  
dp/p = 0.000%

#### Elements of the low-energy beam transport line

1	param slit	0.0	0.000000	0.000000	0.000000	0.0000	0.0000
2	d1 drift	0.0	0.400000	0.000000	0.000000	0.0000	0.0000
3	d2 drift	0.0	0.300000	0.000000	0.000000	0.0000	0.0000
4	d3 drift	0.0	1.600000	0.000000	0.000000	0.0000	0.0000
5	d4 drift	0.0	0.300000	0.000000	0.000000	0.0000	0.0000
6	d5 drift	0.0	0.457200	0.000000	0.000000	0.0000	0.0000
7	d6 drift	0.0	0.633850	0.000000	0.000000	0.0000	0.0000
8	d7 drift	0.0	0.200000	0.000000	0.000000	0.0000	0.0000
9	d8 drift	0.0	0.633850	0.000000	0.000000	0.0000	0.0000
10	d9 drift	0.0	0.946600	0.000000	0.000000	0.0000	0.0000
11	d10 drift	0.0	0.300000	0.000000	0.000000	0.0000	0.0000
12	d11 drift	0.0	0.850000	0.000000	0.000000	0.0000	0.0000
13	d12 drift	0.0	0.850000	0.000000	0.000000	0.0000	0.0000
14	d13 drift	0.0	0.300000	0.000000	0.000000	0.0000	0.0000
15	d14 drift	0.0	1.600000	0.000000	0.000000	0.0000	0.0000
16	q1 quad	1.2	0.100000	-0.431809	0.000000	0.0000	0.0000
17	q2 quad	2.2	0.100000	0.780228	0.000000	0.0000	0.0000
18	q3 quad	3.2	0.100000	-1.191100	0.000000	0.0000	0.0000
19	q4 quad	4.2	0.100000	1.138408	0.000000	0.0000	0.0000
20	q5 quad	0.0	0.100000	1.537801	0.000000	0.0000	0.0000
21	q6 quad	5.2	0.100000	-0.015168	0.000000	0.0000	0.0000
22	q7 quad	6.2	0.100000	-1.073487	0.000000	0.0000	0.0000
23	q8 quad	7.2	0.100000	1.324245	0.000000	0.0000	0.0000
24	q9 quad	8.2	0.100000	1.011914	0.000000	0.0000	0.0000
25	q10 quad	9.2	0.100000	-1.746145	0.000000	0.0000	0.0000
26	e edge	0.0	13.870000	0.270239	0.025000	0.0000	0.0000
27	b bend	0.0	0.440695	0.270239	0.000000	0.0000	0.0000
28	sep bend	0.0	0.445059	-0.158965	0.000000	0.0000	0.0000

**The structure of the lattice**

```

1:  d1    q1    d2    q2    d3    q3    d4
8:  q4    d5    e     b     e     d6    q5
15: d7    d7    q5    d8    e     b     e
22: d9    q6    d10   q7    d11   q8    d12
29: q9    d13   q10   d14   sep

```

**Machine consists of 1 period****Initial Twiss parameters**

## Transport mode

```

betax = 4.3750  alphax = 0.0000
betay = 4.3750  alphay = 0.0000
etax  = 0.0000  eta'x  = 0.0000
etay  = 0.0000  eta'y  = 0.0000

```

**Fit Twiss parameters for a machine of 1 period**

variable	target value	weight	location
1 betax	6.7724	100.000	@end
2 betay	3.3311	30.000	@end
3 alphax	0.0000	20.000	@end
4 alphay	0.0000	20.000	@end
5 etax	-0.1100	10.000	@end
6 etay	0.0000	10.000	@end
7 eta'x	-0.5000	10.000	@end
8 bxmax	10.0000	1.000	@end
9 bymax	10.0000	1.000	@end

**Scales** x<cm> y<cm> e<cm> ey<cm> vsize<cm>

```
Sc 5.000 5.000 5.000 5.000 5.000 21
```

**To calculate the beam parameters at the end of the beam line**

\* LBT of Siam Photon Source By Ritthikrai

```

Total length = 11.998    Total bend = 71.000, 0.000 degrees
betax = 6.7724 meters   alphax = -0.0000  1/gam = 6.7724; z= -0.0000
betay = 3.3311 meters   alphay = 0.0000  1/gam = 3.3311; z= 0.0000
eta x = -0.1139 meters  eta' x = -0.5000  psix = 445.54 degrees
eta y = 0.0000 meters   eta' y = 0.0000  psiy = 291.36 degrees
x  = 0.2177 cm         x'  = 0.3215  r12 = 0.0000
y  = 0.1527 cm         y'  = 0.4584  r34 = -0.0000
m(1,6)= -0.1139       m(2,6)= -0.5000  m(5,6)= -0.1298
m(3,6)= 0.0000        m(4,6)= 0.0000  resolves: -3.8243%

```

### To track the Twiss parameters through every element of the lattice

\* LBT of Siam Photon Source By Ritthikrai

elemt	lth (m)	sum l (m)	betax (m)	alphax (rad)	etax (m)	eta'x (rad)	psix (deg)	betay (m)	alphay (rad)	etay (m)	eta'y (rad)	psiy (deg)
	0.	0.	4.38	0.00	0.00	0.00	0.	4.38	0.00	0.00	0.00	0.
d1	0.40	0.40	4.41	-0.09	0.00	0.00	5.2	4.41	-0.09	0.00	0.00	5.2
q1	0.10	0.50	4.57	-1.56	0.00	0.00	6.5	4.29	1.27	0.00	0.00	6.5
d2	0.30	0.80	5.58	-1.78	0.00	0.00	9.9	3.58	1.09	0.00	0.00	10.9
q2	0.10	0.90	5.61	1.44	0.00	0.00	10.9	3.58	-1.00	0.00	0.00	12.5
d3	1.60	2.50	2.40	0.56	0.00	0.00	36.8	8.19	-1.89	0.00	0.00	29.7
q3	0.10	2.60	2.51	-1.64	0.00	0.00	39.	7.85	5.19	0.00	0.00	30.4
d4	0.30	2.90	3.62	-2.08	0.00	0.00	44.8	5.06	4.12	0.00	0.00	33.2
q4	0.10	3.00	3.73	1.01	0.00	0.00	46.4	4.66	-0.05	0.00	0.00	34.4
d5	0.46	3.46	2.92	0.76	0.00	0.00	54.3	4.75	-0.14	0.00	0.00	39.9
e	0.00	3.46	2.92	-0.68	0.00	0.00	54.3	4.75	1.66	0.00	0.00	39.9
b	0.44	3.90	1.59	2.88	0.18	0.77	64.6	3.44	1.31	0.00	0.00	46.2
e	0.00	3.90	1.59	2.09	0.18	0.86	64.6	3.44	2.62	0.00	0.00	46.2
d6	0.63	4.53	0.30	-0.05	0.73	0.86	131.8	1.04	1.17	0.00	0.00	65.8
q5	0.10	4.63	0.31	-0.04	0.77	-0.00	150.7	0.93	-0.07	0.00	0.00	71.7
d7	0.20	4.83	0.45	-0.69	0.77	-0.00	183.3	1.01	-0.29	0.00	0.00	83.6
d7	0.20	5.03	0.86	-1.34	0.77	-0.00	202.1	1.16	-0.50	0.00	0.00	94.3
q5	0.10	5.13	1.04	-0.45	0.73	-0.86	208.0	1.42	-2.17	0.00	0.00	98.8
d8	0.63	5.77	2.08	-1.18	0.18	-0.86	233.5	5.78	-4.71	0.00	0.00	111.6
e	0.00	5.77	2.08	-2.20	0.18	-0.77	233.5	5.78	-2.51	0.00	0.00	111.6
b	0.44	6.21	2.34	1.77	-0.00	0.00	243.6	8.24	-3.07	0.00	0.00	115.3
e	0.00	6.21	2.34	0.61	-0.00	0.00	243.6	8.24	0.06	0.00	0.00	115.3
d9	0.95	7.15	1.71	0.06	-0.00	0.00	271.8	8.24	-0.06	0.00	0.00	121.9
q6	0.10	7.25	1.71	-0.02	-0.00	0.00	275.2	8.24	0.02	0.00	0.00	122.6
d10	0.30	7.55	1.77	-0.20	-0.00	0.00	285.1	8.23	-0.01	0.00	0.00	124.6
q7	0.10	7.65	1.97	-1.78	-0.00	-0.00	288.2	7.60	6.18	0.00	0.00	125.4
d11	0.85	8.50	6.52	-3.58	-0.00	-0.00	301.9	0.82	1.80	0.00	0.00	145.3
q8	0.10	8.60	6.59	2.88	-0.00	0.00	302.8	0.57	0.75	0.00	0.00	153.8
d12	0.85	9.45	2.71	1.68	-0.00	0.00	314.4	1.27	-1.57	0.00	0.00	248.3
q9	0.10	9.55	2.21	3.23	-0.00	0.00	316.7	1.72	-3.10	0.00	0.00	252.2
d13	0.30	9.85	0.73	1.68	-0.00	0.00	330.3	4.13	-4.94	0.00	0.00	258.7
q10	0.10	9.95	0.52	0.53	-0.00	0.00	339.8	4.59	0.61	0.00	0.00	260.0
d14	1.60	11.55	5.11	-3.40	0.00	0.00	441.4	3.39	0.13	0.00	0.00	283.9
sep	0.45	12.00	6.77	-0.00	-0.11	-0.50	445.5	3.33	0.00	0.00	0.00	291.5

beta x min = 0.297      beta y min = 0.573  
 beta x max = 6.772      beta y max = 8.238  
 eta x min = -0.114      eta y min = 0.000  
 eta x max = 0.771      eta y max = 0.000

### To track the beam size through every element of the lattice

x

\* LBT of Siam Photon Source By Ritthikrai

elemt	lth	sum l	x	x'	etax	psix	x+disp	y	y'	etay	psiy	y+disp
	(m)	(m)	(cm)	(mrad)	(m)	(deg)	(cm)	(cm)	(mrad)	(m)	(deg)	(cm)
d1	0.40	0.40	0.18	0.40	0.00	5.2	0.18	0.18	0.40	0.00	5.2	0.18
q1	0.10	0.50	0.18	0.72	0.00	6.5	0.18	0.17	0.65	0.00	6.5	0.17
d2	0.30	0.80	0.20	0.72	0.00	9.9	0.20	0.16	0.65	0.00	10.9	0.16
q2	0.10	0.90	0.20	0.62	0.00	10.9	0.20	0.16	0.62	0.00	12.5	0.16
d3	1.60	2.50	0.13	0.62	0.00	36.8	0.13	0.24	0.62	0.00	29.7	0.24
q3	0.10	2.60	0.13	1.01	0.00	39.1	0.13	0.23	1.58	0.00	30.4	0.23
d4	0.30	2.90	0.16	1.01	0.00	44.8	0.16	0.19	1.58	0.00	33.2	0.19
q4	0.10	3.00	0.16	0.61	0.00	46.4	0.16	0.18	0.39	0.00	34.4	0.18
d5	0.46	3.46	0.14	0.61	0.00	54.3	0.14	0.18	0.39	0.00	39.9	0.18
e	0.00	3.46	0.14	0.59	0.00	54.3	0.14	0.18	0.74	0.00	39.9	0.18
b	0.44	3.90	0.11	2.02	0.18	64.6	0.11	0.16	0.74	0.00	46.2	0.16
e	0.00	3.90	0.11	1.54	0.18	64.6	0.11	0.16	1.26	0.00	46.2	0.16
d6	0.63	4.53	0.05	1.54	0.73	131.8	0.05	0.09	1.26	0.00	65.8	0.09
q5	0.10	4.63	0.05	1.51	0.77	150.7	0.05	0.08	0.87	0.00	71.7	0.08
d7	0.20	4.83	0.06	1.51	0.77	183.3	0.06	0.08	0.87	0.00	83.6	0.08
d7	0.20	5.03	0.08	1.51	0.77	202.1	0.08	0.09	0.87	0.00	94.3	0.09
q5	0.10	5.13	0.09	0.90	0.73	208.0	0.09	0.10	1.67	0.00	98.8	0.10
d8	0.63	5.77	0.12	0.90	0.18	233.5	0.12	0.20	1.67	0.00	111.6	0.20
e	0.00	5.77	0.12	1.41	0.18	233.5	0.12	0.20	0.94	0.00	111.6	0.20
b	0.44	6.21	0.13	1.11	-0.00	243.6	0.13	0.24	0.94	0.00	115.3	0.24
e	0.00	6.21	0.13	0.64	-0.00	243.6	0.13	0.24	0.29	0.00	115.3	0.24
d9	0.95	7.15	0.11	0.64	-0.00	271.8	0.11	0.24	0.29	0.00	121.9	0.24
q6	0.10	7.25	0.11	0.64	-0.00	275.2	0.11	0.24	0.29	0.00	122.6	0.24
d10	0.30	7.55	0.11	0.64	-0.00	285.1	0.11	0.24	0.29	0.00	124.6	0.24
q7	0.10	7.65	0.12	1.22	-0.00	288.2	0.12	0.23	1.90	0.00	125.4	0.23
d11	0.85	8.50	0.21	1.22	-0.00	301.9	0.21	0.08	1.90	0.00	145.3	0.08
q8	0.10	8.60	0.21	0.99	-0.00	302.8	0.21	0.06	1.38	0.00	153.8	0.06
d12	0.85	9.45	0.14	0.99	-0.00	314.4	0.14	0.09	1.38	0.00	248.3	0.09
q9	0.10	9.55	0.12	1.91	-0.00	316.7	0.12	0.11	2.07	0.00	252.2	0.11
d13	0.30	9.85	0.07	1.91	-0.00	330.3	0.07	0.17	2.07	0.00	258.7	0.17
q10	0.10	9.95	0.06	1.31	-0.00	339.8	0.06	0.18	0.46	0.00	260.0	0.18
d14	1.60	11.55	0.19	1.31	0.00	441.4	0.19	0.15	0.46	0.00	283.9	0.15
sep	0.45	12.00	0.22	0.32	-0.11	445.5	0.22	0.15	0.46	0.00	91.5	0.15

beta x min = 0.297      beta y min = 0.573  
 beta x max = 6.772      beta y max = 8.238  
 eta x min = -0.114      eta y min = 0.000  
 eta x max = 0.771      eta y max = 0.000

### Give exact maximum and minimum of the Twiss parameters

cp

\* LBT of Siam Photon Source By Ritthikrai

elemt	lth (m)	sum l (m)	betax (m)	alphax (rad)	etax (m)	eta'x (rad)	psix ( deg)	x (mm)	betay (m)	alphay (rad)	psiy (deg)	y (mm)
	0.	0.	4.38	0.00	0.00	0.00	0.	2	4.38	0.00	0.	2
d1	0.40	0.40	4.41	-0.09	0.00	0.00	5.2	2	4.41	-0.09	5.2	2
q1	0.10	0.50	4.57	-1.56	0.00	0.00	6.5	2	4.29	1.27	6.5	2
d2	0.30	0.80	5.58	-1.78	0.00	0.00	9.9	2	3.58	1.09	10.9	2
q2	0.10	0.90	5.61	1.44	0.00	0.00	10.9	2	3.58	-1.00	12.5	2
d3	1.60	2.50	2.40	0.56	0.00	0.00	36.8	1	8.19	-1.89	29.7	2
q3	0.10	2.60	2.51	-1.64	0.00	0.00	39.1	1	7.85	5.19	30.4	2
d4	0.30	2.90	3.62	-2.08	0.00	0.00	44.8	2	5.06	4.12	33.2	2
q4	0.10	3.00	3.73	1.01	0.00	0.00	46.4	2	4.66	-0.05	34.4	2
d5	0.46	3.46	2.92	0.76	0.00	0.00	54.3	1	4.75	-0.14	39.9	2
e	0.00	3.46	2.92	-0.68	0.00	0.00	54.3	1	4.75	1.66	39.9	2
b	0.44	3.90	1.59	2.88	0.18	0.77	64.6	1	3.44	1.31	46.2	2
e	0.00	3.90	1.59	2.09	0.18	0.86	64.6	1	3.44	2.62	46.2	2
d6	0.63	4.53	0.30	-0.05	0.73	0.86	131.8	0	1.04	1.17	65.8	1
q5	0.10	4.63	0.31	-0.04	0.77	-0.00	150.7	0	0.93	-0.07	71.7	1
d7	0.20	4.83	0.45	-0.69	0.77	-0.00	183.3	1	1.01	-0.29	83.6	1
d7	0.20	5.03	0.86	-1.34	0.77	-0.00	202.1	1	1.16	-0.50	94.3	1
q5	0.10	5.13	1.04	-0.45	0.73	-0.86	208.0	1	1.42	-2.17	98.8	1
d8	0.63	5.77	2.08	-1.18	0.18	-0.86	233.5	1	5.78	-4.71	111.6	2
e	0.00	5.77	2.08	-2.20	0.18	-0.77	233.5	1	5.78	-2.51	111.6	2
b	0.44	6.21	2.34	1.77	-0.00	0.00	243.6	1	8.24	-3.07	115.3	2
e	0.00	6.21	2.34	0.61	-0.00	0.00	243.6	1	8.24	0.06	115.3	2
d9	0.95	7.15	1.71	0.06	-0.00	0.00	271.8	1	8.24	-0.06	121.9	2
q6	0.10	7.25	1.71	-0.02	-0.00	0.00	275.2	1	8.24	0.02	122.6	2
d10	0.30	7.55	1.77	-0.20	-0.00	0.00	285.1	1	8.23	-0.01	124.6	2
q7	0.10	7.65	1.97	-1.78	-0.00	-0.00	288.2	1	7.60	6.18	125.4	2
d11	0.85	8.50	6.52	-3.58	-0.00	-0.00	301.9	2	0.82	1.80	145.3	1
q8	0.10	8.60	6.59	2.88	-0.00	0.00	302.8	2	0.57	0.75	153.8	1
d12	0.85	9.45	2.71	1.68	-0.00	0.00	314.4	1	1.27	-1.57	248.3	1
q9	0.10	9.55	2.21	3.23	-0.00	0.00	316.7	1	1.72	-3.10	252.2	1
d13	0.30	9.85	0.73	1.68	-0.00	0.00	330.3	1	4.13	-4.94	258.7	2
q10	0.10	9.95	0.52	0.53	-0.00	0.00	339.8	1	4.59	0.61	260.0	2
d14	1.60	11.55	5.11	-3.40	0.00	0.00	441.4	2	3.39	0.13	283.9	2
sep	0.45	12.00	6.77	-0.00	-0.11	-0.50	445.5	2	3.33	0.00	291.5	2

Extremes ..max: betax[33] = 6.7724; betay[6] = 8.2414; eta[14] = 0.7715

[at el#] ..min: betax[13] = 0.2967; betay[28] = 0.3657; eta[27] = -0.0000

## F.2 The Results of Calculations for the Booster Synchrotron (SYN) by the Program LATTICE

Beam rigidity = 3.3373450 t-m  
 x,y emittance = 0.024868 0.002487 cm-mrad  
 dp/p = 0.000%

### Elements of the lattice

1	param	slit	0.0	0.000000	0.000000	0.000000	0.0000
2	d1	drift	0.0	1.037500	0.000000	0.000000	0.0000
3	d2	drift	0.0	0.300000	0.000000	0.000000	0.0000
4	q1	quad	1.2	0.250000	4.836936	0.000000	0.0000
5	q2	quad	2.2	0.250000	-3.676933	0.000000	0.0000
6	e	edge	0.0	15.000000	1.101430	0.027500	0.0000
7	b	bend	0.0	1.586504	1.101434	0.000000	0.0000

### The structure of the lattice

1:	d1	q1	d2	e	b	e	d2
8:	q2	d2	e	b	e	d2	q1
15:	d1						

### Fit parameters for a machine of 6 periods

variable	target value	weight	location
1 nux	2.2500	1.000	@end
2 nu y	1.2500	1.000	@end

### To calculate the beam parameters just at the end of the beam line

\* Booster Sychrotron by Ritthikrai  
 Matched functions for 6 periods  
 Total length = 43.188 Total bend = 360.000, 0.000 degrees  
 betax = 6.7673 meters alphax = -0.0000 nu x = 2.25000  
 betay = 3.3345 meters alphay = -0.0000 nu y = 1.25000  
 eta x = 1.8621 meters eta' x = 0.0000 gamtr = 2.35684  
 eta y = 0.0000 meters eta' y = 0.0000

### Calculate the various parameters

\* Booster Sychrotron by Ritthikrai

nu x	=	2.250	nu y	=	1.250
tr gamma	=	2.357	compaction	=	0.18003
beta x min	=	1.142	beta y min	=	3.335
beta x max	=	6.926	beta y max	=	14.030
eta x min	=	0.932	eta y min	=	0.000
eta x max	=	1.862	eta y max	=	0.000
dnux/(dp/p)	=	-0.995	dnu y/(dp/p)	=	-2.195
normalized x	=	-0.442	normalized y	=	-1.756



Space charge integrals: avg beam half width, height = 0.1010, 0.0407 cm.

Synchrotron integrals: I1 = 7.779082 m-1 , I2 = 2.073658 m-1

I3 = 0.684376 m-2 , I4 = -0.048267 m-1 , I5 = 0.393778 m-1

I5/(I2-I4) = 0.185576 I3/(2\*I2+I4) = 0.166960

Functions for electron storage rings:

D = -0.02328, Jx = 1.023, Je = 1.977

Natural rms x emittance = 0.273562 pi mm-mrad

Natural rms energy spread = 0.497 MeV

Synchrotron radiation = 0.029349 MeV/turn

Damping times (sec): Horiz: 0.009599, Vert: 0.009822, Energy: 0.004969

### To track the Twiss parameters through every element of the lattice

c

\* Booster Sychrotron by Ritthikrai

elemt	lth (m)	sum l (m)	betax (m)	alphax (rad)	etax (m)	eta'x (rad)	psix (deg)	betay (m)	alphay (rad)	etay (m)	eta'y (rad)	psiy (deg)
	0.	0.	6.77	-0.00	1.86	0.00	0.	3.33	-0.00	0.00	0.00	0.
d1	1.04	1.04	6.93	-0.15	1.86	0.00	8.7	3.66	-0.31	0.00	0.00	17.3
q1	0.25	1.29	6.40	2.20	1.78	-0.66	10.8	4.18	-1.86	0.00	0.00	21.0
d2	0.30	1.59	5.16	1.93	1.58	-0.66	13.8	5.39	-2.17	0.00	0.00	24.6
e	0.00	1.59	5.16	1.47	1.58	-0.52	13.8	5.39	-1.72	0.00	0.00	24.6
b	1.59	3.17	1.42	0.67	0.98	-0.22	47.9	12.68	-2.88	0.00	0.00	35.7
e	0.00	3.17	1.42	0.54	0.98	-0.13	47.9	12.68	-1.80	0.00	0.00	35.7
d2	0.30	3.47	1.18	0.27	0.94	-0.13	61.3	13.79	-1.90	0.00	0.00	37.0
q2	0.25	3.72	1.18	-0.27	0.94	0.13	73.7	13.79	1.90	0.00	0.00	38.0
d2	0.30	4.02	1.42	-0.54	0.98	0.13	87.1	12.68	1.80	0.00	0.00	39.3
e	0.00	4.02	1.42	-0.67	0.98	0.22	87.1	12.68	2.88	0.00	0.00	39.3
b	1.59	5.61	5.16	-1.47	1.58	0.52	121.2	5.39	1.72	0.00	0.00	50.4
e	0.00	5.61	5.16	-1.93	1.58	0.66	121.2	5.39	2.17	0.00	0.00	50.4
d2	0.30	5.91	6.40	-2.20	1.78	0.66	124.2	4.18	1.86	0.00	0.00	54.0
q1	0.25	6.16	6.93	0.15	1.86	0.00	126.3	3.66	0.31	0.00	0.00	57.7
d1	1.04	7.20	6.77	-0.00	1.86	0.00	135.0	3.33	-0.00	0.00	0.00	75.0

nu x = 2.250 nu y = 1.250

tr gamma = 2.357 compaction = 0.18003

beta x min = 1.176 beta y min = 3.335

beta x max = 6.926 beta y max = 13.791

eta x min = 0.940 eta y min = 0.000

eta x max = 1.862 eta y max = 0.000

### To track the beam size through of every element of the lattice

x

\* Booster Sychrotron by Ritthikrai

elemt	lth	sum l	x	x'	etax	psix	x+disp	y	y'	etay	psiy	y+disp
	(m)	(m)	(cm)	(mrad)	(m)	(deg)	(cm)	(cm)	(mrad)	(m)	(deg)	(cm)
d1	1.04	1.04	0.13	0.19	1.86	8.7	0.13	0.03	0.09	0.00	17.3	0.03
q1	0.25	1.29	0.13	0.48	1.78	10.8	0.13	0.03	0.16	0.00	21.0	0.03
d2	0.30	1.59	0.11	0.48	1.58	13.8	0.11	0.04	0.16	0.00	24.6	0.04
e	0.00	1.59	0.11	0.39	1.58	13.8	0.11	0.04	0.13	0.00	24.6	0.04
b	1.59	3.17	0.06	0.50	0.98	47.9	0.06	0.06	0.13	0.00	35.7	0.06
e	0.00	3.17	0.06	0.48	0.98	47.9	0.06	0.06	0.09	0.00	35.7	0.06
d2	0.30	3.47	0.05	0.48	0.94	61.3	0.05	0.06	0.09	0.00	37.0	0.06
q2	0.25	3.72	0.05	0.48	0.94	73.7	0.05	0.06	0.09	0.00	38.0	0.06
d2	0.30	4.02	0.06	0.48	0.98	87.1	0.06	0.06	0.09	0.00	39.3	0.06
e	0.00	4.02	0.06	0.50	0.98	87.1	0.06	0.06	0.13	0.00	39.3	0.06
b	1.59	5.61	0.11	0.39	1.58	121.2	0.11	0.04	0.13	0.00	50.4	0.04
e	0.00	5.61	0.11	0.48	1.58	121.2	0.11	0.04	0.16	0.00	50.4	0.04
d2	0.30	5.91	0.13	0.48	1.78	124.2	0.13	0.03	0.16	0.00	54.0	0.03
q1	0.25	6.16	0.13	0.19	1.86	126.3	0.13	0.03	0.09	0.00	57.7	0.03
d1	1.04	7.20	0.13	0.19	1.86	135.0	0.13	0.03	0.09	0.00	75.0	0.03

nu x = 2.250            nu y = 1.250  
 tr gamma = 2.357        compaction = 0.18003  
 beta x min = 1.176      beta y min = 3.335  
 beta x max = 6.926      beta y max = 13.791  
 eta x min = 0.940       eta y min = 0.000  
 eta x max = 1.862       eta y max = 0.000

### Give exact maximum and minimum of the Twiss parameters

cp

\* Booster Sychrotron by Ritthikrai

elemt	lth	sum l	betax	alphax	etax	eta'x	psix	x	betay	alphay	psiy	y
	(m)	(m)	(m)	(rad)	(m)	(rad)	(deg)	(mm)	(m)	(rad)	(deg)	(mm)
	0.	0.	6.77	-0.00	1.86	0.00	0.	1	3.33	-0.00	0.	0
d1	1.04	1.04	6.93	-0.15	1.86	0.00	8.7	1	3.66	-0.31	17.3	0
q1	0.25	1.29	6.40	2.20	1.78	-0.66	10.8	1	4.18	-1.86	21.0	0
d2	0.30	1.59	5.16	1.93	1.58	-0.66	13.8	1	5.39	-2.17	24.6	0
e	0.00	1.59	5.16	1.47	1.58	-0.52	13.8	1	5.39	-1.72	24.6	0
b	1.59	3.17	1.42	0.67	0.98	-0.22	47.9	1	12.68	-2.88	35.7	1
e	0.00	3.17	1.42	0.54	0.98	-0.13	47.9	1	12.68	-1.80	35.7	1
d2	0.30	3.47	1.18	0.27	0.94	-0.13	61.3	1	13.79	-1.90	37.0	1
q2	0.25	3.72	1.18	-0.27	0.94	0.13	73.7	1	13.79	1.90	38.0	1
d2	0.30	4.02	1.42	-0.54	0.98	0.13	87.1	1	12.68	1.80	39.3	1
e	0.00	4.02	1.42	-0.67	0.98	0.22	87.1	1	12.68	2.88	39.3	1
b	1.59	5.61	5.16	-1.47	1.58	0.52	121.2	1	5.39	1.72	50.4	0
e	0.00	5.61	5.16	-1.93	1.58	0.66	121.2	1	5.39	2.17	50.4	0
d2	0.30	5.91	6.40	-.20	1.78	0.66	124.2	1	4.18	1.86	54.0	0
q1	0.25	6.16	6.93	0.15	1.86	0.00	126.3	1	3.66	0.31	57.7	0
d1	1.04	7.20	6.77	-0.00	1.86	0.00	135.0	1	3.33	-0.00	75.0	0

Extremes ..max: betax[ 2] = 6.9287; betay[ 8] = 14.0296; eta[ 0] = 1.8621  
 [at el#] ..min: betax[ 8] = 1.1422; betay[ 0] = 3.3345; eta[ 8] = 0.9315  
 nux = 2.2500;    nu y = 1.2500  
 dnux/(dp/docy) = 0.0000;    dnuy/dp = 0.0000  
 4L/(mb^2g^3) \* dnux/(dQ) = -0.0000;    dnuy/(dQ) = -0.0000

### F.3 The Results of Calculations for the High-Energy Transport Line (HBT) by the Program LATTICE

Beam rigidity = 3.3373450 t-m  
 x,y emittance = 0.024868 0.024868 cm-mrad  
 dp/p = 0.000%

#### Elements of the lattice

e								
2	d	drift	0.0	0.300000	0.000000	0.000000	0.0000	0.0000
3	d1	drift	0.0	4.000000	0.000000	0.000000	0.0000	0.0000
4	d2	drift	0.0	0.500000	0.000000	0.000000	0.0000	0.0000
5	d3	drift	0.0	10.586480	0.000000	0.000000	0.0000	0.0000
6	d4a	drift	0.0	0.898128	0.000000	0.000000	0.0000	0.0000
7	d4b	drift	0.0	0.898128	0.000000	0.000000	0.0000	0.0000
8	d4c	drift	0.0	0.898128	0.000000	0.000000	0.0000	0.0000
9	d4d	drift	0.0	0.898128	0.000000	0.000000	0.0000	0.0000
10	d4e	drift	0.0	0.898128	0.000000	0.000000	0.0000	0.0000
11	d4f	drift	0.0	0.898128	0.000000	0.000000	0.0000	0.0000
12	d4g	drift	0.0	0.898128	0.000000	0.000000	0.0000	0.0000
13	d4h	drift	0.0	0.898128	0.000000	0.000000	0.0000	0.0000
14	d4i	drift	0.0	0.898128	0.000000	0.000000	0.0000	0.0000
15	d4j	drift	0.0	0.898128	0.000000	0.000000	0.0000	0.0000
16	d5	drift	0.0	0.500000	0.000000	0.000000	0.0000	0.0000
17	d6	drift	0.0	10.586480	0.000000	0.000000	0.0000	0.0000
18	d7	drift	0.0	0.500000	0.000000	0.000000	0.0000	0.0000
19	d8	drift	0.0	1.375000	0.000000	0.000000	0.0000	0.0000
20	d9	drift	0.0	0.875600	0.000000	0.000000	0.0000	0.0000
21	q1	quad	1.2	0.400000	-5.836873	0.000000	0.0000	0.0000
22	q2	quad	2.2	0.300000	7.310100	0.000000	0.0000	0.0000
23	q3	quad	3.2	0.300000	-7.468121	0.000000	0.0000	0.0000
24	q4	quad	4.2	0.400000	6.079376	0.000000	0.0000	0.0000
25	q5	quad	5.2	0.600000	3.320636	0.000000	0.0000	0.0000
26	q6	quad	6.2	0.400000	-4.337961	0.000000	0.0000	0.0000
27	q7	quad	7.2	0.300000	4.782795	0.000000	0.0000	0.0000
28	q8	quad	8.2	0.300000	-4.855686	0.000000	0.0000	0.0000
29	eh1	edge	0.0	2.000000	0.465979	0.018000	0.0000	0.0000
30	bh1	bend	0.0	0.500002	0.465979	0.000000	0.0000	0.0000
31	eh2	edge	0.0	1.000000	0.465979	0.018000	0.0000	0.0000
32	bh2	bend	0.0	0.250001	0.465979	0.000000	0.0000	0.0000
33	ev1	vedge	0.0	8.750000	1.000523	0.023000	0.0000	0.0000
34	bv1	vbend	0.0	1.018801	1.000523	0.000000	0.0000	0.0000
35	ev2	vedge	0.0	-8.750000	-1.000523	0.023000	0.0000	0.0000
36	bv2	vbend	0.0	1.018801	-1.000523	0.000000	0.0000	0.0000
37	Sep1	bend	0.0	0.872577	-1.002205	0.000000	0.0000	0.0000
38	Sep2	bend	0.0	0.727802	1.200484	0.000000	0.0000	0.0000

**Structures of the lattice**

l

```

1:  Sep1    d1     eh1    bh1     eh1    d2     q1
8:  d       q2     d3     q3     d      q4     d4a
5:  d4b    d4c    d4d    d4e    d4f    d4g    d4h
2:  d4i    d4j    bv1    d5     q5     d      q6
9:  d6     q7     d      q8     d7    bv2    d8
6:  eh2    bh2    eh2    d8     Sep2

```

**Initial Twiss parameters (injected from SYN)**

t

Transport mode

```

betax = 6.7673  alphax = 0.0000
betay = 3.3345  alphay = 0.0000
etax  = 1.8621  eta'x  = 0.0000
etay  = 0.0000  eta'y  = 0.0000

```

**Machine consists of 1 period****Fit Twiss parameters for a machine of 1 period**

variable	target value	weight	location
1 betax	13.3849	100.000	@end
2 betay	4.5803	100.000	@end
3 bxmax	16.0000	1.000	@end
4 bymax	22.0000	1.000	@end
5 alphax	0.0000	10.000	@end
6 alphay	0.0000	10.000	@end
7 etax	0.0000	10.000	@end
8 eta'x	0.0000	10.000	@end

**To calculate the beam parameters just at the end of the beam line**

g

\* HBT of Siam Photon Source by Ritthikrai

```

Total length = 46.992 Total bend = 5.987, 0.000 degrees
betax = 13.3850 meters  alphax = 0.6878  1/gam = 9.0864; z= 6.2497
betay = 4.5825 meters  alphay = -0.0000  1/gam = 4.5825; z= -0.0002
eta x = 0.2286 meters  eta' x = 0.0554    psix = 407.18 degrees
eta y = -0.1029 meters  eta' y = -0.6905    psiy = 394.19 degrees
x   = 0.1824 cm        x'   = 0.1654    r12 = -0.5667
y   = 0.0338 cm        y'   = 0.0737    r34 = 0.0000
m(1,6)= -1.5513        m(2,6)= 0.2904  m(5,6)= 1.3596
m(3,6)= -0.1029        m(4,6)= -0.6905  resolves: -0.2352%

```

### To track the Twiss parameters through the beam line

c

\* HBT of Siam Photon Source by Ritthikrai

elemnt	lth	sum l	betax	alphax	etax	eta'x	psix	betay	alphay	etay	eta'y	psiy
	(m)	(m)	(m)	(rad)	(m)	(rad)	(deg)	(m)	(rad)	(m)	(rad)	(deg)
	0.	0.	6.77	0.00	1.86	0.00	0.	3.33	0.00	0.00	0.00	0.
Sep1	0.87	0.87	6.42	0.39	1.68	-0.40	7.5	3.56	-0.26	0.00	0.00	14.7
d1	4.00	4.87	6.20	-0.33	0.07	-0.40	46.8	10.45	-1.46	0.00	0.00	55.6
eh1	0.00	4.87	6.20	-0.36	0.07	-0.40	46.8	10.45	-1.41	0.00	0.00	55.6
bh1	0.50	5.37	6.58	-0.39	-0.12	-0.33	51.3	11.94	-1.56	0.00	0.00	58.2
eh1	0.00	5.37	6.58	-0.42	-0.12	-0.33	51.3	11.94	-1.50	0.00	0.00	58.2
d2	0.50	5.87	7.04	-0.51	-0.28	-0.33	55.6	13.51	-1.64	0.00	0.00	60.4
q1	0.40	6.27	9.72	-6.80	-0.46	-0.59	58.5	11.19	6.89	0.00	0.00	62.2
d	0.30	6.57	14.24	-8.26	-0.64	-0.59	59.9	7.45	5.59	0.00	0.00	64.1
q2	0.30	6.87	16.35	1.69	-0.75	-0.13	61.0	5.62	0.90	0.00	0.00	66.8
d3	10.59	17.46	6.99	-0.80	-2.07	-0.13	159.0	22.75	-2.52	0.00	0.00	177.4
q3	0.30	17.76	9.07	-6.58	-2.33	-1.58	161.3	19.81	11.64	0.00	0.00	178.1
d	0.30	18.06	13.45	-8.04	-2.80	-1.58	162.8	13.45	9.58	0.00	0.00	179.2
q4	0.40	18.46	15.86	2.62	-3.00	0.59	164.3	9.74	0.58	0.00	0.00	181.3
d4a	0.90	19.36	11.55	2.17	-2.47	0.59	168.1	8.81	0.46	0.00	0.00	186.9
d4b	0.90	20.26	8.05	1.73	-1.94	0.59	173.5	8.09	0.33	0.00	0.00	193.0
d4c	0.90	21.15	5.34	1.28	-1.42	0.59	181.3	7.61	0.21	0.00	0.00	199.5
d4d	0.90	22.05	3.44	0.84	-0.89	0.59	193.4	7.34	0.09	0.00	0.00	206.5
d4e	0.90	22.95	2.33	0.39	-0.36	0.59	211.9	7.29	-0.04	0.00	0.00	213.5
d4f	0.90	23.85	2.02	-0.05	0.17	0.59	236.4	7.47	-0.16	0.00	0.00	220.5
d4g	0.90	24.75	2.52	-0.50	0.70	0.59	259.8	7.86	-0.28	0.00	0.00	227.2
d4h	0.90	25.64	3.81	-0.94	1.22	0.59	276.7	8.48	-0.41	0.00	0.00	233.5
d4i	0.90	26.54	5.90	-1.39	1.75	0.59	287.6	9.32	-0.53	0.00	0.00	239.3
d4j	0.90	27.44	8.79	-1.83	2.28	0.59	294.8	10.38	-0.65	0.00	0.00	244.6
bv1	1.02	28.46	13.04	-2.34	2.88	0.59	300.3	10.83	0.23	0.15	0.30	250.0
d5	0.50	28.96	15.50	-2.58	3.17	0.59	302.3	10.63	0.18	0.30	0.30	252.7
q5	0.60	29.56	13.15	6.02	2.96	-1.30	304.5	14.68	-7.72	0.55	0.55	255.6
d	0.30	29.86	9.79	5.17	2.57	-1.30	306.1	19.69	-8.96	0.72	0.55	256.6
q6	0.40	30.26	7.72	0.35	2.30	-0.05	308.8	22.70	1.96	0.86	0.13	257.7
d6	10.59	40.85	16.58	-1.19	1.72	-0.05	378.1	5.11	-0.29	2.26	0.13	337.0
q7	0.30	41.15	15.20	5.60	1.59	-0.77	379.1	6.01	-2.83	2.45	1.14	340.1
d	0.30	41.45	12.03	4.96	1.36	-0.77	380.4	7.85	-3.29	2.79	1.14	342.6
q8	0.30	41.75	10.64	-0.10	1.21	-0.22	382.0	8.80	0.26	2.95	-0.13	344.7
d7	0.50	42.25	10.76	-0.15	1.10	-0.22	384.6	8.57	0.20	2.88	-0.13	348.0
bv2	1.02	43.26	11.17	-0.25	0.88	-0.22	390.0	7.54	0.78	2.46	-0.68	355.1
d8	1.38	44.64	12.02	-0.38	0.58	-0.22	396.8	5.78	0.49	1.52	-0.68	367.2
eh2	0.00	44.64	12.02	-0.41	0.58	-0.22	396.8	5.78	0.50	1.52	-0.69	367.2
bh2	0.25	44.89	12.22	-0.37	0.53	-0.19	398.0	5.55	0.45	1.35	-0.69	369.7
eh2	0.00	44.89	12.22	-0.40	0.53	-0.18	398.0	5.55	0.46	1.35	-0.69	369.7
d8	1.38	46.26	13.50	-0.53	0.28	-0.18	404.1	4.70	0.16	0.40	-0.69	385.3
Sep2	0.73	46.99	13.39	0.69	0.23	0.06	407.2	4.58	-0.00	-0.10	-0.69	394.3

beta x min = 2.023      beta y min = 3.334  
 beta x max = 16.584    beta y max = 22.751  
 eta x min = -3.002     eta y min = -0.103  
 eta x max = 3.175      eta y max = 2.946

### Give exact maximum and minimum of the Twiss parameters

cp

\* HBT of Siam Photon Source by Ritthikrai

elemt	lth	sum l	betax	alphax	etax	eta'x	psix	x	betay	alphay	psiy	y
	(m)	(m)	(m)	(rad)	(m)	(rad)	( deg)	(mm)	(m)	(rad)	(deg)	(mm)
	0.	0.	6.77	0.00	1.86	0.00	0.	1	3.33	0.00	0.	0
Sep1	0.87	0.87	6.42	0.39	1.68	-0.40	7.5	1	3.56	-0.26	14.7	0
d1	4.00	4.87	6.20	-0.33	0.07	-0.40	46.8	1	10.45	-1.46	55.6	1
eh1	0.00	4.87	6.20	-0.36	0.07	-0.40	46.8	1	10.45	-1.41	55.6	1
bh1	0.50	5.37	6.58	-0.39	-0.12	-0.33	51.3	1	11.94	-1.56	58.2	1
eh1	0.00	5.37	6.58	-0.42	-0.12	-0.33	51.3	1	11.94	-1.50	58.2	1
d2	0.50	5.87	7.04	-0.51	-0.28	-0.33	55.6	1	13.51	-1.64	60.4	1
q1	0.40	6.27	9.72	-6.80	-0.46	-0.59	58.5	2	11.19	6.89	62.2	1
d	0.30	6.57	14.24	-8.26	-0.64	-0.59	59.9	2	7.45	5.59	64.1	0
q2	0.30	6.87	16.35	1.69	-0.75	-0.13	61.0	2	5.62	0.90	66.8	0
d3	10.59	17.46	6.99	-0.80	-2.07	-0.13	159.0	1	22.75	-2.52	177.4	1
q3	0.30	17.76	9.07	-6.58	-2.33	-1.58	161.3	2	19.81	11.64	178.1	1
d	0.30	18.06	13.45	-8.04	-2.80	-1.58	162.8	2	13.45	9.58	179.2	1
q4	0.40	18.46	15.86	2.62	-3.00	0.59	164.3	2	9.74	0.58	181.3	0
d4a	0.90	19.36	11.55	2.17	-2.47	0.59	168.1	2	8.81	0.46	186.9	0
d4b	0.90	20.26	8.05	1.73	-1.94	0.59	173.5	1	8.09	0.33	193.0	0
d4c	0.90	21.15	5.34	1.28	-1.42	0.59	181.3	1	7.61	0.21	199.5	0
d4d	0.90	22.05	3.44	0.84	-0.89	0.59	193.4	1	7.34	0.09	206.5	0
d4e	0.90	22.95	2.33	0.39	-0.36	0.59	211.9	1	7.29	-0.04	213.5	0
d4f	0.90	23.85	2.02	-0.05	0.17	0.59	236.4	1	7.47	-0.16	220.5	0
d4g	0.90	24.75	2.52	-0.50	0.70	0.59	259.8	1	7.86	-0.28	227.2	0
d4h	0.90	25.64	3.81	-0.94	1.22	0.59	276.7	1	8.48	-0.41	233.5	0
d4i	0.90	26.54	5.90	-1.39	1.75	0.59	287.6	1	9.32	-0.53	239.3	0
d4j	0.90	27.44	8.79	-1.83	2.28	0.59	294.8	1	10.38	-0.65	244.6	1
bv1	1.02	28.46	13.04	-2.34	2.88	0.59	300.3	2	10.83	0.23	250.0	1
d5	0.50	28.96	15.50	-2.58	3.17	0.59	302.3	2	10.63	0.18	252.7	1
q5	0.60	29.56	13.15	6.02	2.96	-1.30	304.5	2	14.68	-7.72	255.6	1
d	0.30	29.86	9.79	5.17	2.57	-1.30	306.1	2	19.69	-8.96	256.6	1
q6	0.40	30.26	7.72	0.35	2.30	-0.05	308.8	1	22.70	1.96	257.7	1
d6	10.59	40.85	16.58	-1.19	1.72	-0.05	378.1	2	5.11	-0.29	337.0	0
q7	0.30	41.15	15.20	5.60	1.59	-0.77	379.1	2	6.01	-2.83	340.1	0
d	0.30	41.45	12.03	4.96	1.36	-0.77	380.4	2	7.85	-3.29	342.6	0
q8	0.30	41.75	10.64	-0.10	1.21	-0.22	382.0	2	8.80	0.26	344.7	0
d7	0.50	42.25	10.76	-0.15	1.10	-0.22	384.6	2	8.57	0.20	348.0	0
bv2	1.02	43.26	11.17	-0.25	0.88	-0.22	390.0	2	7.54	0.78	355.1	0
d8	1.38	44.64	12.02	-0.38	0.58	-0.22	396.8	2	5.78	0.49	367.2	0
eh2	0.00	44.64	12.02	-0.41	0.58	-0.22	396.8	2	5.78	0.50	367.2	0
bh2	0.25	44.89	12.22	-0.37	0.53	-0.19	398.0	2	5.55	0.45	369.7	0
eh2	0.00	44.89	12.22	-0.40	0.53	-0.18	398.0	2	5.55	0.46	369.7	0
d8	1.38	46.26	13.50	-0.53	0.28	-0.18	404.1	2	4.70	0.16	385.3	0
Sep2	0.73	46.99	13.39	0.69	0.23	0.06	407.2	2	4.58	-0.00	394.3	0

Extremes ..max: betax[30] = 16.6439; betay[11] = 22.8759; eta[26] = 3.2283

[at el#] ..min: betax[19] = 2.0181; betay[10] = 3.0881; eta[13] = -3.0326

### To track the beam size through of every element of the lattice

x

\* HBT of the Siam Photon Source by Ritthikrai

elemnt	lth	sum l	x	x'	etax	psix	x+disp	y	y'	etay	psiy
	(m)	(m)	(cm)	(mrad)	(m)	(deg)	(cm)	(cm)	(mrad)	(m)	(deg)
Sep1	0.87	0.87	0.13	0.21	1.68	7.5	0.13	0.03	0.09	0.00	14.7
d1	4.00	4.87	0.12	0.21	0.07	46.8	0.12	0.05	0.09	0.00	55.6
eh1	0.00	4.87	0.12	0.21	0.07	46.8	0.12	0.05	0.08	0.00	55.6
bh1	0.50	5.37	0.13	0.21	-0.12	51.3	0.13	0.05	0.08	0.00	58.2
eh1	0.00	5.37	0.13	0.21	-0.12	51.3	0.13	0.05	0.08	0.00	58.2
d2	0.50	5.87	0.13	.21	-0.28	55.6	0.13	0.06	0.08	0.00	60.4
q1	0.40	6.27	0.16	1.10	-0.46	58.5	0.16	0.05	0.33	0.00	62.2
d	0.30	6.57	0.19	1.10	-0.64	59.9	0.19	0.04	0.33	0.00	64.1
q2	0.30	6.87	0.20	0.24	-0.75	61.0	0.20	0.04	0.09	0.00	66.8
d3	10.59	17.46	0.13	0.24	-2.07	159.0	0.13	0.08	0.09	0.00	177.4
q3	0.30	17.76	0.15	1.10	-2.33	161.3	0.15	0.07	0.41	0.00	178.1
d	0.30	18.06	0.18	1.10	-2.80	162.8	0.18	0.06	0.41	0.00	179.2
q4	0.40	18.46	0.20	0.35	-3.00	164.3	0.20	0.05	0.06	0.00	181.3
d4a	0.90	19.36	0.17	0.35	-2.47	168.1	0.17	0.05	0.06	0.00	186.9
d4b	0.90	20.26	0.14	0.35	-1.94	173.5	0.14	0.04	0.06	0.00	193.0
d4c	0.90	21.15	0.12	0.35	-1.42	181.3	0.12	0.04	0.06	0.00	199.5
d4d	0.90	22.05	0.09	0.35	-0.89	193.4	0.09	0.04	0.06	0.00	206.5
d4e	0.90	22.95	0.08	0.35	-0.36	211.9	0.08	0.04	0.06	0.00	213.5
d4f	0.90	23.85	0.07	0.35	0.17	236.4	0.07	0.04	0.06	0.00	220.5
d4g	0.90	24.75	0.08	0.35	0.70	259.8	0.08	0.04	0.06	0.00	227.2
d4h	0.90	25.64	0.10	0.35	1.22	276.7	0.10	0.05	0.06	0.00	233.5
d4j	0.90	27.44	0.15	0.35	2.28	294.8	0.15	0.05	0.06	0.00	244.6
bv1	1.02	28.46	0.18	0.35	2.88	300.3	0.18	0.05	0.05	0.15	250.0
d5	0.50	28.96	0.20	0.35	3.17	302.3	0.20	0.05	0.05	0.30	252.7
q5	0.60	29.56	0.18	0.84	2.96	304.5	0.18	0.06	0.32	0.55	255.6
d	0.30	29.86	0.16	0.84	2.57	306.1	0.16	0.07	0.32	0.72	256.6
q6	0.40	30.26	0.14	0.19	2.30	308.8	0.14	0.08	0.07	0.86	257.7
d6	10.59	40.85	0.20	0.19	1.72	378.1	0.20	0.04	0.07	2.26	337.0
q7	0.30	41.15	0.19	0.73	1.59	379.1	0.19	0.04	0.19	2.45	340.1
d	0.30	41.45	0.17	0.73	1.36	380.4	0.17	0.04	0.19	2.79	342.6
q8	0.30	41.75	0.16	0.15	1.21	382.0	0.16	0.05	0.05	2.95	344.7
d7	0.50	42.25	0.16	0.15	1.10	384.6	0.16	0.05	0.05	2.88	348.0
bv2	1.02	43.26	0.17	0.15	0.88	390.0	0.17	0.04	0.07	2.46	355.1
d8	1.38	44.64	0.17	0.15	0.58	396.8	0.17	0.04	0.07	1.52	367.2
eh2	0.00	44.64	0.17	0.16	0.58	396.8	0.17	0.04	0.07	1.52	367.2
bh2	0.25	44.89	0.17	0.15	0.53	398.0	0.17	0.04	0.07	1.35	369.7
eh2	0.00	44.89	0.17	0.15	0.53	398.0	0.17	0.04	0.07	1.35	369.7
d8	1.38	46.26	0.18	0.15	0.28	404.1	0.18	0.03	0.07	0.40	385.3
Sep2	0.73	46.99	0.18	0.17	0.23	407.2	0.18	0.03	0.07	-0.10	394.3

beta x min = 2.023      beta y min = 3.334  
 beta x max = 16.584     beta y max = 22.751  
 eta x min = -3.002     eta y min = -0.103  
 eta x max = 3.175      eta y max = 2.946

## F.4 The Results of Calculations for the Storage Ring (STR) without Chromaticities Compensation by the Program LATTICE

Beam rigidity = 3.3373450 t-m  
 x,y emittance = 0.006726 0.000673 cm-mrad  
 dp/p = 0.000%

### Elements of the lattice

e								
1	param	slit	0.0	0.000000	0.000000	0.000000	0.0000	0.0000
2	d1	drift	0.0	3.500000	0.000000	0.000000	0.0000	0.0000
3	d2	drift	0.0	0.400000	0.000000	0.000000	0.0000	0.0000
4	d3	drift	0.0	0.405000	0.000000	0.000000	0.0000	0.0000
5	d4	drift	0.0	0.600000	0.000000	0.000000	0.0000	0.0000
6	d5	drift	0.0	1.624000	0.000000	0.000000	0.0000	0.0000
7	q1	quad	1.2	0.290000	9.198042	0.000000	0.0000	0.0000
8	q2	quad	2.2	0.290000	-9.573120	0.000000	0.0000	0.0000
9	q3	quad	3.2	0.290000	8.410067	0.000000	0.0000	0.0000
10	q4	quad	4.2	0.145000	-6.888579	0.000000	0.0000	0.0000
11	b1	bend	0.0	0.818778	1.200480	0.000000	0.0000	0.0000
12	b2	bend	0.0	1.364629	1.200480	0.000000	0.0000	0.0000
13	dsf	drift	0.0	0.205000	0.000000	0.000000	0.0000	0.0000
14	dsd	drift	0.0	0.230000	0.000000	0.000000	0.0000	0.0000
15	sf	sex	5.2	0.000001	0.000000	0.000000	0.0000	0.0000
16	sd	sex	6.2	0.000001	0.000000	0.000000	0.0000	0.0000

### Structures of the lattice

l							
1:	d1	q1	d2	q2	d3	b1	b2
8:	d4	q3	dsf	sf	d5	sd	dsd
15:	q4	q4	dsd	sd	d5	sf	dsf
22:	q3	d4	b2	b1	d3	q2	d2
29:	q1	d1					

### Machine consists of 4 periods

#### Calculate the parameters

g  
 \* STR of Siam Photon Source by Ritthikrai  
 Matched functions for 4 periods  
 Total length = 81.299 Total bend = 359.999, 0.000 degrees  
 betax = 13.3849 meters alphax = -0.0000 nu x = 4.76000  
 betay = 4.5803 meters alphay = -0.0000 nu y = 2.82000  
 eta x = -0.0000 meters eta' x = -0.0000 gamtr = 6.83314  
 eta y = 0.0000 meters eta' y = 0.0000



**Calculate the various parameters**

ch

\* STR of Siam Photon Source by Ritthikrai

nu x	=	4.760	nu y	=	2.820
tr gamma	=	6.833	compaction	=	0.02142
beta x min	=	0.531	beta y min	=	1.561
beta x max	=	14.300	beta y max	=	19.354
eta x min	=	-0.000	eta y min	=	0.000
eta x max	=	1.316	eta y max	=	0.000
dnux/(dp/p)	=	-7.648	dnuy/(dp/p)	=	-6.727
normalized x	=	-1.607	normalized y	=	-2.386

Space charge integrals: avg beam half width, height = 0.0640, 0.0203 cm.

Synchrotron integrals: I1 = 1.744828 m-1 , I2 = 2.260124 m-1

I3 = 0.812992 m-2 , I4 = 0.225767 m-1 , I5 = 0.102107 m-1

I5/(I2-I4) = 0.050192 I3/(2\*I2+I4) = 0.171300

Functions for electron storage rings:

D = 0.09989, Jx = 0.900, Je = 2.100

Natural rms x emittance = 0.073989 pi mm-mrad

Natural rms energy spread = 0.503 MeV

Synchrotron radiation = 0.031988 MeV/turn

Damping times (sec): Horiz: 0.018847, Vert: 0.016964, Energy: 0.008079

**F.5 The Results of Calculations for the Storage Ring (STR) with Compensation Chromaticities by the Program LATTICE**

Beam rigidity = 3.3373450 t-m

x,y emittance = 0.006726 0.000673 cm-mrad

dp/p = 0.000%

**Elements of the lattice**

1 param	slit	0.0	0.000000	0.000000	0.000000	0.0000	0.0000
2 d1	drift	0.0	3.500000	0.000000	0.000000	0.0000	0.0000
3 d2	drift	0.0	0.400000	0.000000	0.000000	0.0000	0.0000
4 d3	drift	0.0	0.405000	0.000000	0.000000	0.0000	0.0000
5 d4	drift	0.0	0.600000	0.000000	0.000000	0.0000	0.0000
6 d5	drift	0.0	1.624000	0.000000	0.000000	0.0000	0.0000
7 q1	quad	1.2	0.290000	9.198045	0.000000	0.0000	0.0000
8 q2	quad	2.2	0.290000	-9.573124	0.000000	0.0000	0.0000
9 q3	quad	3.2	0.290000	8.410067	0.000000	0.0000	0.0000
10 q4	quad	4.2	0.145000	-6.888579	0.000000	0.0000	0.0000
11 b1	bend	0.0	0.818778	1.200480	0.000000	0.0000	0.0000
12 b2	bend	0.0	1.364629	1.200480	0.000000	0.0000	0.0000
13 dsf	drift	0.0	0.205000	0.000000	0.000000	0.0000	0.0000
14 dsd	drift	0.0	0.230000	0.000000	0.000000	0.0000	0.0000
15 sf	sex	0.0	0.000001	6877662.751800	0.000000	0.0000	0.0000
16 sd	sex	0.0	0.000001	-10317118.549900	0.000000	0.0000	0.0000

**Structures of the lattice**

l

1:	d1	q1	d2	q2	d3	b1	b2
8:	d4	q3	dsf	sf	d5	sd	dsd
15:	q4	q4	dsd	sd	d5	sf	dsf
22:	q3	d4	b2	b1	d3	q2	d2
29:	q1	d1					

**Machine consists of 4 periods****To calculate the beam parameters just at the end of the beam line**

g

\* STR of Siam Photon Source by Ritthikrai

Matched functions for 4 periods

Total length = 81.299 Total bend = 359.999, 0.000 degrees  
 betax = 13.3849 meters alphax = 0.0000 nu x = 4.76000  
 betay = 4.5803 meters alphay = 0.0000 nu y = 2.82000  
 eta x = -0.0000 meters eta' x = -0.0000 gamtr = 6.83314  
 eta y = 0.0000 meters eta' y = 0.0000

**Calculate the various parameters**

ch

\* STR of Siam Photon Source by Ritthikrai

nu x	=	4.760	nu y	=	2.820
tr gamma	=	6.833	compaction	=	0.02142
beta x min	=	0.531	beta y min	=	1.561
beta x max	=	14.300	beta y max	=	19.354
eta x min	=	-0.000	eta y min	=	0.000
eta x max	=	1.316	eta y max	=	0.000
dnux/(dp/p)	=	0.000	dnuy/(dp/p)	=	-0.000
normalized x	=	0.000	normalized y	=	-0.000

Space charge integrals: avg beam half width, height = 0.0640, 0.0203 cm.

Synchrotron integrals: I1 = 1.744828 m-1 , I2 = 2.260124 m-1

I3 = 0.812992 m-2 , I4 = 0.225767 m-1 , I5 = 0.102108 m-1

I5/(I2-I4) = 0.050192 I3/(2\*I2+I4) = 0.171300

Functions for electron storage rings:

D = 0.09989, Jx = 0.900, Je = 2.100

Natural rms x emittance = 0.073989 pi mm-mrad

Natural rms energy spread = 0.503 MeV

Synchrotron radiation = 0.031988 MeV/turn

Damping times (sec): Horiz: 0.018847, Vert: 0.016964, Energy: 0.008079

### To track the Twiss parameters through every element of the lattice

c

\* STR of Siam Photon Source by Ritthikrai

elemt	lth	sum l	betax	alphax	etax	eta'x	psix	betay	alphay	etay	eta'y	psiy
	(m)	(m)	(m)	(rad)	(m)	(rad)	(deg)	(m)	(rad)	(m)	(rad)	(deg)
	0.	0.	13.38	0.00	-0.00	-0.00	0.	4.58	0.00	0.00	0.00	0.
d1	3.50	3.50	14.30	-0.26	-0.00	-0.00	14.7	7.25	-0.76	0.00	0.00	37.4
q1	0.29	3.79	11.37	9.58	-0.00	0.00	15.9	9.61	-7.96	0.00	0.00	39.5
d2	0.40	4.19	5.01	6.31	-0.00	0.00	18.9	17.04	-10.64	0.00	0.00	41.2
q2	0.29	4.48	2.78	1.98	-0.00	0.00	23.6	18.99	4.46	0.00	0.00	42.1
d3	0.41	4.89	1.47	1.26	-0.00	0.00	35.1	15.56	4.01	0.00	0.00	43.5
b1	0.82	5.70	0.55	-0.16	0.12	0.29	99.3	9.73	3.11	0.00	0.00	47.3
b2	1.36	7.07	4.03	-2.18	0.81	0.71	161.4	3.28	1.61	0.00	0.00	61.3
d4	0.60	7.67	7.17	-3.04	1.24	0.71	167.8	1.74	0.95	0.00	0.00	75.8
q3	0.29	7.96	7.39	2.33	1.31	-0.24	170.0	1.60	-0.44	0.00	0.00	86.2
dsf	0.21	8.16	6.47	2.15	1.26	-0.24	171.7	1.81	-0.59	0.00	0.00	93.1
sf	0.00	8.16	6.47	2.15	1.26	-0.24	171.7	1.81	-0.59	0.00	0.00	93.1
d5	1.62	9.79	1.78	0.74	0.87	-0.24	200.3	5.68	-1.80	0.00	0.00	123.5
sd	0.00	9.79	1.78	0.74	0.87	-0.24	200.3	5.68	-1.80	0.00	0.00	123.5
dsd	0.23	10.02	1.48	0.54	0.81	-0.24	208.4	6.55	-1.97	0.00	0.00	125.7
q4	0.15	10.16	1.41	-0.00	0.80	-0.00	214.2	6.84	0.00	0.00	0.00	126.9
q4	0.15	10.31	1.48	-0.54	0.81	0.24	220.0	6.55	1.97	0.00	0.00	128.1
dsd	0.23	10.54	1.78	-0.74	0.87	0.24	228.1	5.68	1.80	0.00	0.00	130.3
sd	0.00	10.54	1.78	-0.74	0.87	0.24	228.1	5.68	1.80	0.00	0.00	130.3
d5	1.62	12.16	6.47	-2.15	1.26	0.24	256.7	1.81	0.59	0.00	0.00	160.7
sf	0.00	12.16	6.47	-2.15	1.26	0.24	256.7	1.81	0.59	0.00	0.00	160.7
dsf	0.21	12.37	7.39	-2.33	1.31	0.24	258.4	1.60	0.44	0.00	0.00	167.6
q3	0.29	12.66	7.17	3.04	1.24	-0.71	260.6	1.74	-0.95	0.00	0.00	178.0
d4	0.60	13.26	4.03	2.18	0.81	-0.71	267.0	3.28	-1.61	0.00	0.00	192.5
b2	1.36	14.62	0.55	0.16	0.12	-0.29	329.1	9.73	-3.11	0.00	0.00	206.5
b1	0.82	15.44	1.47	-1.26	-0.00	-0.00	393.3	15.56	-4.01	0.00	0.00	210.3
d3	0.41	15.84	2.78	-1.98	-0.00	-0.00	404.8	18.99	-4.46	0.00	0.00	211.7
q2	0.29	16.13	5.01	-6.31	-0.00	-0.00	409.5	17.04	10.64	0.00	0.00	212.6
d2	0.40	16.53	11.37	-9.58	-0.00	-0.00	412.5	9.61	7.96	0.00	0.00	214.3
q1	0.29	16.82	14.30	0.26	-0.00	-0.00	413.7	7.25	0.76	0.00	0.00	216.4
d1	3.50	20.32	13.38	-0.00	-0.00	-0.00	428.4	4.58	-0.00	0.00	0.00	253.8

elemt l th s um l betax alphax etax eta'x psix betay alphay etay eta'y  
psiy

(m) (m) (m) (m) (rad) (deg) (m) (m) (rad) (deg)

nu x = 4.760 nu y = 2.820

tr gamma = 6.833 compaction = 0.02142

beta x min = 0.546 beta y min = 1.600

beta x max = 14.300 beta y max = 18.994

eta x min = -0.000 eta y min = 0.000

eta x max = 1.307 eta y max = 0.000

### Give exact maximum and minimum of the Twiss parameters

cp

\* STR of the Siam Photon Source by Ritthikrai

elemt	lth	sum l	betax	alphax	etax	eta'x	psix	x	betay	alphay	psiy	y
	(m)	(m)	(m)	(rad)	(m)	(rad)	(deg)	(mm)	(m)	(rad)	(deg)	(mm)
	0.	0.	13.38	0.00	-0.00	-0.00	0.	1	4.58	0.00	0.	0
d1	3.50	3.50	14.30	-0.26	-0.00	-0.00	14.7	1	7.25	-0.76	37.4	0
q1	0.29	3.79	11.37	9.58	-0.00	0.00	15.9	1	9.61	-7.96	39.5	0
d2	0.40	4.19	5.01	6.31	-0.00	0.00	18.9	1	17.04	-10.64	41.2	0
q2	0.29	4.48	2.78	1.98	-0.00	0.00	23.6	0	18.99	4.46	42.1	0
d3	0.41	4.89	1.47	1.26	-0.00	0.00	35.1	0	15.56	4.01	43.5	0
b1	0.82	5.70	0.55	-0.16	0.12	0.29	99.3	0	9.73	3.11	47.3	0
b2	1.36	7.07	4.03	-2.18	0.81	0.71	161.4	1	3.28	1.61	61.3	0
d4	0.60	7.67	7.17	-3.04	1.24	0.71	167.8	1	1.74	0.95	75.8	0
q3	0.29	7.96	7.39	2.33	1.31	-0.24	170.0	1	1.60	-0.44	86.2	0
dsf	0.21	8.16	6.47	2.15	1.26	-0.24	171.7	1	1.81	-0.59	93.1	0
sf	0.00	8.16	6.47	2.15	1.26	-0.24	171.7	1	1.81	-0.59	93.1	0
d5	1.62	9.79	1.78	0.74	0.87	-0.24	200.3	0	5.68	-1.80	123.5	0
sd	0.00	9.79	1.78	0.74	0.87	-0.24	200.3	0	5.68	-1.80	123.5	0
dsd	0.23	10.02	1.48	0.54	0.81	-0.24	208.4	0	6.55	-1.97	125.7	0
q4	0.15	10.16	1.41	-0.00	0.80	-0.00	214.2	0	6.84	0.00	126.9	0
q4	0.15	10.31	1.48	-0.54	0.81	0.24	220.0	0	6.55	1.97	128.1	0
dsd	0.23	10.54	1.78	-0.74	0.87	0.24	228.1	0	5.68	1.80	130.3	0
sd	0.00	10.54	1.78	-0.74	0.87	0.24	228.1	0	5.68	1.80	130.3	0
d5	1.62	12.16	6.47	-2.15	1.26	0.24	256.7	1	1.81	0.59	160.7	0
sf	0.00	12.16	6.47	-2.15	1.26	0.24	256.7	1	1.81	0.59	160.7	0
dsf	0.21	12.37	7.39	-2.33	1.31	0.24	258.4	1	1.60	0.44	167.6	0
q3	0.29	12.66	7.17	3.04	1.24	-0.71	260.6	1	1.74	-0.95	178.0	0
d4	0.60	13.26	4.03	2.18	0.81	-0.71	267.0	1	3.28	-1.61	192.5	0
b2	1.36	14.62	0.55	0.16	0.12	-0.29	329.1	0	9.73	-3.11	206.5	0
b1	0.82	15.44	1.47	-1.26	-0.00	-0.00	393.3	0	15.56	-4.01	210.3	0
d3	0.41	15.84	2.78	-1.98	-0.00	-0.00	404.8	0	18.99	-4.46	211.7	0
q2	0.29	16.13	5.01	-6.31	-0.00	-0.00	409.5	1	17.04	10.64	212.6	0
d2	0.40	16.53	11.37	-9.58	-0.00	-0.00	412.5	1	9.61	7.96	214.3	0
q1	0.29	16.82	14.30	0.26	-0.00	-0.00	413.7	1	7.25	0.76	216.4	0
d1	3.50	20.32	13.38	-0.00	-0.00	-0.00	428.4	1	4.58	-0.00	253.8	0

Extremes ..max: betax[29] = 14.3018; betay[ 4] = 19.3586; eta[22] = 1.3161

[at el#] ..min: betax[25] = 0.5308; betay[22] = 1.5596; eta[ 2] = -0.0000

nux = 4.7600; nuy = 2.8200

dnux/(dp/docy) = 0.0000; dnuy/dp = 0.0000

4L/(mb<sup>2</sup>g<sup>3</sup>) \* dnux/(dQ) = -0.0000; dnuy/(dQ) = -0.0000

### To track the beam size through of every element of the lattice

x

\* STR of the Siam Photon Source by Ritthikrai

elemt	lth	sum l	x	x'	etax	psix	x+disp	y	y'	etay	psiy
	(m)	(m)	(cm)	(mrad)	(m)	(deg)	(cm)	(cm)	(mrad)	(m)	(deg)
d1	3.50	3.50	0.10	0.07	-0.00	14.7	0.10	0.02	0.04	0.00	37.4
q1	0.29	3.79	0.09	0.74	-0.00	15.9	0.09	0.03	0.21	0.00	39.5
d2	0.40	4.19	0.06	0.74	-0.00	18.9	0.06	0.03	0.21	0.00	41.2
q2	0.29	4.48	0.04	0.34	-0.00	23.6	0.04	0.04	0.09	0.00	42.1
d3	0.41	4.89	0.03	0.34	-0.00	35.1	0.03	0.03	0.09	0.00	43.5
b1	0.82	5.70	0.02	0.36	0.12	99.3	0.02	0.03	0.09	0.00	47.3
b2	1.36	7.07	0.05	0.31	0.81	161.4	0.05	0.01	0.09	0.00	61.3
d4	0.60	7.67	0.07	0.31	1.24	167.8	0.07	0.01	0.09	0.00	75.8
q3	0.29	7.96	0.07	0.24	1.31	170.0	0.07	0.01	0.07	0.00	86.2
dsf	0.21	8.16	0.07	0.24	1.26	171.7	0.07	0.01	0.07	0.00	93.1
sf	0.00	8.16	0.07	0.24	1.26	171.7	0.07	0.01	0.07	0.00	93.1
d5	1.62	9.79	0.03	0.24	0.87	200.3	0.03	0.02	0.07	0.00	123.5
sd	0.00	9.79	0.03	0.24	0.87	200.3	0.03	0.02	0.07	0.00	123.5
dsd	0.23	10.02	0.03	0.24	0.81	208.4	0.03	0.02	0.07	0.00	125.7
q4	0.15	10.16	0.03	0.22	0.80	214.2	0.03	0.02	0.03	0.00	126.9
q4	0.15	10.31	0.03	0.24	0.81	220.0	0.03	0.02	0.07	0.00	128.1
dsd	0.23	10.54	0.03	0.24	0.87	228.1	0.03	0.02	0.07	0.00	130.3
sd	0.00	10.54	0.03	0.24	0.87	228.1	0.03	0.02	0.07	0.00	130.3
d5	1.62	12.16	0.07	0.24	1.26	256.7	0.07	0.01	0.07	0.00	160.7
sf	0.00	12.16	0.07	0.24	1.26	256.7	0.07	0.01	0.07	0.00	160.7
dsf	0.21	12.37	0.07	0.24	1.31	258.4	0.07	0.01	0.07	0.00	167.6
q3	0.29	12.66	0.07	0.31	1.24	260.6	0.07	0.01	0.09	0.00	178.0
d4	0.60	13.26	0.05	0.31	0.81	267.0	0.05	0.01	0.09	0.00	192.5
b2	1.36	14.62	0.02	0.36	0.12	329.1	0.02	0.03	0.09	0.00	206.5
b1	0.82	15.44	0.03	0.34	-0.00	393.3	0.03	0.03	0.09	0.00	210.3
d3	0.41	15.84	0.04	0.34	-0.00	404.8	0.04	0.04	0.09	0.00	211.7
q2	0.29	16.13	0.06	0.74	-0.00	409.5	0.06	0.03	0.21	0.00	212.6
d2	0.40	16.53	0.09	0.74	-0.00	412.5	0.09	0.03	0.21	0.00	214.3
q1	0.29	16.82	0.10	0.07	-0.00	413.7	0.10	0.02	0.04	0.00	216.4
d1	3.50	20.32	0.09	0.07	-0.00	428.4	0.09	0.02	0.04	0.00	253.8

nu x = 4.760      nu y = 2.820  
 tr gamma = 6.833      compaction = 0.02142  
 beta x min = 0.546      beta y min = 1.600  
 beta x max = 14.300      beta y max = 18.994  
 eta x min = -0.000      eta y min = 0.000  
 eta x max = 1.307      eta y max = 0.000

## F.6 The Results of Calculations for the Storage Ring (STR) by the Program BETA

OPTION(%%, \$, Z, VI, AX, X, DE, MO, FI, DIAG, SY, GR, TR, CO,  
 NUDP, XXP, ZXP, LDP, XZ, EXZ, DEFQ, DEFD, DEFM, AL  
 AJ, AJ2, SX, SXLD, LDSX, AVAR, NLOG, MO2) : mo

Structure as RING(BETA) or TRANSFER LINE(BEAM) (RI/TL) [RI]:

```

32
D1 SD .35000000E+01
QF1 QP .28999999E+00 .27560966E+01
D2 SD .40000001E+00
QD2 QP .28999999E+00 -.28684850E+01
D3 SD .40500000E+00
B1 DI .29452431E+00 .27800000E+01 .00000000E+00 .00000000E+00
B2 DI .49087384E+00 .27800000E+01 .00000000E+00 .00000000E+00
D4 SD .60000002E+00
QF3 QP .28999999E+00 .25199873E+01
D5 SD .20500000E+00
SF SX .10000000E-05 .10304093E+07
D6 SD .16240000E+01
SD SX .10000000E-05 -.15457075E+07
D7 SD .23000000E+00
QD4 QP .28999999E+00 -.20640895E+01
D8 SD .23000000E+00
D9 SD .16240000E+01
D10 SD .20500000E+00
QF3 QP .28999999E+00 .25199873E+01
D11 SD .60000002E+00
B2 DI .49087384E+00 .27800000E+01 .00000000E+00 .00000000E+00
B1 DI .29452431E+00 .27800000E+01 .00000000E+00 .00000000E+00
D12 SD .40500000E+00
QD2 QP .28999999E+00 -.28684850E+01
D13 SD .40000001E+00
QF1 QP .28999999E+00 .27560966E+01
D14 SD .14890000E+01
D15 SD .20109999E+01
RF CA .12000000E+06 .32000000E+02 .10000000E+10
K1 KI .00000000E+00 .00000000E+00 .00000000E+00
NEXT ?:
121
D1 QF1 D2 QD2 D3 B1 B2 D4 QF3 D5
SF D6 SD D7 QD4 D8 SD D9 SF D10
QF3 D11 B2 B1 D12 QD2 D13 QF1 D14 RF
D15 D1 QF1 D2 QD2 D3 B1 B2 D4 QF3
D5 SF D6 SD D7 QD4 D8 SD D9 SF
D10 QF3 D11 B2 B1 D12 QD2 D13 QF1 D14
D15 D1 QF1 D2 QD2 D3 B1 B2 D4 QF3
D5 SF D6 SD D7 QD4 D8 SD D9 SF
D10 QF3 D11 B2 B1 D12 QD2 D13 QF1 D14

```

D15 D1 QF1 D2 QD2 D3 B1 B2 D4 QF3  
 D5 SF D6 SD D7 QD4 D8 SD D9 SF  
 D10 QF3 D11 B2 B1 D12 QD2 D13 QF1 D14  
 D15

NEXT ?:

NUMBER OF SUPERPERIODS [ 1]:

PARTICLE [E ]:

FIRST OR SECOND ORDER(1 OU 2):

OPTION : BETA

STRUCTURE: E:\The results\strgood.str

0/ 121

### FIRST-ORDER MATRIX

```

6.280E-02 -1.336E+01 0.000E+00 0.000E+00 7.506E-10 1.245E-06 0.000E+00
7.456E-02 6.280E-02 0.000E+00 0.000E+00 -1.253E-11 -9.906E-08 0.000E+00
0.000E+00 0.000E+00 4.258E-01 -4.144E+00 0.000E+00 0.000E+00 0.000E+00
0.000E+00 0.000E+00 1.975E-01 4.258E-01 0.000E+00 0.000E+00 0.000E+00
-9.902E-08 1.245E-06 0.000E+00 0.000E+00 1.000E+00 1.741E+00 0.000E+00
2.737E-11 2.490E-10 0.000E+00 0.000E+00 2.966E-04 1.000E+00 0.000E+00

```

MACHINE RADIUS = 12.939185

CELL LENGTH = 81.299301

NUX= .760001 NUZ= .820000 NUS=\*\*\*\*\*

NEXT PAGE ?

The beam matrix

```

1.3385E+01
-4.4531E-09 7.4711E-02
0.0000E+00 0.0000E+00 4.5803E+00
0.0000E+00 0.0000E+00 -1.3013E-08 2.1833E-01
-2.9413E-10 -9.9247E-08 -5.2709E-15 1.6561E-16 1.3184E-13
-1.0592E-10 1.9987E-11 2.4016E-17 -5.2465E-18 -2.6549E-17 6.1854E-21

```

### CLOSED ORBIT

0.0000E+00 0.0000E+00 0.0000E+00 0.0000E+00 0.0000E+00 0.0000E+00

### CHROMATIC CLOSED ORBIT

1.3286E-06 1.0269E-11 0.0000E+00 0.0000E+00 0.0000E+00 0.0000E+00

ALPHAP= 2.142E-02 ETA= 2.142E-02

W= 1.000E+09 E0= 5.110E+05

V/C= 1.000E+00 GAMMA= 1.958E+03

NEXT PAGE ?

0/ 121

	DAMPING TIME (s)	PARTITION NUMBER	EMITTANCE INVARIANT	PROJECTION	DP/P=0
X	1.8893E-02	9.0040E-01	7.3411E-08		
Z	1.7011E-02	1.0000E+00			
S	8.1021E-03	2.0996E+00			

X	-1.7072E-01		-6.6299E-07	6.6299E-07	6.6299E-07
Z	-3.4233E+29		-6.5383E-05	6.5383E-05	6.5383E-05
S	0.0000E+00		0.0000E+00	6.9735E-24	6.9735E-24

COUPLING		0.0000E+00	9.8618E+01	9.8618E+01	
----------	--	------------	------------	------------	--

ENERGY SPREAD	5.0220E-04
ENERGY LOSS/TURN (MeV)	3.1900E-02

I1	1.7397E+00
I2	2.2601E+00
I3	8.1300E-01
I4	2.2510E-01
I5	1.0149E-01

NEXT PAGE ?

### 200 HARMONICS

D	.11621E+03	NUX-	4	.11077E+03	.95317E+00
G	.15503E+03	NUX-	4	.24520E+03	.15817E+01
DG	.24349E+03	NUX-	4	.16481E+03	.67685E+00
F	-.16878E+02	3*NUX-	16	-.13627E+02	.80737E+00
L	-.70231E+02	NUX+2*NUZ-	12	-.91374E+02	.13010E+01
H	-.80839E+01	NUX-2*NUZ-	0	-.45813E+02	.56672E+01

### BETATRON TUNES

NUX=	4.760002	NUZ=	2.820000
------	----------	------	----------

### TUNE SHIFTS WITH AMPLITUDE

DNUX/(EX/PI)=	-.49183E+02	DNUZ/(EX/PI)=	-.90670E+02
DNUX/(EZ/PI)=	-.90670E+02	DNUZ/(EZ/PI)=	-.19178E+02

NEXT PAGE ?



## **Curriculum Vitae**

Mr. Ritthikrai Chai-Ngam was born on March 2<sup>nd</sup>, 1976 in Roi-Et Province. He received the Duang Prathep Scholarship from Duang Pratheep Foundation while he was a high school student in Roi-Et. Then, he graduated B.Sc. (Physics) from Srinakharinwirot University in 1998. He was supported by Chai-Yong-Lim-Thongkul Scholarship. After that, he joined the School of Physics, Institute of Science, Suranaree University of Technology by the support of Mahasarakham University.